

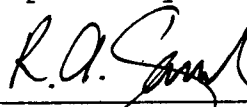
IOW-40-199-1
Revision 0
December 1982
25.2640.0199

DUANE ARNOLD ENERGY CENTER
PLANT UNIQUE ANALYSIS REPORT
VOLUME 1
GENERAL CRITERIA AND
LOADS METHODOLOGY

Prepared for:
Iowa Electric Light and Power Company

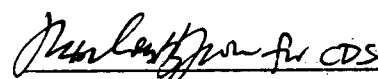
Prepared by:
NUTECH Engineers, Inc.
San Jose, California

Prepared by:




R. A. Sanchez, P.E.
Unit Supervisor

Approved by:

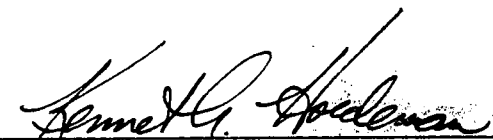


Dr. C. D. Sawyer
Engineering Director


Issued by:



H. J. Sund
Project Manager



for Dr. A. B. Higginbotham, P.E.
Senior Vice President
San Jose Operations



K. A. Hoedeman, P.E.
Project General Manager

Date: 12/15/82

REVISION CONTROL SHEET

TITLE: Duane Arnold Energy Center
Plant Unique Analysis Report
Volume 1

Hamzah Alhadi
H. Alhadi/Consultant I

HA
INITIALS

R. D. Carignan
R. D. Carignan/Principal Engineer

RDC
INITIALS

R. A. Sanchez
R. A. Sanchez/Unit Supervisor

RAS
INITIALS

W. J. Steffey
W. J. Steffey/Principal Engineer

WJS
INITIALS

Vijay Kumar
V. Kumar/Project Engineer

VK
INITIALS

EFFEC- TIVE PAGE (S)	REV	PRE- PARED	ACCURACY CHECK	CRITERIA CHECK	EFFEC- TIVE PAGE (S)	REV	PRE- PARED	ACCURACY CHECK	CRITERIA CHECK
1-v	0	<u>RDC</u>	<u>WJS</u>	<u>WJS</u>	1-1.10	0	<u>RDC</u>	<u>WJS</u>	<u>WJS</u>
1-vi					1-1.11				
1-vii					1-1.12				
1-viii					1-1.13				
1-ix					1-1.14				
1-x					1-1.15				
1-xi					1-1.16				
1-xii					1-1.17				
1-xiii					1-1.18				
1-xiv					1-1.19				
1-xv					1-1.20				
1-xvi					1-2.1				
1-1.1					1-2.2				
1-1.2					1-2.3				
1-1.3					1-2.4				
1-1.4					1-2.5				
1-1.5					1-2.6				
1-1.6					1-2.7				
1-1.7					1-2.8				
1-1.8					1-2.9				
1-1.9	0				1-2.10	0			
					1-2.11				

QEP-001.4-00

REVISION CONTROL SHEET
(Continuation)

TITLE: Duane Arnold Energy Center
Plant Unique Analysis Report
Volume 1

EFFECTIVE PAGE(S)	REV	PRE- PARED	ACCURACY CHECK	CRITERIA CHECK	EFFECTIVE PAGE(S)	REV	PRE- PARED	ACCURACY CHECK	CRITERIA CHECK
1-2.12	0	RAS	WJS	WJS	1-4.7	0	RAS	HA	HA
1-2.13					1-4.8				
1-2.14					1-4.9				
1-2.15					1-4.10				
1-2.16					1-4.11				
1-2.17					1-4.12				
1-2.18					1-4.13				
1-2.19					1-4.14				
1-2.20					1-4.15				
1-2.21					1-4.16				
1-2.22					1-4.17				
1-2.23					1-4.18				
1-2.24					1-4.19				
1-2.25					1-4.20				
1-2.26					1-4.21				
1-2.27					1-4.22				
1-2.28					1-4.23				
1-2.29					1-4.24				
1-2.30					1-4.25				
1-2.31					1-4.26				
1-3.1		RAS	HA	HA	1-4.27				
1-3.2					1-4.28				
1-3.3					1-4.29				
1-3.4					1-4.30				
1-3.5					1-4.31				
1-3.6					1-4.32				
1-3.7					1-4.33				
1-3.8					1-4.34				
1-3.9					1-4.35				
1-3.10					1-4.36				
1-3.11					1-4.37				
1-3.12		WJS	VK	VK	1-4.38				
1-3.13					1-4.39				
1-3.14					1-4.40				
1-3.15					1-4.41				
1-3.16		RAS	HA	HA	1-4.42				
1-4.1					1-4.43				
1-4.2					1-4.44				
1-4.3					1-4.45				
1-4.4					1-4.46				
1-4.5					1-4.47				
1-4.6	0				1-4.48	0			

00-4.100-979

QEP-001.4-0

IOW-40-199-1
Revision 0

1-iii

nutech
ENGINEERS

REVISION CONTROL SHEET
(Continuation)

TITLE: Duane Arnold Energy Center
Plant Unique Analysis Report
Volume 1

1-291-04-WOI
1-291-04-WOI
1-291-04-WOI

EFEC-TIVE PAGE (S)	REV	PRE-PARED	ACCURACY CHECK	CRITERIA CHECK	EFEC-TIVE PAGE (S)	REV	PRE-PARED	ACCURACY CHECK	CRITERIA CHECK
1-4.49	0	Ras	HA	HA	1-4.91	0	Ras	HA	HA
1-4.50					1-4.92				
1-4.51					1-4.93				
1-4.52					1-4.94				
1-4.53					1-4.95				
1-4.54					1-4.96		WJS	VK	VK
1-4.55					1-4.97		WJS	VK	VK
1-4.56					1-4.98		Ras	HA	HA
1-4.57					1-4.99				
1-4.58					1-4.100				
1-4.59					1-4.101				
1-4.60					1-4.102				
1-4.61					1-4.103				
1-4.62					1-4.104				
1-4.63					1-4.105				
1-4.64					1-4.106				
1-4.65					1-4.107				
1-4.66					1-4.108				
1-4.67					1-4.109				
1-4.68					1-4.110				
1-4.69					1-4.111				
1-4.70					1-4.112				
1-4.71					1-4.113				
1-4.72					1-4.114				
1-4.73					1-4.115				
1-4.74					1-4.116				
1-4.75					1-4.117				
1-4.76					1-5.1				
1-4.77					1-5.2				
1-4.78					1-5.3				
1-4.79					1-5.4				
1-4.80					1-5.5				
1-4.81					1-5.6				
1-4.82					1-5.7				
1-4.83					1-5.8				
1-4.84					1-5.9				
1-4.85					1-5.10				
1-4.86					1-5.11				
1-4.87					1-5.12				
1-4.88					1-6.1				
1-4.89					1-6.2	0			
1-4.90	0								

QEP-001.4-00

IOW-40-199-1
Revision 0

1-iv

1-291-04-WOI

nutech
ENGINEERS

ABSTRACT

The primary containment for the Duane Arnold Energy Center (DAEC) was designed, erected, pressure-tested, and ASME Code N-stamped during the early 1970's for the Iowa Electric Light and Power Company by the Chicago Bridge and Iron Company. Since that time new requirements have been generated. These requirements affect the design and operation of the primary containment system and are defined in the Nuclear Regulatory Commission's Safety Evaluation Report NUREG-0661. The requirements to be addressed include an assessment of additional containment design loads postulated to occur during a loss-of-coolant accident or a safety relief valve discharge event, as well as an assessment of the effects that these postulated events have on the operational characteristics of the containment system.

This plant unique analysis report documents the efforts undertaken to address and resolve each of the applicable NUREG-0661 requirements and demonstrates, in accordance with NUREG-0661 acceptance criteria, that the design of the primary containment system is adequate and that original design safety margins have been restored. The report is composed of the following six volumes and appendix.

- o Volume 1 - GENERAL CRITERIA AND LOADS METHODOLOGY
- o Volume 2 - SUPPRESSION CHAMBER ANALYSIS
- o Volume 3 - VENT SYSTEM ANALYSIS
- o Volume 4 - INTERNAL STRUCTURES ANALYSIS
- o Volume 5 - SAFETY RELIEF VALVE DISCHARGE LINE PIPING ANALYSIS
- o Volume 6 - TORUS ATTACHED PIPING AND SUPPRESSION CHAMBER PENETRATIONS ANALYSES
- o Appendix A - DAEC RESPONSES TO CURRENT CONTAINMENT AND PIPING LICENSING ISSUES

Volume 1 provides introductory and background information regarding the reevaluation of the suppression chamber design. This includes a description of the DAEC pressure suppression containment system, a description of the structural and mechanical acceptance criteria, and the hydrodynamic loads development methodology used in the analysis. This document has been prepared by NUTECH Engineers, Inc. (NUTECH), acting as an agent to the Iowa Electric Light and Power Company.

1.1-1

The volume number precedes each number assigned to pages, sections, subsections, tables, and figures within a given volume.

7.1-1

8.1-1

01.1-1

01.1-1

41.1-1

1.2-1

2.2-1

3.2-1

41.2-1

20.2-1

70.2-1

80.2-1

1.3-1

2.3-1

4.3-1

5.3-1

8.3-1

TABLE OF CONTENTS

ABSTRACT	1-v
LIST OF ACRONYMS	1-x
LIST OF TABLES	1-xii
LIST OF FIGURES	1-xiv
1-1.0 INTRODUCTION	1-1.1
1-1.1 Scope of Analysis	1-1.5
1-1.2 General Description of the Containment System	1-1.7
1-1.3 Review of Phenomena	1-1.9
1-1.3.1 LOCA-Related Phenomena	1-1.10
1-1.3.2 SRV Discharge Phenomena	1-1.12
1-1.4 Evaluation Philosophy	1-1.14
1-2.0 PLANT UNIQUE CHARACTERISTICS	1-2.1
1-2.1 Plant Configuration	1-2.2
1-2.1.1 Suppression Chamber	1-2.6
1-2.1.2 Vent System	1-2.14
1-2.1.3 Internal Structures	1-2.22
1-2.1.4 SRV Discharge Piping	1-2.27
1-2.2 Operating Parameters	1-2.29
1-3.0 PLANT UNIQUE ANALYSIS CRITERIA	1-3.1
1-3.1 Hydrodynamic Loads: NRC Acceptance Criteria	1-3.2
1-3.1.1 LOCA-Related Load Applications	1-3.4
1-3.1.2 SRV Discharge Load Applications	1-3.6
1-3.1.3 Other Considerations	1-3.8

TABLE OF CONTENTS

(Continued)

<u>Page</u>		<u>Page</u>
06.4-1	1-3.2 Component Analysis: Structural Acceptance Criteria	1-3.9
	1-3.2.1 Classification of Components	1-3.10
06.4-1	1-3.2.2 Service Level Assignments	1-3.11
	1-3.2.3 Other Considerations	1-3.16
07.4-1		
1-4.0	HYDRODYNAMIC LOADS DEVELOPMENT METHODOLOGY AND	
07.4-1	EVENT SEQUENCE SUMMARY	1-4.1
07.4-1	1-4.1 LOCA-Related Loads	1-4.3
10.4-1	1-4.1.1 Containment Pressure and Temperature Response	1-4.5
10.4-1	1-4.1.2 Vent System Discharge Loads	1-4.6
10.4-1	1-4.1.3 Pool Swell Loads on the Suppression Chamber Shell	1-4.8
001.4-1	1-4.1.4 Pool Swell Loads on Elevated Structures	1-4.10
001.4-1	1-4.1.4.1 Impact and Drag Loads on the Vent System	1-4.11
001.4-1	1-4.1.4.2 Impact and Drag Loads on Other Structures	1-4.15
001.4-1	1-4.1.4.3 Pool Swell Froth Impingement Loads	1-4.16
1.4-1	1-4.1.4.4 Pool Fallback Loads	1-4.22
00.4-1	1-4.1.5 LOCA Waterjet Loads on Submerged Structures	1-4.25
11.4-1	1-4.1.6 LOCA Bubble-Induced Loads on Submerged Structures	1-4.32
1.4-1	1-4.1.7 Condensation Oscillation Loads	1-4.36
	1-4.1.7.1 CO Loads on the Suppression Chamber Shell	1-4.37
	1-4.1.7.2 CO Loads on the Downcomers and Vent System	1-4.48
	1-4.1.7.3 CO Loads on Submerged Structures	1-4.56

TABLE OF CONTENTS

(Concluded)

	<u>Page</u>
1-4.1.8 Chugging Loads	1-4.60
1-4.1.8.1 Chugging Loads on the Suppression Chamber Shell	1-4.62
1-4.1.8.2 Chugging Downcomer Lateral Loads	1-4.70
1-4.1.8.3 Chugging Loads on Submerged Structures	1-4.72
1-4.2 Safety Relief Valve Discharge Loads	1-4.76
1-4.2.1 SRV Actuation Cases	1-4.81
1-4.2.2 SRV Discharge Line Clearing Loads	1-4.87
1-4.2.3 SRV Loads on the Suppression Chamber Shell	1-4.92
1-4.2.4 SRV Loads on Submerged Structures	1-4.100
1-4.3 Event Sequence	1-4.105
1-4.3.1 Design Basis Accident	1-4.108
1-4.3.2 Intermediate Break Accident	1-4.114
1-4.3.3 Small Break Accident	1-4.116
1-5.0 SUPPRESSION POOL TEMPERATURE MONITORING SYSTEM	1-5.1
1-5.1 Suppression Pool Temperature Response to SRV Transients	1-5.2
1-5.2 Suppression Pool Temperature Monitoring System Design	1-5.11
1-6.0 LIST OF REFERENCES	1-6.1

LIST OF ACRONYMS

ADS	Automatic Depressurization System
ASME	American Society of Mechanical Engineers
BDC	Bottom Dead Center
BWR	Boiling Water Reactor
CDF	Cumulative Distribution Function
CO	Condensation Oscillation
DAEC	Duane Arnold Energy Center
DBA	Design Basis Accident
DC/VH	Downcomer/Vent Header
FSAR	Final Safety Analysis Report
FSI	Fluid-Structure Interaction
FSTF	Full-Scale Test Facility
HPCI	High Pressure Coolant Injection
IBA	Intermediate Break Accident
ID	Inside Diameter
I&C	Instrumentation & Control
IR	Inside Radius
LDR	Load Definition Report (Mark I Containment Program)
LOCA	Loss-of-Coolant Accident
LTP	Long-Term Program
MCF	Modal Correction Factors
NEP	Non-Exceedance Probability
NOC	Normal Operating Conditions
NPS	Nominal Pipe Size

LIST OF ACRONYMS

(Concluded)

NRC	Nuclear Regulatory Commission	100	200
NSSS	Nuclear Steam Supply System	100	200
OBE	Operating Basis Earthquake	100	200
OD	Outside Diameter	100	200
PUAAG	Plant Unique Analysis Application Guide	100	200
PUA	Plant Unique Analysis	100	200
PUAR	Plant Unique Analysis Report	100	200
PULD	Plant Unique Load Definition	100	200
QSTF	Quarter-Scale Test Facility	100	200
RCIC	Reactor Core Isolation Cooling	100	200
RHRS	Residual Heat Removal System	100	200
RPV	Reactor Pressure Vessel	100	200
RSEL	Resultant-Static-Equivalent Load	100	200
SBA	Small Break Accident	100	200
SORV	Stuck-Open Safety Relief Valve	100	200
SPTMS	Suppression Pool Temperature Monitoring System	100	200
SRSS	Square Root of the Sum of the Squares	100	200
SRV	Safety Relief Valve	100	200
SRVDL	Safety Relief Valve Discharge Line	100	200
SSE	Safe Shutdown Earthquake	100	200
STP	Short-Term Program	100	200

LIST OF TABLES

<u>Number</u>	<u>Title</u>	<u>Page</u>
1-1.0-1	DAEC Containment Modification Status	1-1.4
1-2.2-1	Suppression Chamber Operating Parameters	1-2.30
1-3.2-1	Event Combinations and Service Levels for Class MC Components and Internal Structures	1-3.12
1-3.2-2	Event Combinations and Service Levels for Class 2 and 3 Piping	1-3.14
1-4.0-1	Plant Unique Analysis/NUREG-0661 Load Sections Cross-Reference	1-4.2
1-4.1-1	Hydrodynamic Mass and Acceleration Drag Volumes for Two-Dimensional Structural Components (Length L For All Structures)	1-4.29
1-4.1-2	Plant Unique Parameters for LOCA Bubble Drag Load Development	1-4.34
1-4.1-3	DBA Condensation Oscillation Torus Shell Pressure Amplitudes	1-4.41
1-4.1-4	FSTF Response to Condensation Oscillation	1-4.43
1-4.1-5	Condensation Oscillation Onset and Duration	1-4.44
1-4.1-6	Downcomer Internal Pressure Loads for DBA Condensation Oscillation	1-4.51
1-4.1-7	Downcomer Internal Pressure Loads For IBA Condensation Oscillation	1-4.52
1-4.1-8	Condensation Oscillation Loads on the Vent System	1-4.53
1-4.1-9	Amplitudes at Various Frequencies for Condensation Oscillation Source Function for Loads on Submerged Structures	1-4.59
1-4.1-10	Chugging Onset and Duration	1-4.65
1-4.1-11	Post-Chug Rigid Wall Pressure Amplitudes on Torus Shell Bottom Dead Center	1-4.66

LIST OF TABLES
(Concluded)

<u>Number</u>	<u>Title</u>	<u>Page</u>
1-4.1-12	Amplitudes at Various Frequencies for Chugging Source Function for Loads on Submerged Structures	1-4.74
1-4.2-1	SRV Load Case/Initial Conditions	1-4.86
1-4.2-2	Plant Unique Initial Conditions for Actuation Cases Used for SRVDL Clearing Transient Load Development	1-4.90
1-4.2-3	SRVDL Analysis Parameters	1-4.91
1-4.2-4	Comparison of Analysis and Monticello Test Results	1-4.96
1-4.2-5	Comparison of Analysis and DAEC Test Results	1-4.97
1-4.3-1	SRV and LOCA Structural Loads	1-4.107
1-4.3-2	Event Timing Nomenclature	1-4.109
1-4.3-3	SRV Discharge Load Cases for Mark I Structural Analysis	1-4.110
1-5.1-1	Summary of DAEC Pool Temperature Response to SRV Transients	1-5.6
1-5.1-2	Summary of DAEC Pool Temperature Response to Additional SRV Transients	1-5.9

LIST OF FIGURES

<u>Number</u>	<u>Title</u>	<u>Page</u>
1-2.1-1	Elevation View of Containment	1-2.4
1-2.1-2	Plan View of Containment	1-2.5
1-2.1-3	Suppression Chamber Section - Mid-Vent Line Bay	1-2.9
1-2.1-4	Suppression Chamber Section - Miter Joint	1-2.10
1-2.1-5	T-quencher and Support Locations	1-2.11
1-2.1-6	T-quencher and T-quencher Supports - Plan View and Elevation	1-2.12
1-2.1-7	SRV Elbow Support Beam	1-2.13
1-2.1-8	Vent Header Plan View	1-2.16
1-2.1-9	Vent-Line-to-Vent-Header Intersection	1-2.17
1-2.1-10	Developed View of Vent Header and Vent Deflector System	1-2.18
1-2.1-11	Downcomer-to-Vent-Header Intersection	1-2.19
1-2.1-12	Vacuum Breaker Penetration - Plan View	1-2.20
1-2.1-13	SRV Penetration in Vent Line	1-2.21
1-2.1-14	Catwalk Frame	1-2.23
1-2.1-15	Catwalk Support at Ring Beam	1-2.24
1-2.1-16	Catwalk Support in the Non-Vent Bay	1-2.25
1-2.1-17	Monorail Supports	1-2.26
1-2.1-18	SRV Pipe Routing in Suppression Chamber - Plan View	1-2.28
1-4.1-1	Pulse Shape for Water Impact on Cylindrical Targets	1-4.13
1-4.1-2	Pulse Shape for Water Impact on Flat Targets	1-4.14
1-4.1-3	Froth Impingement Zone - Region I	1-4.20

LIST OF FIGURES
(Continued)

<u>Number</u>	<u>Title</u>	<u>Page</u>
1-4.1-4	Froth Impingement Zone - Region II	1-4.21
1-4.1-5	Quarter-Scale Downcomer Water Slug Ejection, Test 8	1-4.31
1-4.1-6	Quarter-Scale Drywell Pressure Time-History	1-4.35
1-4.1-7	Condensation Oscillation Baseline Rigid Wall Pressure Amplitudes on Torus Shell Bottom Dead Center	1-4.45
1-4.1-8	Mark I Condensation Oscillation - Torus Vertical Cross-Sectional Distribution for Pressure Oscillation Amplitude	1-4.46
1-4.1-9	Mark I Condensation Oscillation - Multiplier Factor to Account for the Effect of the Pool-to-Vent Area Ratio	1-4.47
1-4.1-10	Downcomer Internal Pressure Loading for DBA CO	1-4.54
1-4.1-11	Downcomer Internal Pressure Loading for IBA CO	1-4.55
1-4.1-12	Typical Chug Cycle Average Pressure Trace on the Torus Shell	1-4.61
1-4.1-13	Mark I Chugging - Torus Asymmetric Longitudinal Distribution for Pressure Amplitude	1-4.67
1-4.1-14	Mark I Chugging - Torus Vertical Cross-Sectional Distribution for Pressure Amplitude	1-4.68
1-4.1-15	Post-Chug Rigid Wall Pressure Amplitudes on Torus Shell Bottom Dead Center	1-4.69
1-4.2-1	T-quencher Arm Hole Pattern - Elevation Views	1-4.78
1-4.2-2	T-quencher Arm Hole Pattern - Section Views	1-4.79
1-4.2-3	T-quencher and SRV Line	1-4.80

LIST OF FIGURES
(Concluded)

<u>Number</u>	<u>Title</u>	<u>Page</u>
1-4.2-4	Comparison of Predicted and Measured Shell Pressure Time-Histories for Monticello Test 801	1-4.98
1-4.2-5	Modal Correction Factors for Analysis of SRV Discharge Torus Shell Loads	1-4.99
1-4.3-1	Loading Condition Combinations for the Vent Header, Main Vents, Downcomers, and Torus Shell During a DBA	1-4.111
1-4.3-2	Loading Condition Combinations for Submerged Structures During a DBA	1-4.112
1-4.3-3	Loading Condition Combinations for Small Structures Above Suppression Pool During a DBA	1-4.113
1-4.3-4	Loading Condition Combinations for the Vent Header, Main Vents, Downcomers, Torus Shell, and Submerged Structures During an IBA	1-4.115
1-4.3-5	Loading Condition Combinations for the Vent Header, Main Vents, Downcomers, Torus Shell, and Submerged Structures During a SBA	1-4.117
1-5.1-1	Local Pool Temperature Limit for Duane Arnold Energy Center	1-5.10

The primary containment for the Duane Arnold Energy Center was designed, erected, leak-tested and N-stamped in accordance with the ASME Boiler and Pressure Vessel Code during the early 1970's. Subsequently, while in the course of performing large-scale testing for the Mark III containment system and in-plant testing for the Mark I containment system, new suppression chamber hydrodynamic loads were identified. The new loads are related to the postulated loss-of-coolant accident (LOCA) and safety relief valve (SRV) operation.

The identification of these new loads presented an open item for all utilities with Mark I containments. To determine the magnitude, time characteristics, etc., of the dynamic loads in a timely manner and to identify courses of action needed to resolve any outstanding concerns, the utilities with Mark I containments formed the Mark I Owners Group. The Mark I Owners Group established a program which consisted of two parts: 1) a Short-Term Program (STP) which was completed in 1976, and 2) a Long-Term Program (LTP) which was completed with the submittal

DESIGN OF
MARK I
CONTAINMENT
PROGRAM

STRUCTURAL
ANALYSIS
APPLICATION
GUIDE

of the Mark I Containment Program Load Definition Report (LDR) (Reference 1), the Mark I Containment Program Structural Acceptance Criteria Plant Unique Analysis Application Guide (PUAAG) (Reference 2) and supporting reports on experimental and analytical tasks of the Long-Term Program. The NRC reviewed these LTP generic documents and issued acceptance criteria to be used during the implementation of the Mark I plant unique analyses. The NRC acceptance criteria are described in Appendix A of NUREG-0661 (Reference 3).

The objective of the LTP was to establish final design loads and load combinations to verify that existing or modified containment and related structures are capable of withstanding these loads with acceptable design margins. To meet the objectives of the LTP, Iowa Electric Light and Power Company implemented a containment study program that provided analysis, design, and modification, if required, in a timely manner. Table 1-1.0-1 shows the containment modification status.

This PUAR documents the results of the evaluation of the Duane Arnold Energy Center suppression chamber,

vent system, safety relief valve discharge lines, suppression chamber internal structures, torus attached piping, and suppression chamber penetrations which was performed in accordance with the requirements of NUREG-0661.

Accordingly, with the submittal of this PUAR, Iowa Electric Light and Power Company has addressed the requirements of NUREG-0661 for the Duane Arnold Energy Center.

Table 1-1.0-1

DAEC CONTAINMENT MODIFICATION STATUS

523 87000

DESCRIPTION		APPROXIMATE MODIFICATION DATES
SUPPRESSION CHAMBER	COLUMN HOLD-DOWN BRACKETS	1976
	REINFORCEMENT (SADDLES)	12/80
	RING BEAM DRAIN HOLE ENLARGEMENT	4/80
	RING BEAM STIFFENERS	3/83
	ADDITIONAL SADDLE BRACKETS & ANCHOR BOLTS	3/83
VENT SYSTEM	DRYWELL-TO-WETWELL ΔP	1976
	DOWNCOMER SHORTENING	4/80
	VENT HEADER DEFLECTORS	3/81
	VENT LINE SRV PENETRATIONS	3/83
INTERNAL STRUCTURES	CATWALK SUPPORT COLUMNS	3/81
	CATWALK BRACING AND HANGERS	3/83
	ELECTRICAL CONDUIT AND NITROGEN LINE SUPPORTS (ON CATWALK)	3/83
	SPRAY HEADER BRACKETS	3/81 & 3/83
SRVDL PIPING	ADJUSTMENT OF SRV SET POINTS	1978
	T-QUENCHERS AND T-QUENCHER SUPPORTS	4/80 & 3/83
	SRVDL SUPPORTS FOR LINES 6,9,10 AND 11	3/81 & 3/83
	SRVDL SUPPORTS FOR LINES 7 AND 8	3/83
	ELBOW SUPPORT BEAMS	3/83
	MAIN STEAM SNUBBERS	3/83
	DRYWELL FLOOR STEEL	3/81 & 3/83

The following structural and mechanical elements are addressed in the various volumes of this report.

o Suppression Chamber (Torus)

- The suppression chamber shell with associated penetrations, reinforcing rings and support attachments
- The suppression chamber supports
- The vent lines between the drywell and the vent header, including SRV penetrations
- The local region of the drywell at the vent line penetration
- The bellows between the vent lines and the suppression chamber shell
- The vent header and downcomers
- The vent header supports
- The vent header deflectors and their supports
- The vacuum breaker nozzle penetrations to the vent header
- The suction strainers

o Internal Structures

- The internal structural elements (including the monorail and the catwalk) and their supports

- Suppression chamber thermowells

- The spray headers and support bracketry

- The electrical conduit and nitrogen lines for the vacuum breakers

o The safety relief valve (SRV) discharge piping and supports

o Torus attached piping

o Suppression chamber penetrations

o Miscellaneous

- The instrumentation and control (I&C) conduit and tubing inside or attached to the suppression chamber

- The Suppression Pool Temperature Monitoring System (SPTMS)

The Mark I containment is a pressure suppression system which houses the Boiling Water Reactor (BWR) pressure vessel, the reactor coolant recirculating loops, and other branch connections of the Nuclear Steam Supply System (NSSS). The containment consists of a drywell, a suppression chamber (wetwell or torus) which is approximately half-filled with water, and a vent system which connects the drywell to the wetwell suppression pool. The suppression chamber is toroidal in shape and is located below the drywell, encircling it. The drywell-to-wetwell vents are connected to a vent header contained within the airspace of the wetwell. Downcomers project downward from the vent header and terminate below the water surface of the suppression pool. The suppression chamber is described in greater detail in Sections 1-2.1.1 through 1-2.1.3 and in Volumes 2 through 4.

BWR's utilize safety relief valves (SRV's) attached to the main steam lines as a means of primary system overpressure protection. The outlet of each valve is connected to discharge piping which is routed to the suppression pool. The discharge lines end in

T-quencher discharge devices. The SRV discharge lines are described in greater detail in Section 1-2.1.4 and in Volume 5.

exhaust

discharge

SRV discharge

hydrogen

discharge

discharge

discharge

discharge

The following subsections provide a brief qualitative description of the various phenomena that could occur during the course of a postulated LOCA and during SRV actuations. A detailed description of the hydrodynamic loads which these phenomena could impose upon the suppression chamber and related structures is given in the LDR (Reference 1). Section 1-4.0 presents the load definition procedures used to develop the DAEC hydrodynamic loads.

Immediately following a postulated design basis accident (DBA), the pressure and temperature of the drywell and vent system atmosphere rapidly increase. As a result of the drywell pressure increase, the water initially present in the downcomers is forced into the suppression pool until the downcomers clear of water. Following downcomer water clearing, the downcomer air, which is essentially at drywell pressure, is exposed to the relatively low pressure in the wetwell, producing a downward reaction force on the suppression chamber. The consequent bubble expansion causes the pool water to swell in the suppression chamber (pool swell), compressing the airspace above the pool. This airspace compression results in an upward reaction force on the suppression chamber. Eventually, the bubbles "break through" to the suppression chamber airspace, equalizing the pressures. An air/water froth mixture continues upward as a result of the momentum previously imparted to the water slug, causing impingement loads on elevated structures. The transient loads associated with this rapid drywell air venting to the pool typically last for three to five seconds.

Following air carryover, there is an intense flow of steam through the vent system. The discharge of steam into the pool and the subsequent condensation cause pool pressure oscillations which are transmitted to submerged structures and the suppression chamber shell. This phenomenon is referred to as condensation oscillation (CO). As the reactor vessel depressurizes, the rate of steam flow to the vent system decreases. Steam condensation during this period of reduced steam flow is characterized by movement of the water/steam interface up and down within the downcomer as the steam volumes are condensed and replaced by surrounding pool water. This phenomenon is referred to as chugging.

Postulated intermediate break accidents (IBA) and small break accidents (SBA) produce drywell pressure transients slow enough that the dynamic effects of vent clearing and pool swell are negligible. CO and chugging occur for an IBA, however, and chugging occurs for an SBA.

1-1.3.2 SRV Discharge Phenomena

DAEC is equipped with six SRV's to control primary system pressure transients. The SRV's are mounted on the main steam lines inside the drywell with discharge pipes routed down the main vents into the suppression pool. When an SRV is actuated, steam released from the primary system is discharged into the suppression pool, where it condenses.

Prior to the initial actuation of an SRV, the safety relief valve discharge lines (SRVDL's) contain air at atmospheric pressure and suppression pool water in the submerged portion of the piping. Following SRV actuation, steam enters the SRVDL, compressing the air within the line and expelling the water slug into the suppression pool. During water clearing, the SRVDL undergoes a transient pressure loading.

Once the water has been cleared from the T-quencher discharge device, the compressed air enters the pool in the form of high-pressure bubbles. These bubbles expand, resulting in an outward acceleration of the surrounding pool water. The momentum of the accelerated water results in an overexpansion of the

bubbles, causing the bubble pressure to become negative relative to the ambient pressure of the surrounding pool. This negative bubble pressure slows and reverses the motion of the water, leading to a compression of the bubbles and a positive pressure relative to that of the pool. The bubbles continue to oscillate in this manner as they rise to the pool surface. The positive and negative pressures developed as a result of this phenomenon attenuate with distance and result in an oscillatory pressure loading on the submerged portion of the suppression chamber shell and internal structures.

The development of event sequences, assumptions, load definitions, analysis techniques, and all other facets composing the DAEC plant unique analysis are specifically formulated to provide a conservative evaluation. This section describes, in qualitative terms, some of the conservative elements inherent in the DAEC plant unique analysis.

Event Sequences and Assumptions

Implicit in the analysis of loss-of-coolant accidents is the assumption that the event will occur, although the probability of such pipe breaks is low. No credit is taken for detection of leaks to prevent LOCA's. Furthermore, various sizes of pipe breaks are evaluated to consider various effects. The large, instantaneous pipe breaks are considered in evaluating the initial, rapidly occurring events, such as vent system pressurization and pool swell. Smaller pipe breaks are analyzed to maximize prolonged effects, such as condensation oscillation and chugging.

The various LOCA's analyzed are assumed to occur during plant conditions of maximum interest. For example, the reactor is assumed to be at 102% of rated power; a single failure is assumed; no credit is taken for normal auxiliary power. Operator actions which can mitigate the effects of a LOCA are assumed to be unavailable for a specified period. Other assumptions are also selected to maximize the parameter to be evaluated. This approach results in a conservative evaluation, as the plant conditions are not likely to be in this worst-case situation if a LOCA were to occur.

Test Results and Load Definitions

The load definitions utilized in the DAEC PUA are based on conservative test results and analyses. For example, the LOCA steam condensation loads (condensation oscillation and chugging) are based on tests in the Mark I Full-Scale Test Facility (FSTF). The FSTF is a full-size 1/16 segment of a Mark I suppression chamber. To ensure that appropriately conservative results would be obtained, the FSTF was specifically designed and constructed to promote rapid air and steam flow from the drywell to the

wetwell. While this maximizes hydrodynamic loads, it does not take into account the plant features which would mitigate the effects of the LOCA. Actual Mark I drywells have piping and equipment in the drywell which would absorb some of the energy released during a LOCA. There are other features of the FSTF which are not typical of actual plant configurations, but which contribute to more conservative load definitions. Pre-heating of the drywell to minimize condensation and heat losses is an example of a non-prototypical feature. Additionally, the load definitions developed from FSTF data apply the maximum observed load over the entire period during which the load may occur. This conservative treatment takes no credit for the load variation observed in the tests.

LOCA pool swell loads were developed from similarly conservative tests at the Quarter-Scale Test Facility (QSTF). These tests were performed with the driving medium consisting of 100% noncondensibles. This maximizes the pool swell because this phenomenon would be driven by condensible steam if a LOCA were to occur in an actual plant. The QSTF tests also minimized the loss coefficient and maximized the

drywell pressurization rate, thus maximizing the pool swell loads. The drywell pressurization rate used in the tests was calculated using conservative analytical modeling and initial conditions. Structures above the pool are assumed to be rigid when analyzed for pool swell impact loads. This assumption maximizes loads and is also used to evaluate loads on submerged structures.

The methods used to develop safety relief valve (SRV) loads are based on conservative assumptions, modeling techniques, and full and subscale test data. SRV loads are calculated assuming a minimum SRV opening time, a maximum steam flow rate, and a maximum steam line pressure, all of which maximize the SRV loads. Appropriate assumptions are also applied to conservatively predict SRV load frequency ranges. SRV loads on submerged structures are similarly determined with the additional assumptions that maximize the pressure differential across the structure due to bubble pressure phasing. The conservatism in the SRV load definition approach has been demonstrated by in-plant tests performed at DAEC (Reference 4) and at several other plants. All such tests have confirmed that actual plant responses are significantly less than predicted.

Load Combinations

Conservative assumptions have also been made in developing the combinations of loading phenomena to be evaluated. Many combinations of loading phenomena are investigated, even though it is very unlikely for such combinations of phenomena to occur. For example, mechanistic analysis has shown that an SRV cannot actuate during the pool swell phase of a design basis LOCA. However, that combination of loading phenomena is evaluated. Both the pool swell and SRV load phenomena involve pressurized air bubbles in the pool, and the structural response to these two different bubbles is assumed to be additive. This is a very conservative assumption; however, since two bubbles in a pool cannot physically combine to form one bubble at a pressure higher than either separate bubble. This rationale is also valid for other hydrodynamic phenomena in the pool, such as chugging, which is also combined with SRV discharge.

When evaluating the structural response to combinations of loading phenomena, the peak responses due to the various loading phenomena are assumed to occur at

the same time. While this is not an impossible occurrence, the probability is very remote that the actual responses will combine in that fashion. Furthermore, the initiating events themselves (e.g., LOCA or earthquake) are of extremely low probability.

Analysis Techniques

The methods used for analyzing LOCA and SRV loads also contribute to conservatism. In the analyses, these loads are assumed to be smooth curves of regular or periodic shape. This simplifies load definitions and analyses but maximizes predicted responses. Data from full-scale tests show actual forcing functions to be much less "pure" or "perfect" than those assumed for analyses.

The analyses generally treat a nonlinear problem as a linear, elastic problem with the load "tuned" to the structural frequencies which produce maximum response. The nonlinearities which exist in both the pool and structural dynamics would preclude the attainment of the elastic transient and steady-state responses that are predicted mathematically.

Inherent in the structural analyses are additional conservatisms. Damping is assumed to be low to maximize response, but it is likely to be much higher in reality. Likewise, allowable stress levels are low compared to the expected material capabilities. Conservative boundary conditions are also used in the analyses.

Conclusion

The loads, methods, and results described above and elsewhere in this report demonstrate that the margins of safety which actually existed for the original design loads have been restored. The advancements in understanding the hydrodynamic phenomena and in the structural analyses and modeling techniques have substantially increased since the original design and analysis were completed. This increased understanding and analysis capability is applied to the original loads as well as to the newly defined loads. Thus, the original safety margins have been restored.

This section describes the general plant unique geometric and operating parameters pertinent to the reevaluation of the suppression chamber design. Specific details are provided in subsequent volumes, in which the analyses of individual components are described.

The containment vessel is a Mark I design with a drywell and toroidal suppression chamber (Figures 1-2.1-1 and 1-2.1-2). The structural components affected by the LOCA and SRV discharge loads include the suppression chamber and its supports, the vent system and its supports, and the intersection of the vent lines to the drywell. Other items connected to the suppression chamber, such as the electrical conduit, piping, thermowells, catwalk, monorail, and the horizontal seismic supports, are also included in this plant unique analysis.

The suppression chamber is in the general form of a torus, although it is actually constructed of 16 mitered cyclindrical shell segments (Figure 1-2.1-2). A reinforcing ring with two supporting columns and a saddle is provided at each miter joint.

The suppression chamber is connected to the drywell by eight vent lines. Within the suppression chamber, the vent lines are connected to a common vent header. Also connected to the vent header are downcomers which terminate below the water level of

the suppression pool. A bellows assembly connecting the suppression chamber to the vent line allows for differential movement between the drywell and the suppression chamber.

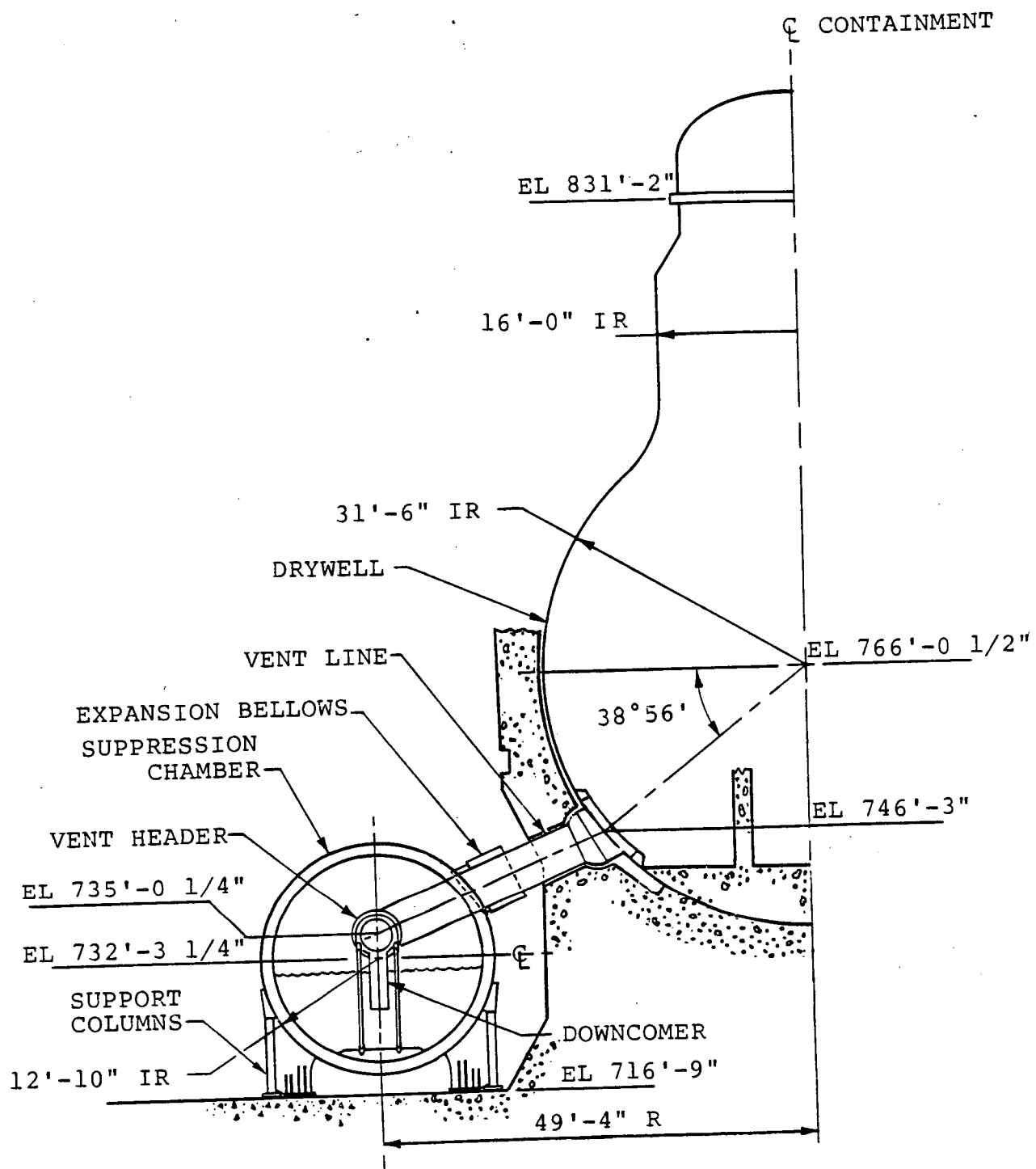


Figure 1-2.1-1

ELEVATION VIEW OF CONTAINMENT

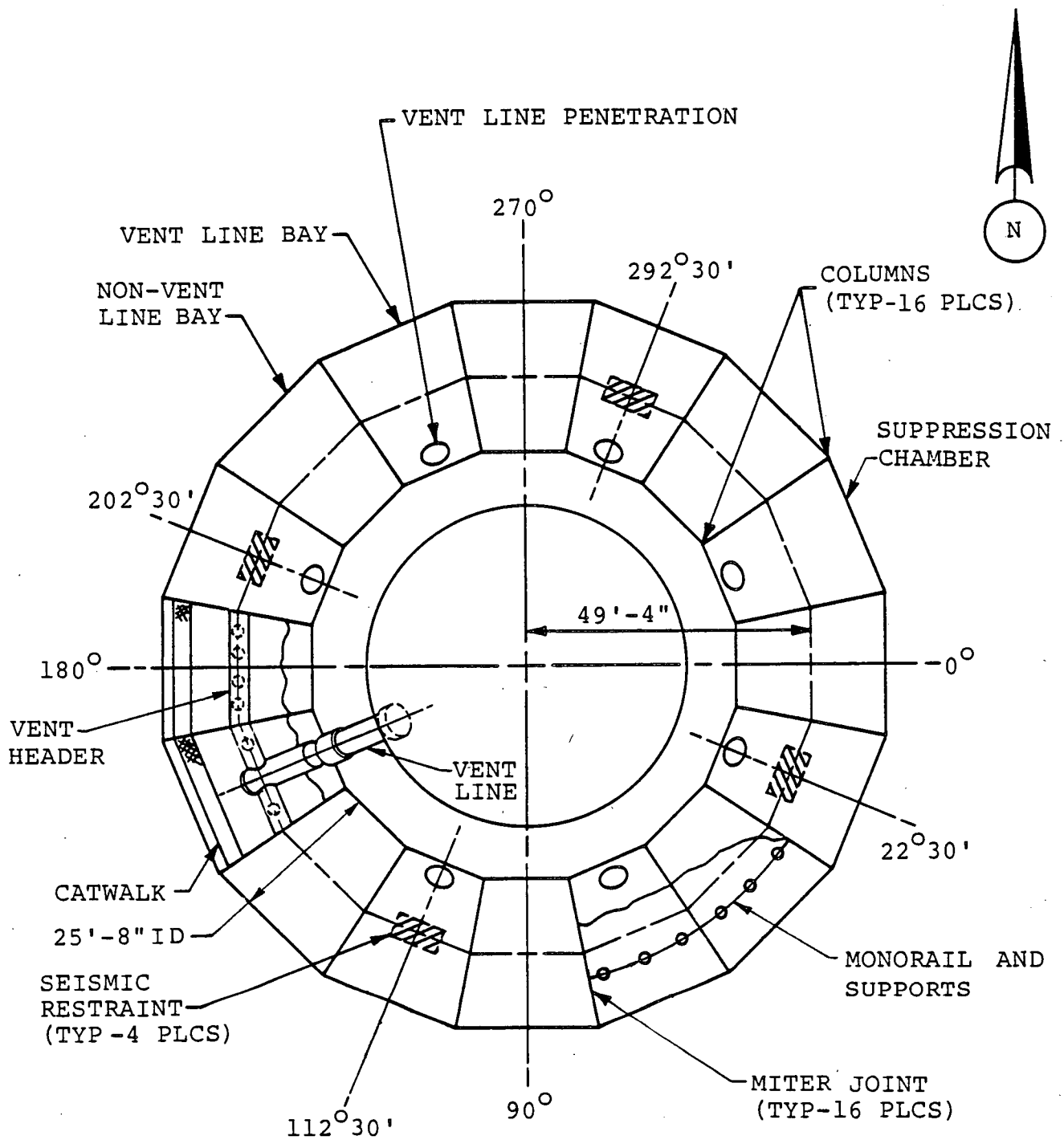


Figure 1-2.1-2

PLAN VIEW OF CONTAINMENT

IOW-40-199-1
Revision 0

1-2.5

1-2.1.1 Suppression Chamber

The inside radius of the mitered cylinders which make up the suppression chamber is 12'10" (Figure 1-2.1-3). The suppression chamber shell thickness is typically 0.500" above the horizontal centerline and 0.534" below the horizontal centerline except at penetration locations, where it is locally thicker.

The suppression chamber shell is reinforced at each miter joint location by a T-shaped ring beam (Figure 1-2.1-4). A typical ring beam is located in a plane parallel to and on the non-vent line bay side of each miter joint. The ring beam is braced laterally with stiffeners connecting the ring beam web to the suppression chamber shell.

The suppression chamber is supported vertically at each miter joint location by inside and outside columns and by local saddle supports (Figure 1-2.1-4). The columns, the associated column connection plates, and the saddle support are located parallel to the miter joint in the plane of the ring beam web.

The column members are constructed from rolled sections with cover plates. The column connections to the suppression chamber shell consist of web plates, flange plates, cover plates, and stiffener plates.

The anchorage of the suppression chamber to the basemat is achieved by a system of base plates, stiffeners, and anchor bolts located at each column and saddle support. Anchor bolts are provided in groups of 6 and 10 for outside saddles and in groups of 6 and 8 for inside saddles. In addition to the two internal column anchor bolts, two more outboard anchor bolts are provided for 12 of the outside columns where SRV discharge loads are applied. The total number of anchor bolts at each miter joint varies from 16 to 24. These bolts provide the principal mechanism for transfer of uplift loads to the basemat.

The DAEC safety relief valve system includes piping which terminates at T-quencher discharge devices in the suppression chamber (Figures 1-2.1-5 and 1-2.1-6). Six SRV discharge line pipes enter the suppression chamber through the vent lines and extend

downward through the vent line shell to a location below the water level where the pipes attach to a T-quencher device.

Each T-quencher device consists of two perforated arms attached to a central ramshead, with 768 holes along one arm and 782 holes along the other arm, both in a graduated hole pattern.

Each T-quencher device is supported by a support beam that spans between the ring beams (Figure 1-2.1-6). The support beam is a 16", Schedule 160 pipe section with field-welded end connections that are reinforced in the ring beam web plate. The device is installed with the arms oriented parallel to the circumferential centerline of the suppression chamber shell bay.

Each of the SRV discharge lines is supported at the elbow by a support beam that spans between the ring beams. This elbow support beam is a built-up box section (Figure 1-2.1-7).

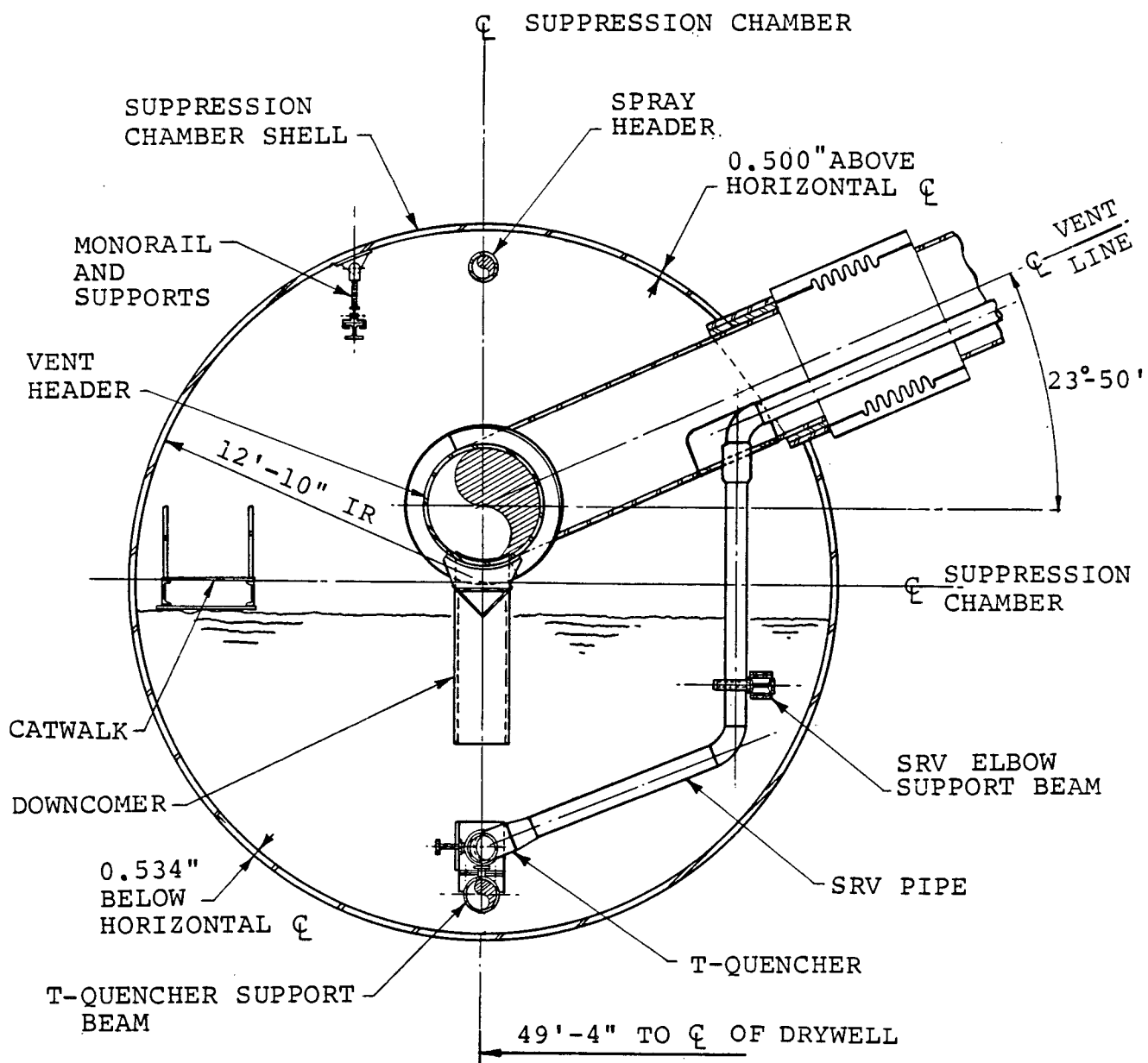
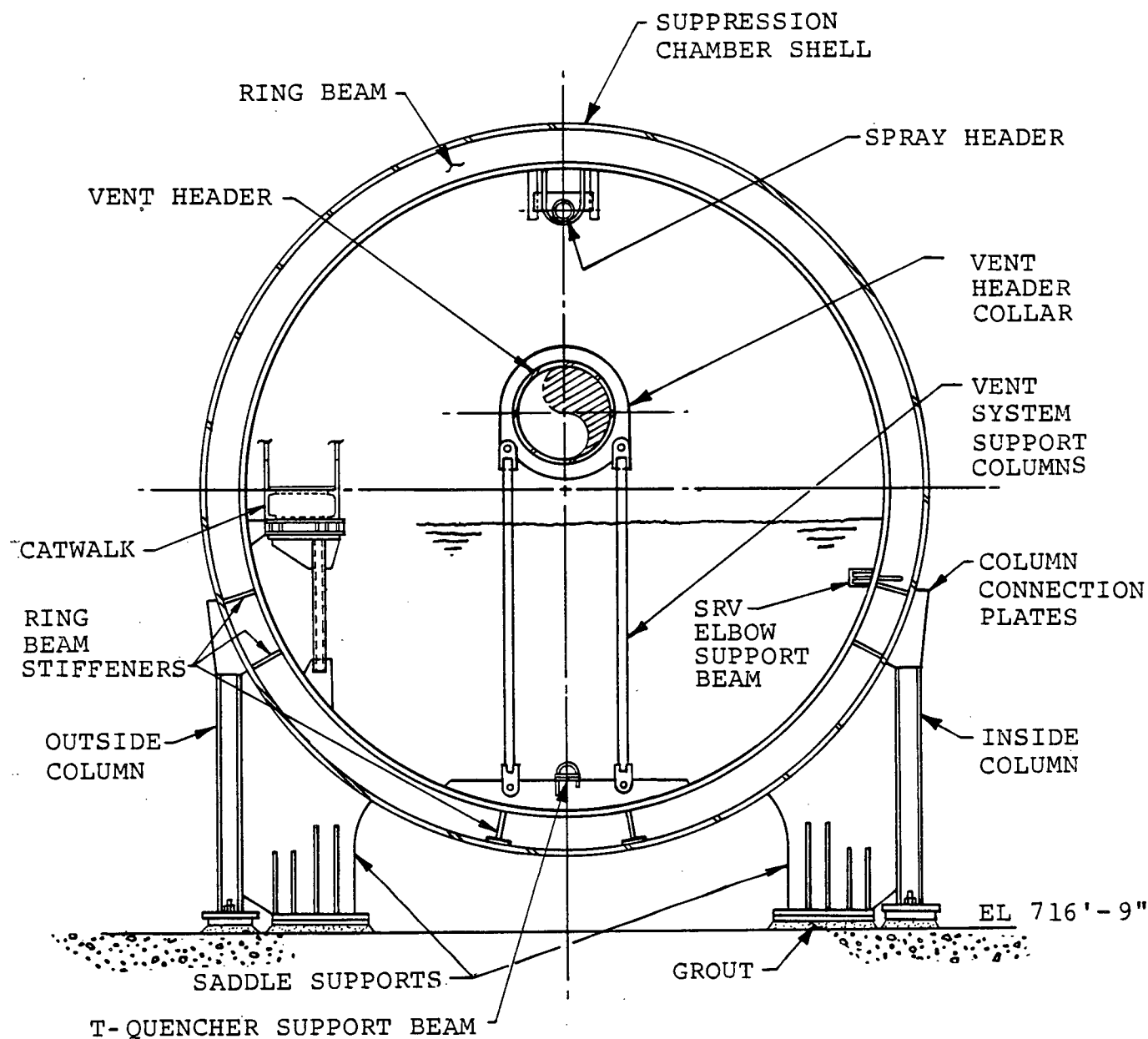


Figure 1-2.1-3

SUPPRESSION CHAMBER SECTION-
MID-VENT LINE BAY

IOW-40-199-1
Revision 0

1-2.9



1. ADDITIONAL TORUS ANCHORAGE NOT SHOWN FOR CLARITY.

Figure 1-2.1-4
SUPPRESSION CHAMBER SECTION -
MITER JOINT

IOW-40-199-1
 Revision 0

1-2.10

nutech
 ENGINEERS

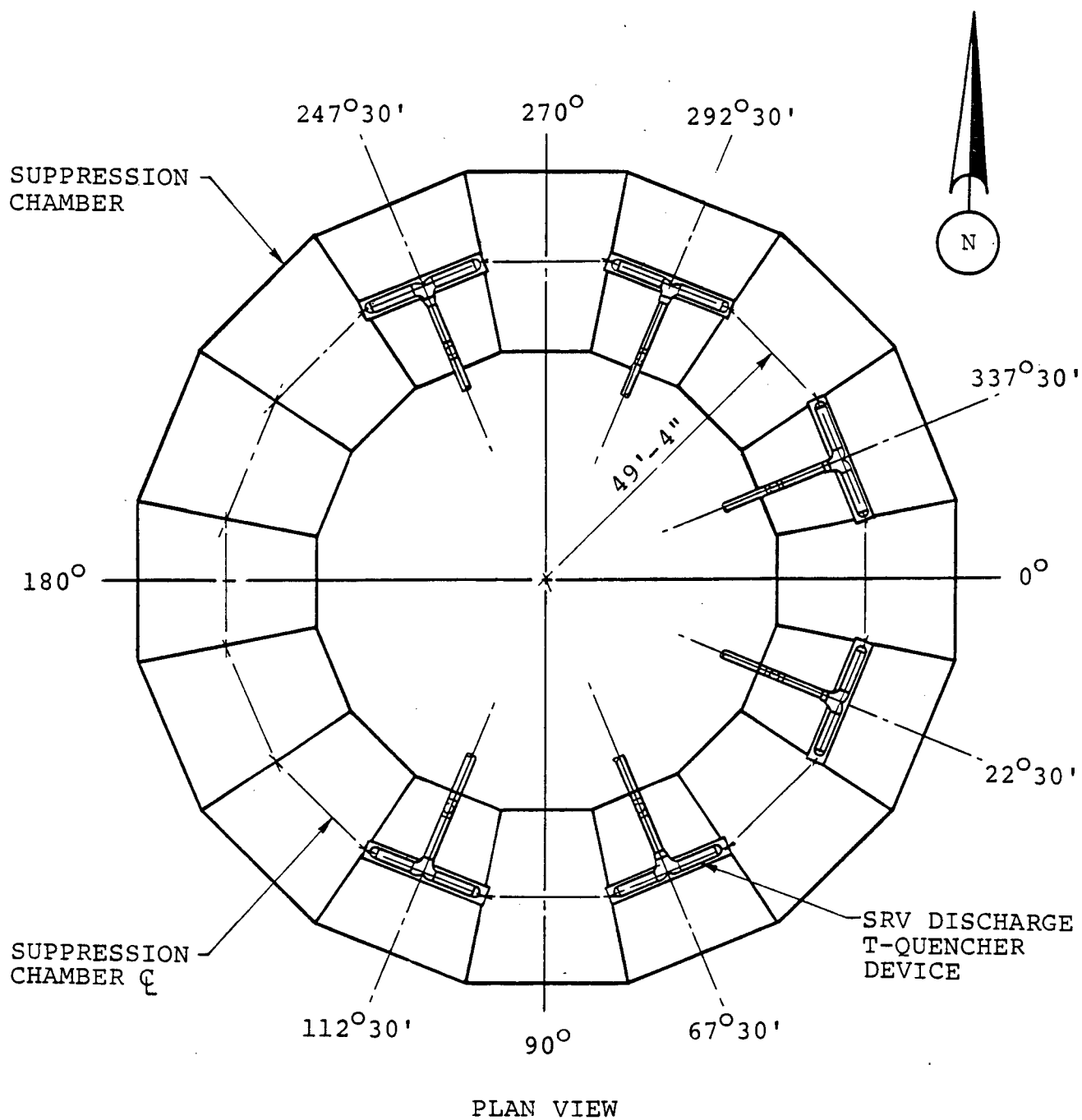
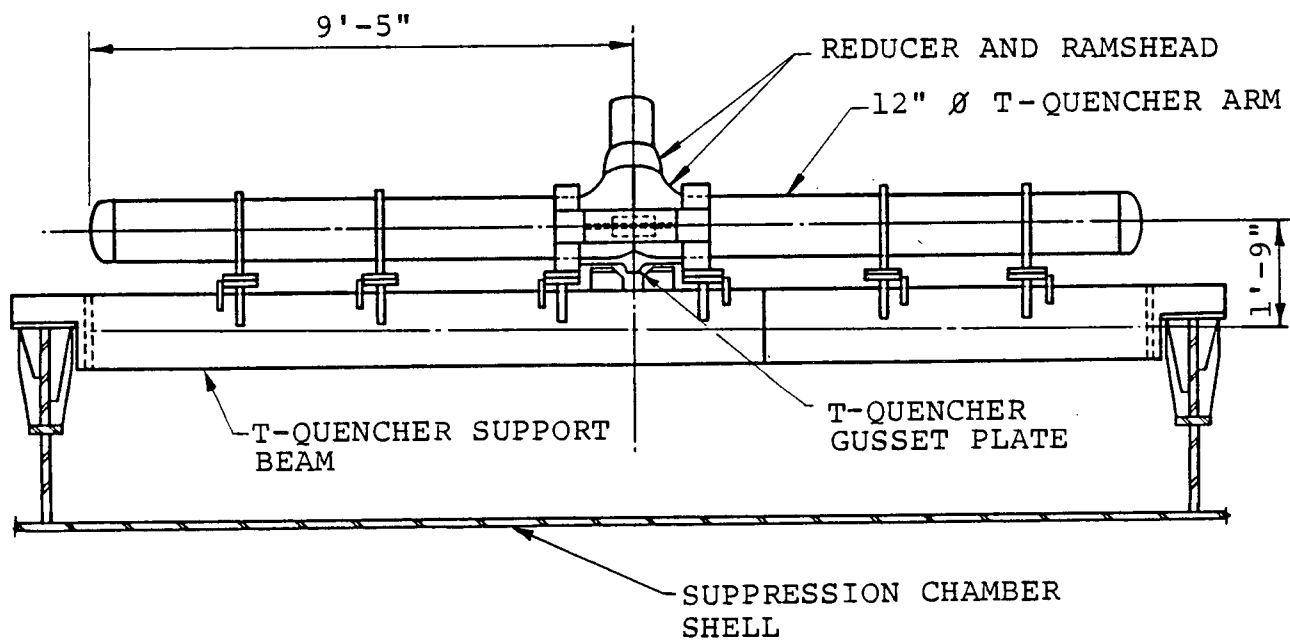
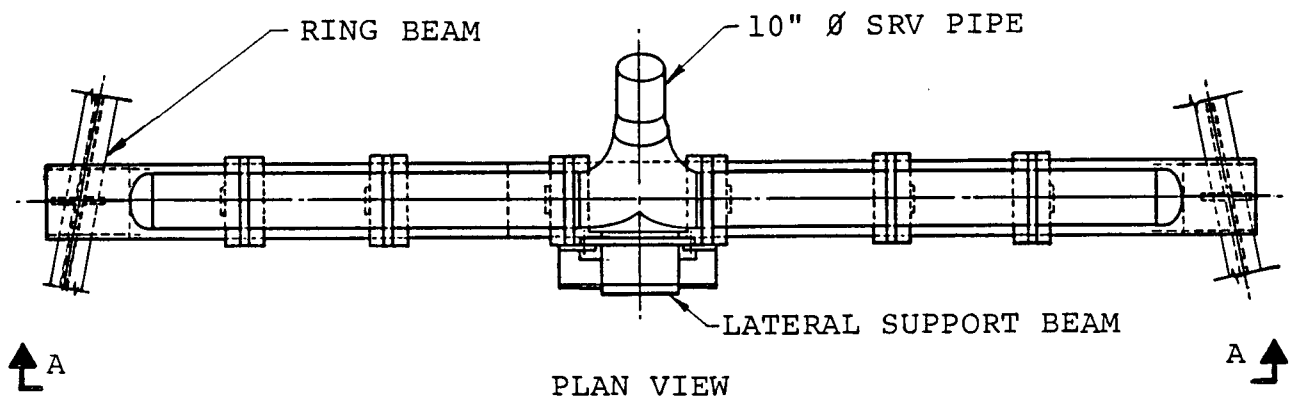


Figure 1-2.1-5

T-QUENCHER AND SUPPORT LOCATIONS

IOW-40-199-1
Revision 0

1-2.11



VIEW A-A

Figure 1-2.1-6

T-QUENCHER AND T-QUENCHER SUPPORTS-
PLAN VIEW AND ELEVATION

IOW-40-199-1
Revision 0

1-2.12

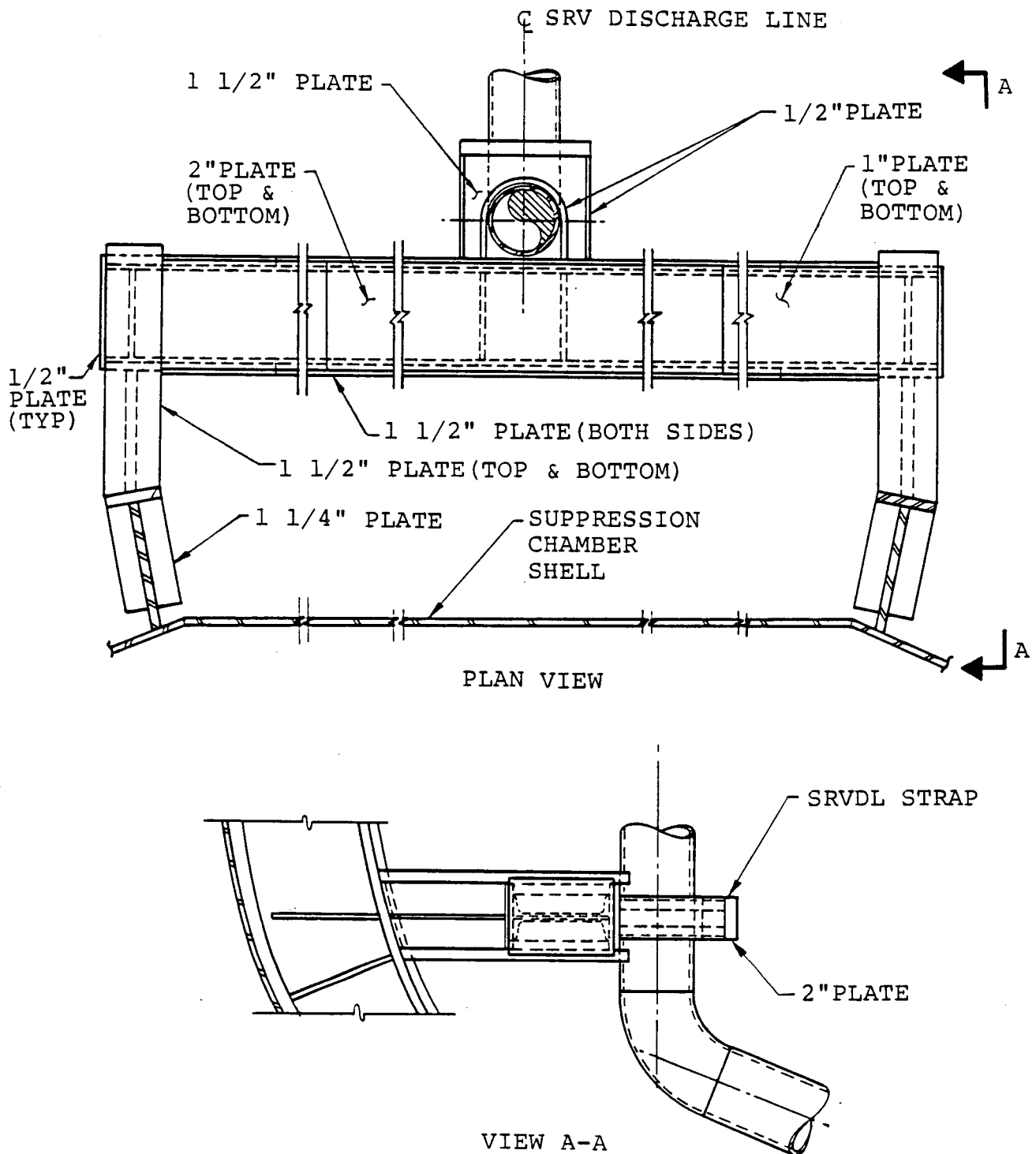


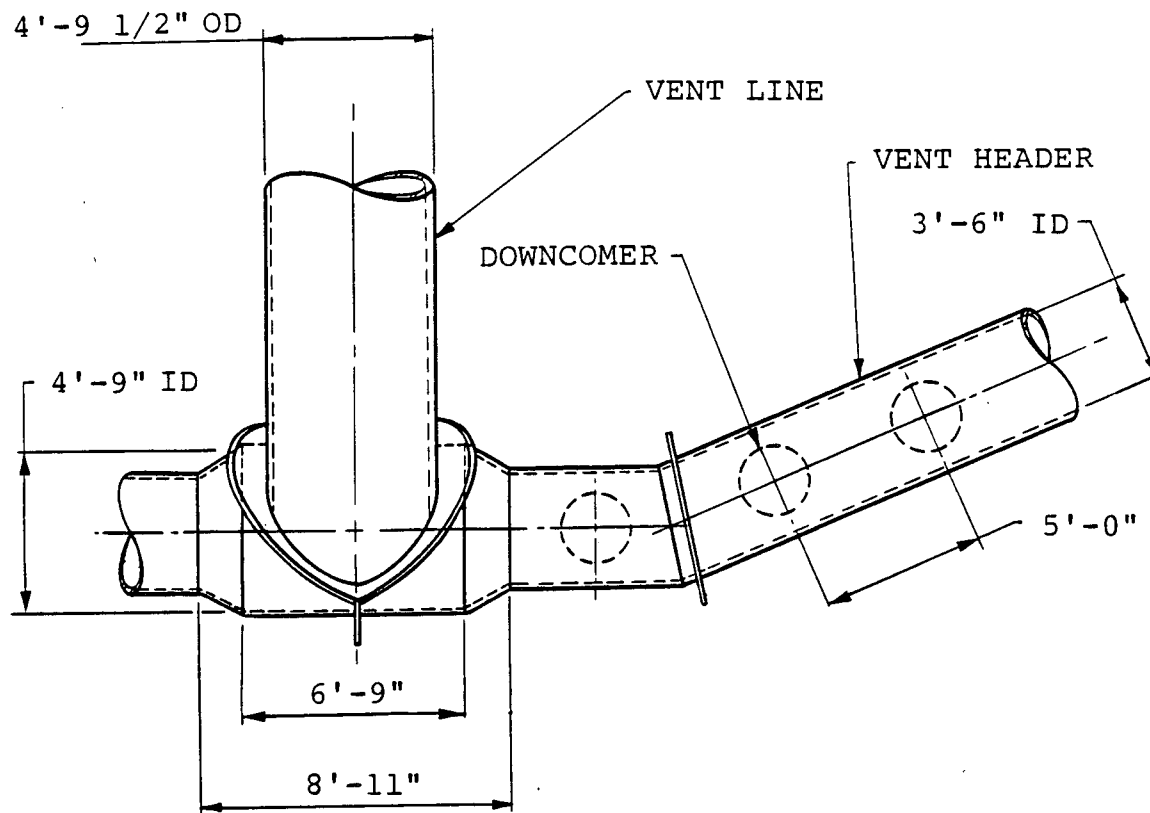
Figure 1-2.1-7
SRV ELBOW SUPPORT BEAM

1-2.1.2 Vent System

The DAEC vent system is constructed from mitered cylindrical segments joined together to form a manifold-like structure which connects the drywell to the suppression chamber (Figure 1-2.1-8). The cylinder connected to the end of the vent line has an inside diameter of 4'9". Beyond the vent line intersection, the vent header inside diameter is 3'6". There are 48 downcomers which protrude from the vent header.

The vent system is supported by two column members at each miter joint location (Figure 1-2.1-4). Figure 1-2.1-9 shows stiffening for the vent-line-to-vent-header intersection. Figures 1-2.1-10 and 1-2.1-11 show the deflector configuration. The deflector is a multi-segmented, wedge-shaped plate assembly. It extends from the centerline of each non-vent bay to the nearest downcomer in the vent line bay. The deflector segments are supported by the downcomers horizontally and vertically by support plates which are welded to the vent header.

The vent system also provides support for the vacuum breakers (Figure 1-2.1-12) and for a portion of the SRV piping inside the vent line and suppression chamber (Figure 1-2.1-13). Loads which act on the SRV piping are transferred to the vent system by the penetration assembly.



1. VENT HEADER DEFLECTOR
NOT SHOWN FOR CLARITY

Figure 1-2.1-8
VENT HEADER PLAN VIEW

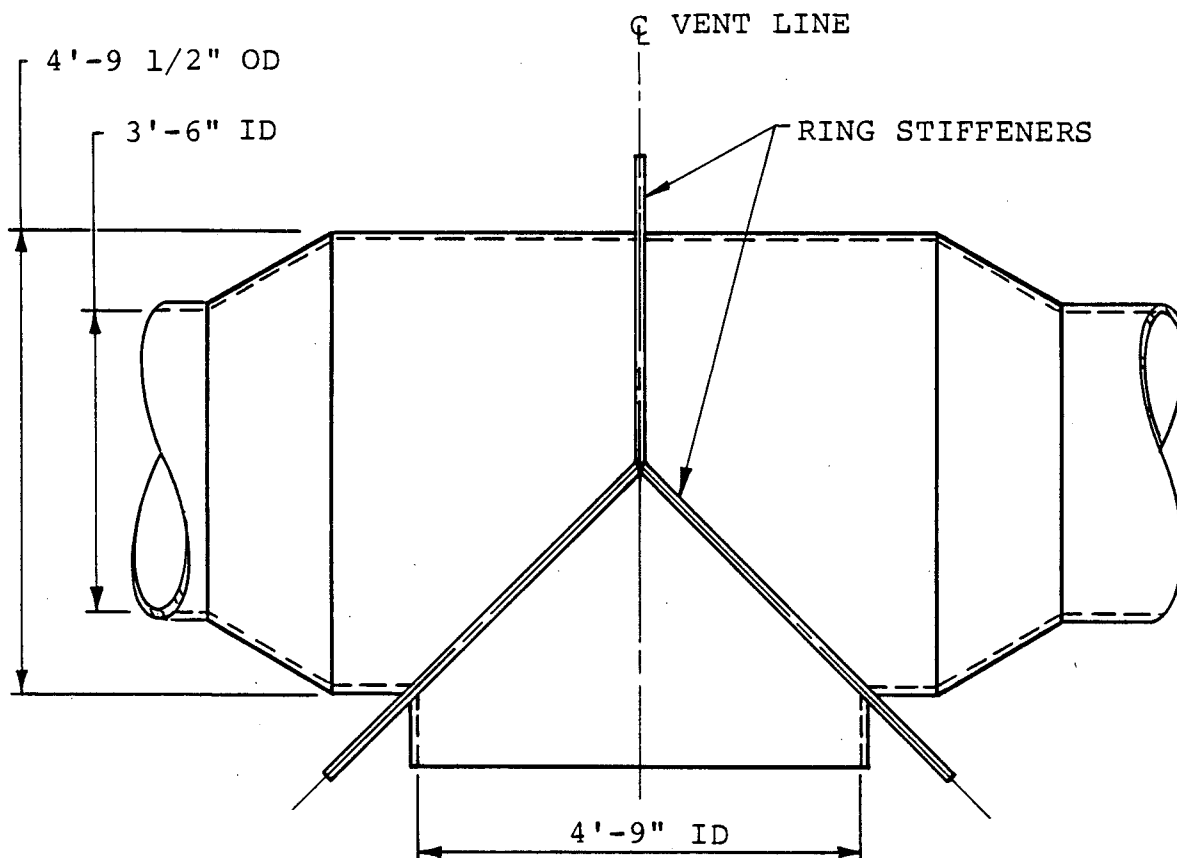
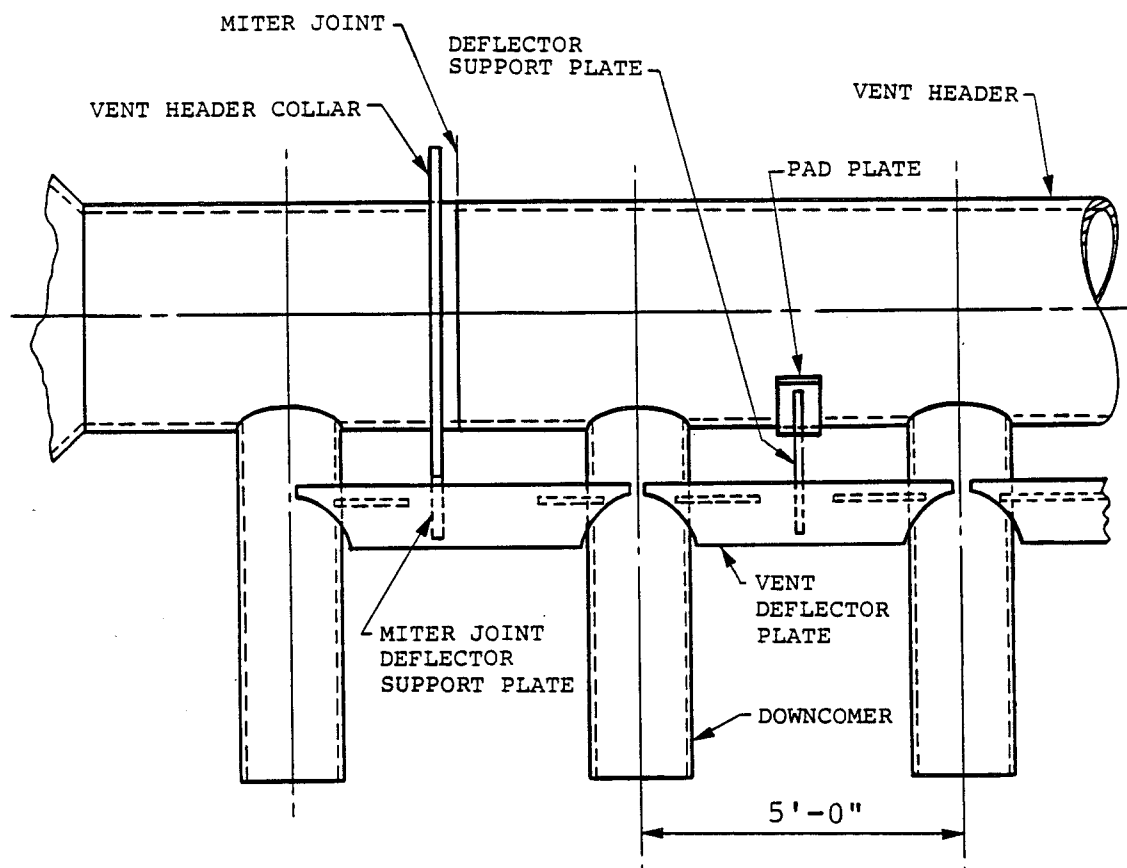


Figure 1-2.1-9

VENT-LINE-TO-VENT-HEADER INTERSECTION

IOW-40-199-1
Revision 0

1-2.17



1. VIEW DEVELOPED NORMAL TO AXES OF VENT HEADER AND DOWNCOMER.
2. VENT HEADER SUPPORT COLUMN DETAILS NOT SHOWN FOR CLARITY.

Figure 1-2.1-10
DEVELOPED VIEW OF VENT HEADER AND VENT DEFLECTOR SYSTEM

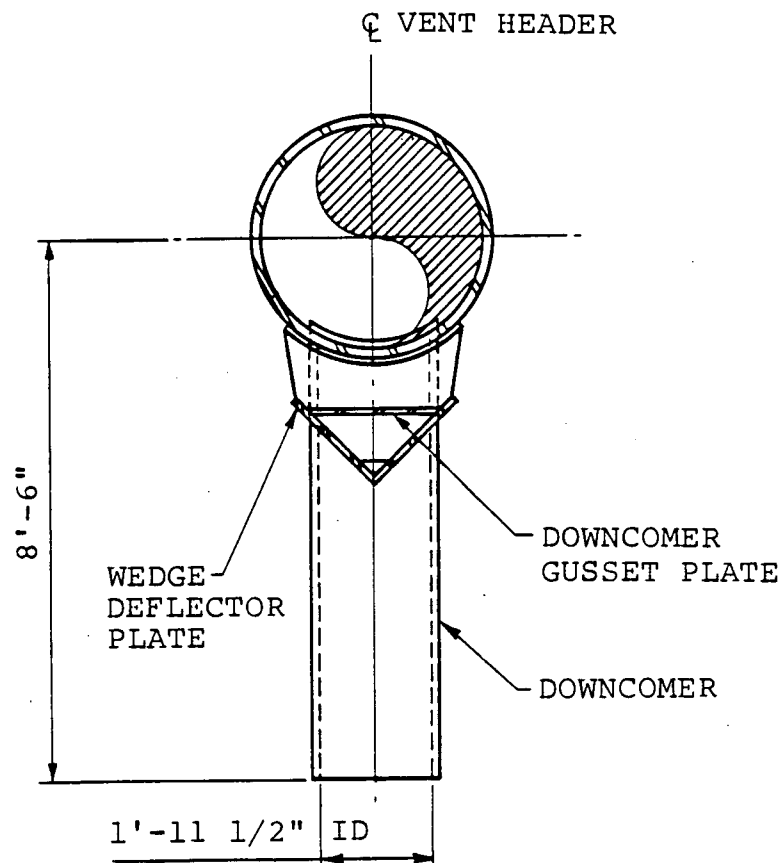


Figure 1-2.1-11.

DOWNCOMER-TO-VENT-HEADER INTERSECTION

IOW-40-199-1
Revision 0

1-2.19

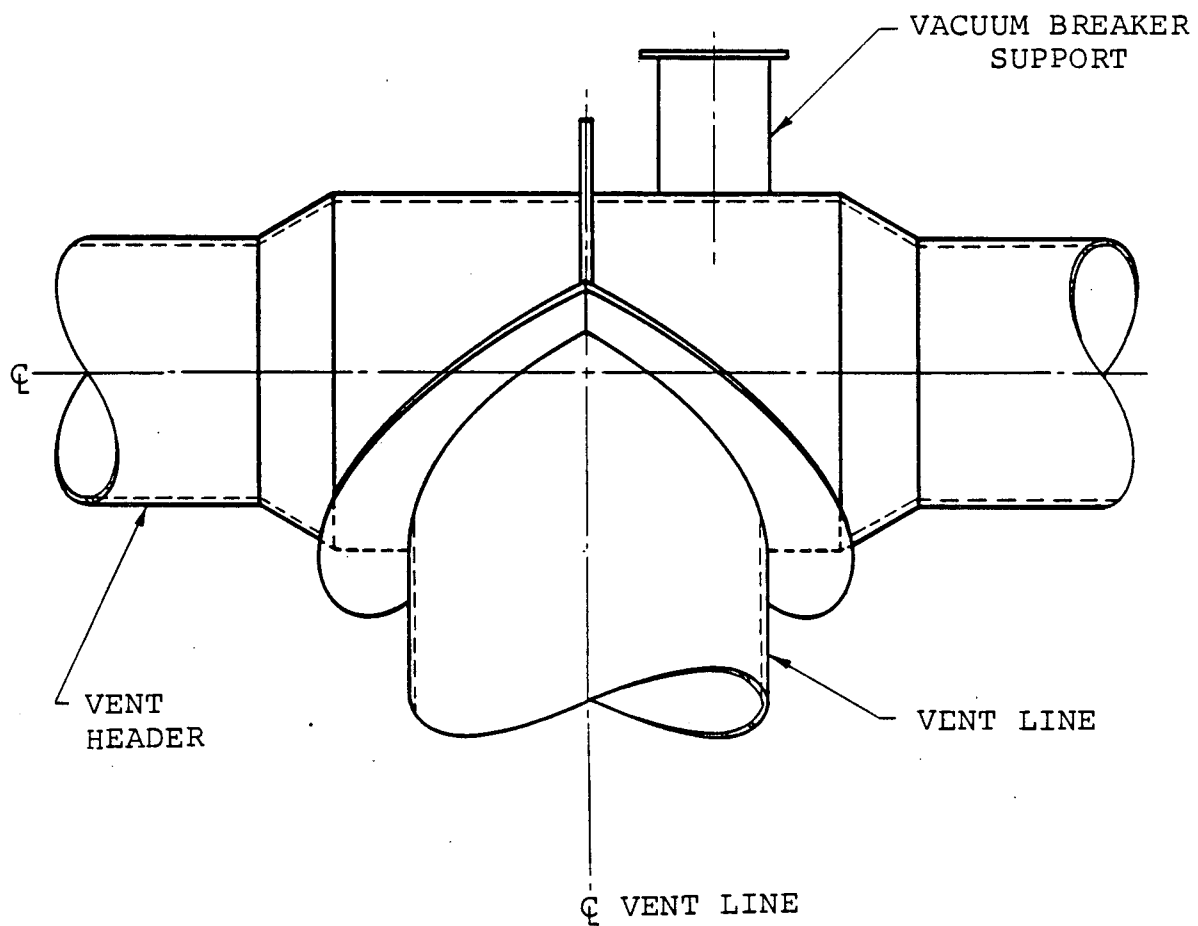
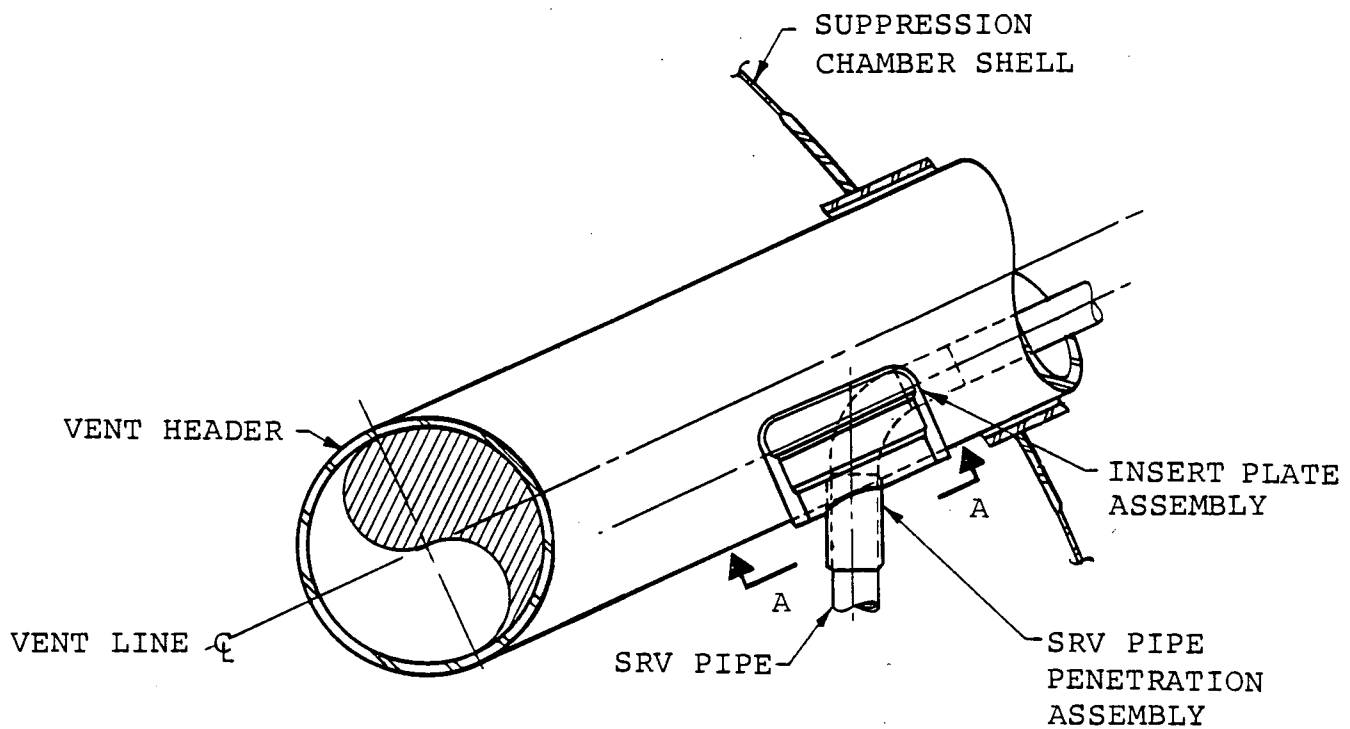


Figure 1-2.1-12

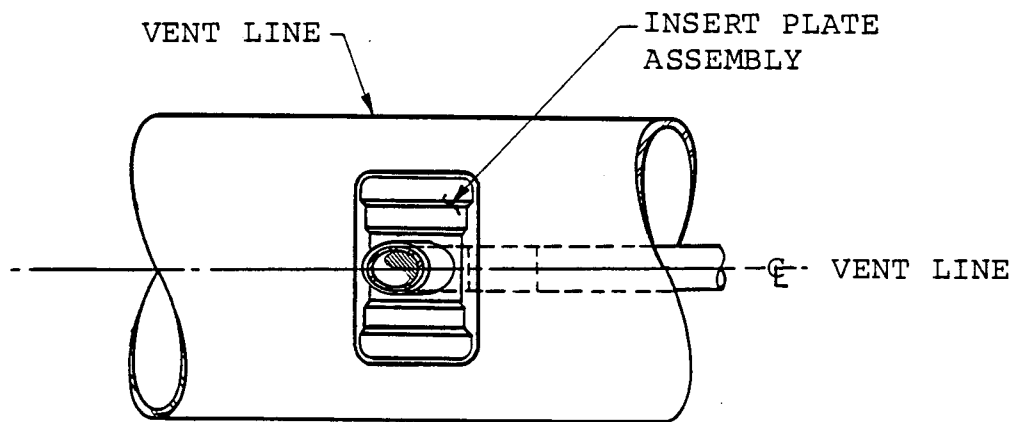
VACUUM BREAKER PENETRATION - PLAN VIEW

IOW-40-199-1
Revision 0

1-2.20



VENT LINE ELEVATION VIEW



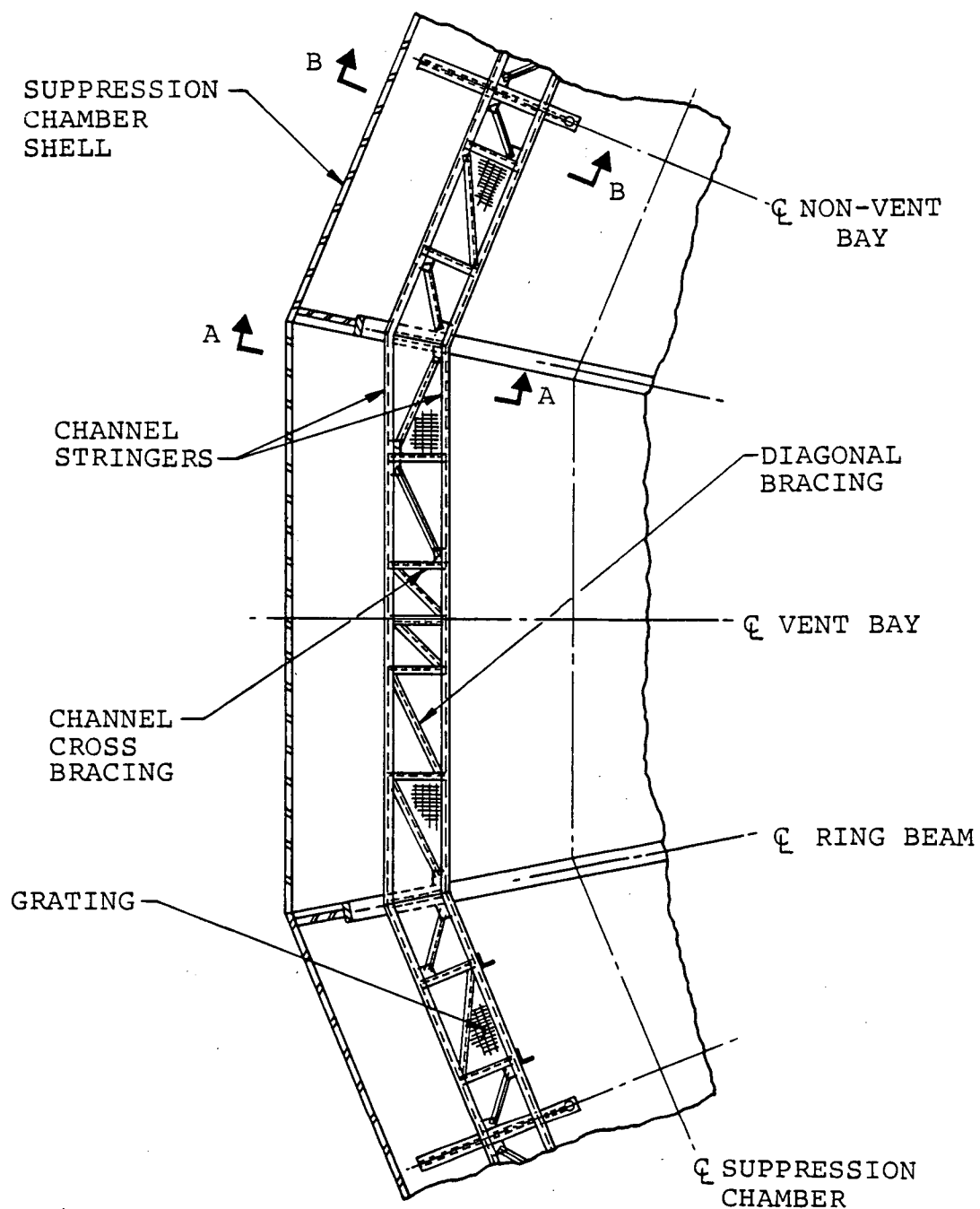
SECTION A-A

Figure 1-2.1-13

SRV PENETRATION IN VENT LINE

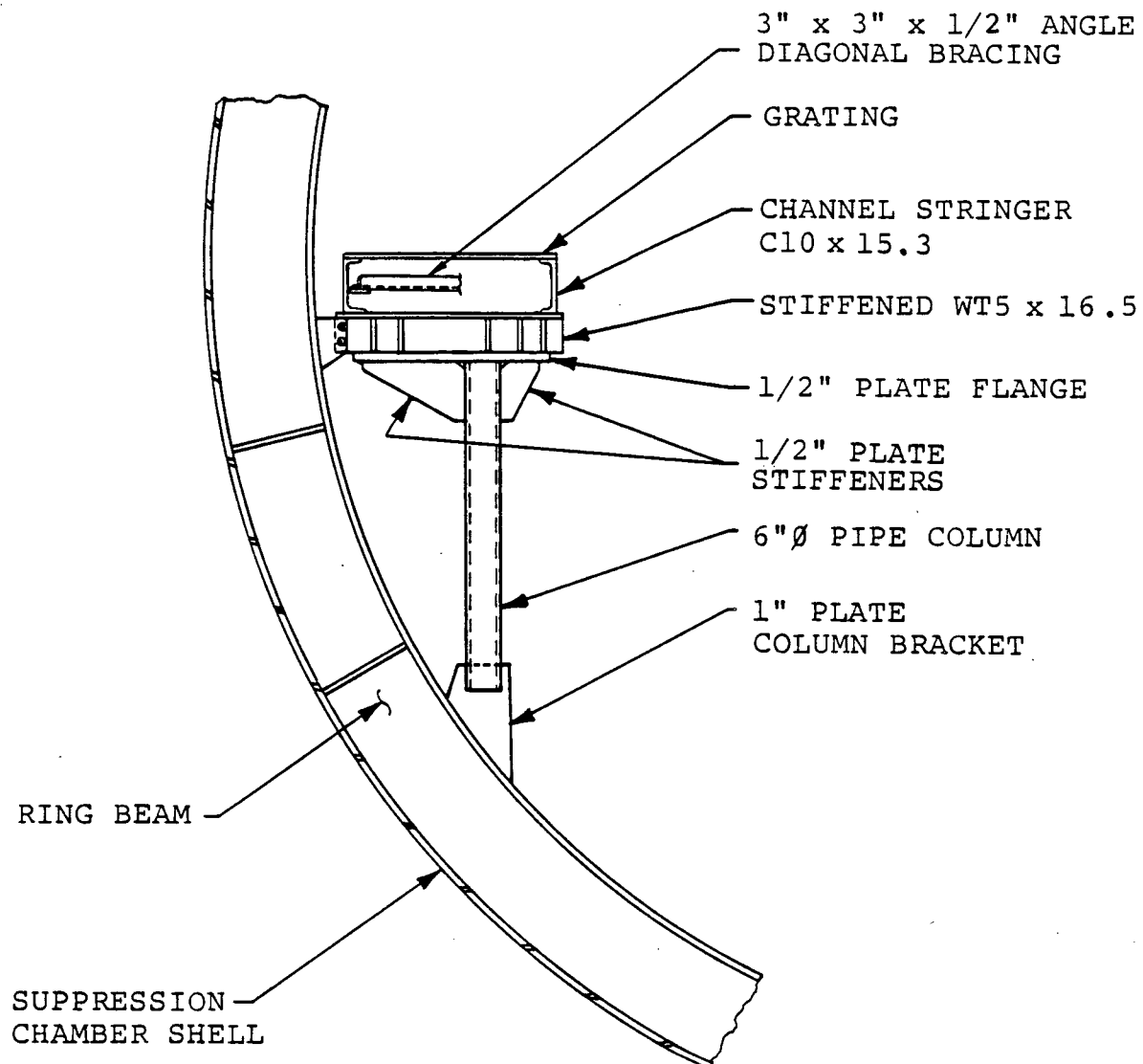
The catwalk is located parallel to the suppression chamber longitudinal axis of each mitered cylinder (Figure 1-2.1-14). The catwalk frame is supported by a pipe column at the miter joint ring beam (Figure 1-2.1-15) and in each non-vent bay by a hanger (Figure 1-2.1-16). The non-vent bay hanger consists of a horizontal beam from the suppression chamber shell to a pipe hanger suspended from the suppression chamber shell (Figure 1-2.1-16). Figures 1-2.1-2 and 1-2.1-3 show the location of the catwalk relative to other major components within the suppression chamber.

The monorail forms a complete circle around the inside of the suppression chamber. The monorail support system consists of a vertical hanger rod, clevis, forged eye nut and beam clamp (Figure 1-2.1-17). Figures 1-2.1-2 and 1-2.1-3 show the location of the monorail relative to the other major components within the suppression chamber.



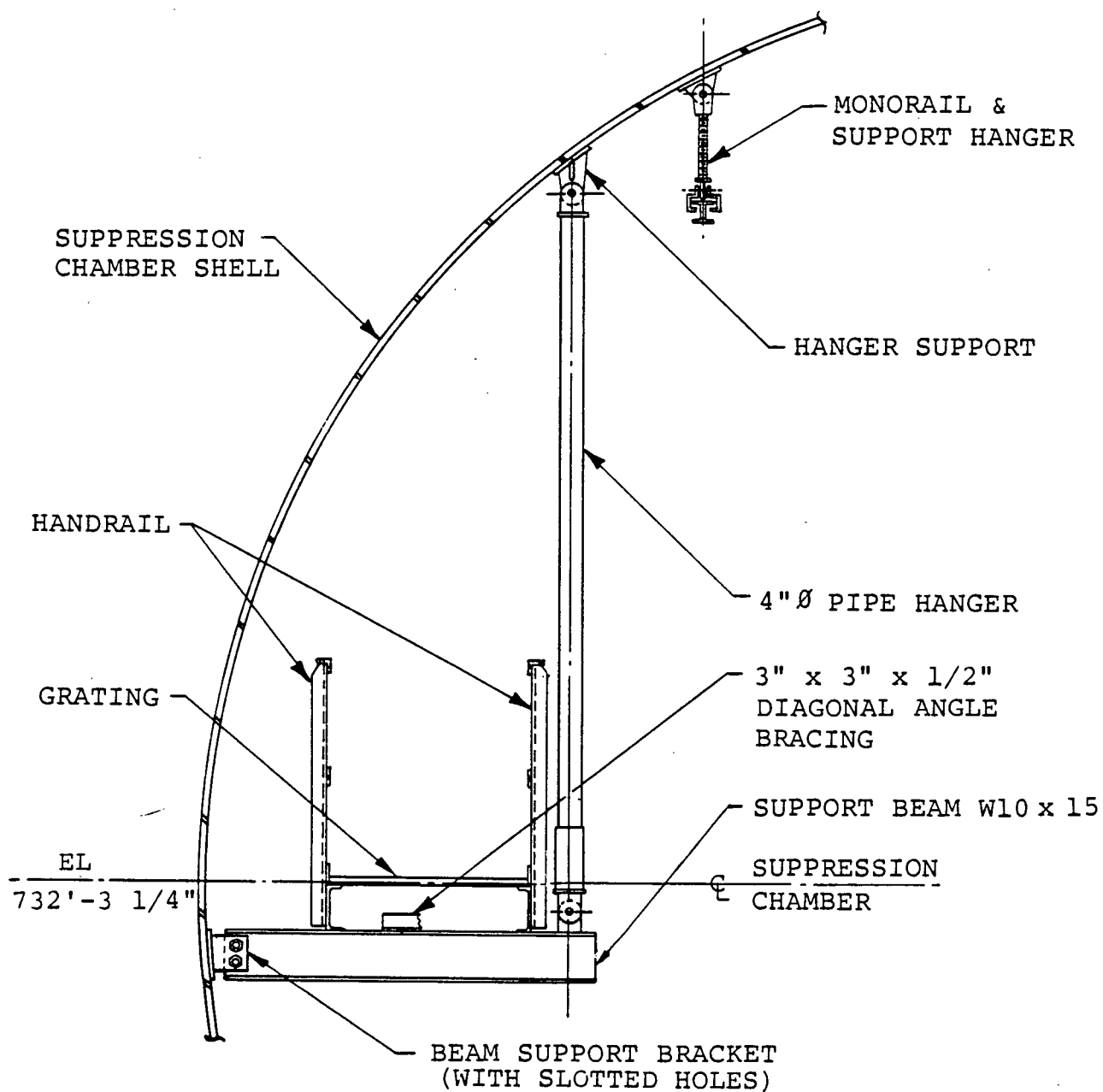
- 1 SEE FIGURE 1-2.1-15 FOR SECTION A-A.
- 2 SEE FIGURE 1-2.1-16 FOR SECTION B-B.

Figure 1-2.1-14
CATWALK FRAME



SECTION A-A
(From Figure 1-2.1-14)

Figure 1-2.1-15
CATWALK SUPPORT AT RING BEAM



SECTION B-B
(From Figure 1-2.1-14)

Figure 1-2.1-16

CATWALK SUPPORT IN THE NON-VENT BAY

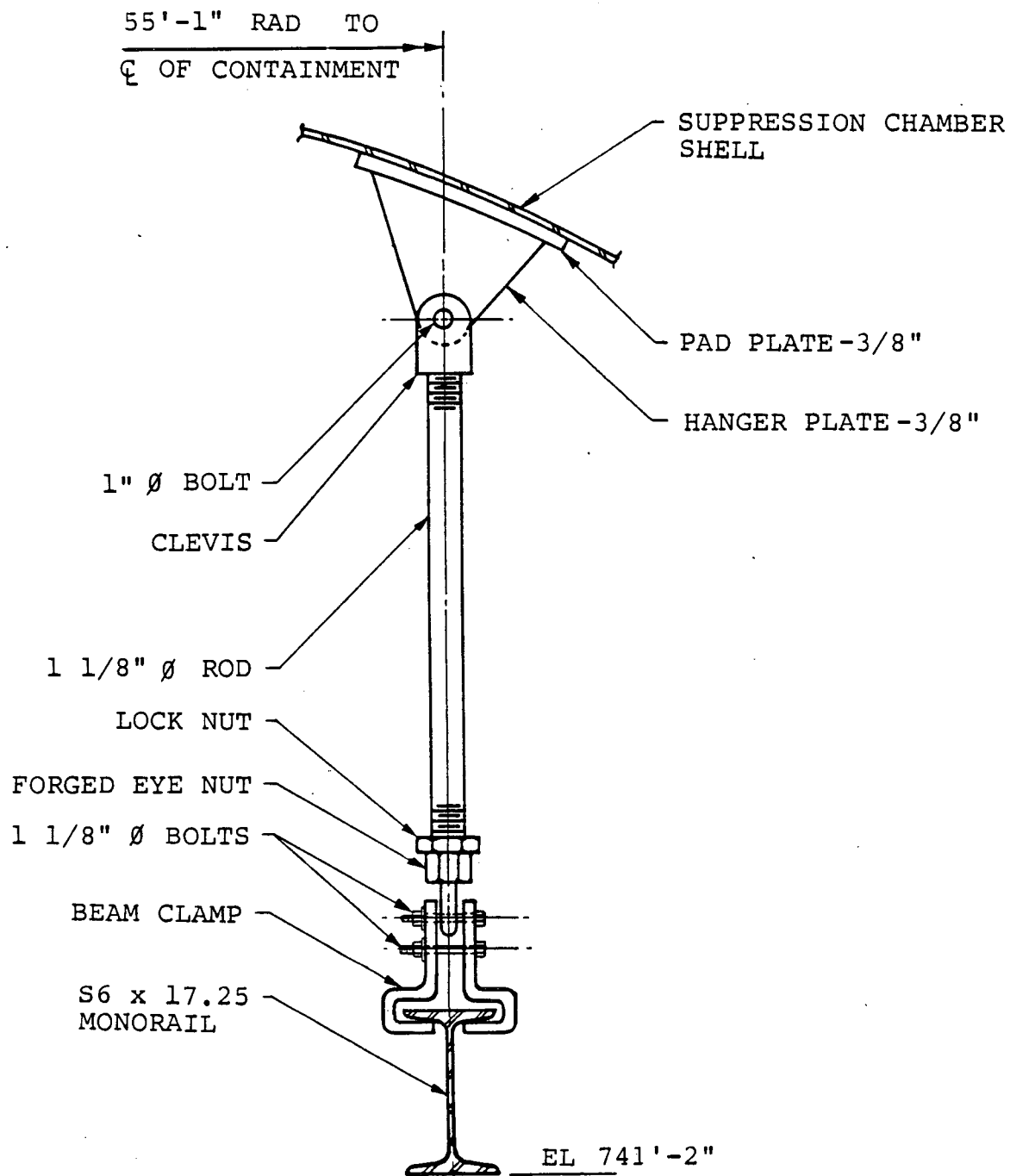


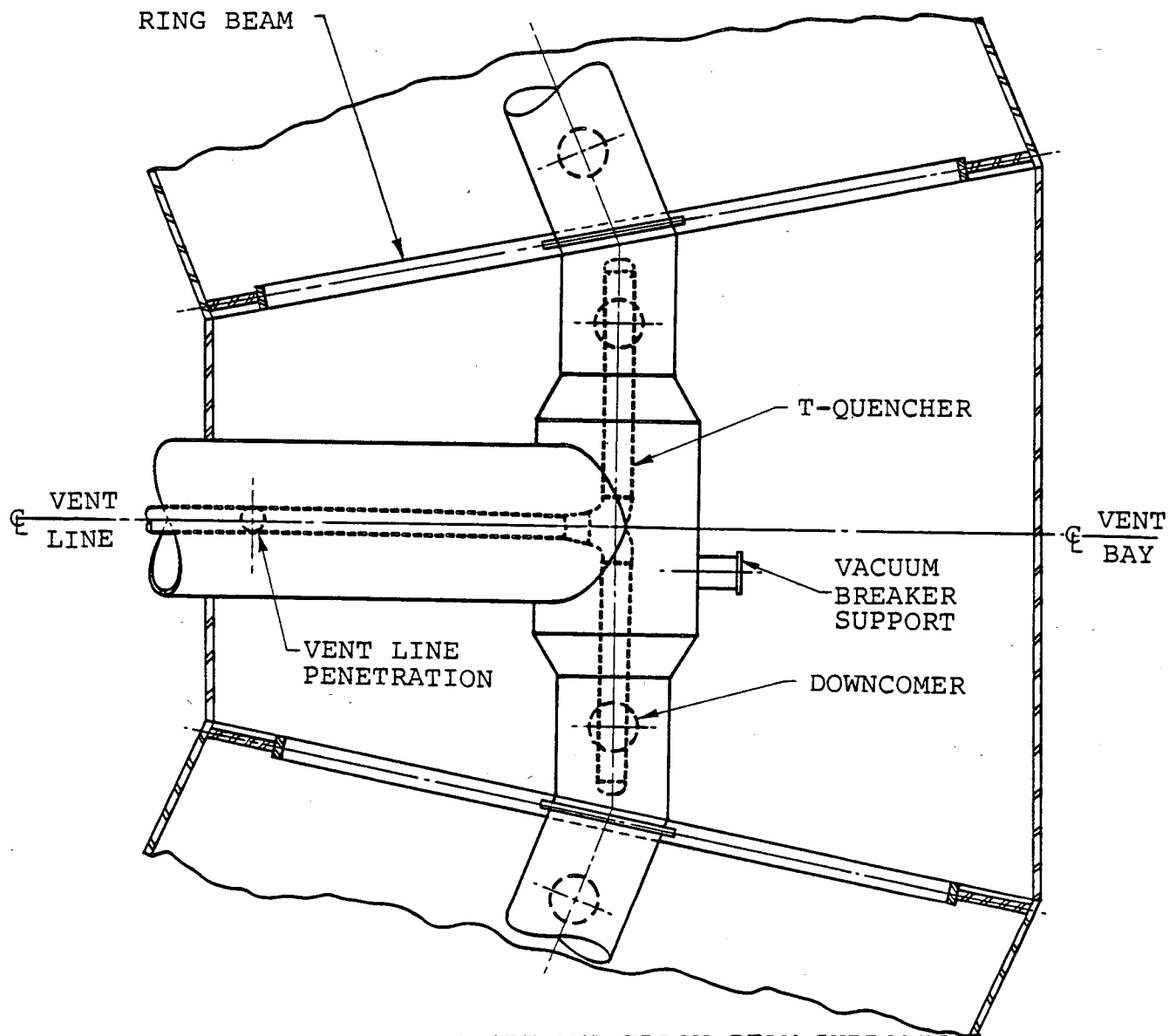
Figure 1-2.1-17

MONORAIL SUPPORTS

1-2.1.4 SRV Discharge Piping

The outlet of each SRV is connected to discharge piping which is routed to the suppression pool. Routing of the SRV discharge piping is such that only six of the vent lines are used, with a single SRV line being routed through each vent line. The SRV piping in the drywell is supported by hangers, struts and snubbers connected to backup steel structures and the vent line.

The use of the vent lines for routing the six SRV lines results in only one SRV line terminating at any one reinforcing beam. The SRV piping exits the vent line through an insert plate (Figure 1-2.1-13) and is then routed to the center of the bay, where the ramshead and T-quencher arms are attached to the T-quencher support beam by bracket supports and a lateral support beam. Figure 1-2.1-18 shows a typical SRV pipe routing in the wetwell.



1. T-QUENCHER SUPPORT AND ELBOW BEAM SUPPORTS
NOT SHOWN FOR CLARITY

Figure 1-2.1-18

SRV PIPE ROUTING IN SUPPRESSION CHAMBER - PLAN VIEW

Plant operating parameters are used to determine many of the hydrodynamic loads utilized in the reevaluation of the DAEC suppression chamber design. Table 1-2.2-1 is a summary of the operating parameters used to determine the DAEC hydrodynamic loads.

Table 1-2.2-1

SUPPRESSION CHAMBER OPERATING PARAMETERS

COMPONENTS	CONDITION/ITEM	VALUE
DRYWELL	FREE AIR VOLUME ⁽¹⁾	118,000 cu ft $\begin{matrix} +0\% \\ -10\% \end{matrix}$
	NORMAL OPERATING PRESSURE	HIGH 2.0 psig LOW -2.0 psig
	NORMAL OPERATING TEMPERATURE	NOMINAL BULK 135°F MAX BULK 148°F MIN BULK 70°F
	PRESSURE SCRAM INITIATION SET POINT	2 psig ± 0.2 psig
	DESIGN INTERNAL PRESSURE	56 psig
	DESIGN EXTERNAL PRESSURE MINUS INTERNAL PRESSURE	2 psid
	DESIGN TEMPERATURE	281°F
SUPPRESSION CHAMBER	POOL VOLUME	MAX (HIGH WATER LEVEL) 61,500 ft ³ MIN (LOW WATER LEVEL) 58,900 ft ³
	FREE AIR VOLUME ⁽²⁾	MIN (HIGH WATER LEVEL) 94,270 ft ³ MAX (LOW WATER LEVEL) 96,870 ft ³
	LOCA VENT SYSTEM DOWNCOMER SUBMERGENCE (DISTANCE OF DOWNCOMER DISCHARGE PLANE BELOW WATER LEVEL)	MIN (LOW WATER LEVEL) 3.00 ft MAX (HIGH WATER LEVEL) 3.39 ft
	WATER LEVEL DISTANCE TO TORUS CENTERLINE	MAX (LOW WATER LEVEL) 2.75 ft MIN (HIGH WATER LEVEL) 2.36 ft
	SUPPRESSION POOL SURFACE EXPOSED TO SUPPRESSION CHAMBER AIRSPACE	7,763 ft ²
	NORMAL OPERATING PRESSURE RANGE	HIGH 2.0 psig LOW -2.0 psig

Table 1-2.2-1

SUPPRESSION CHAMBER OPERATING PARAMETERS

(Concluded)

COMPONENTS	CONDITION/ITEM	VALUE
SUPPRESSION CHAMBER	NORMAL TEMPERATURE RANGE OF SUPPRESSION POOL	HIGH 82°F LOW 50°F
	TECH SPEC MAXIMUM	TECH SPEC 95°F
	NORMAL OPERATING TEMPERATURE RANGE OF SUPPRESSION CHAMBER FREE AIR VOLUME	HIGH 100°F LOW 50°F
	DESIGN INTERNAL PRESSURE	56 psig
	EXTERNAL PRESSURE MINUS INTERNAL PRESSURE	2 psid
	DESIGN TEMPERATURE	281°F
DOWNCOMER	NORMAL OPERATING PRESSURE DIFFERENTIAL (DRYWELL-TO-WETWELL)	ZERO
	ID AT DISCHARGE	1.958 ft
	OD AT DISCHARGE	2 ft
CONTAINMENT	TOTAL NUMBER OF DOWNCOMERS	48
	LONG-TERM POST-LOCA CONTAINMENT LEAK RATE	MAX 2.0%/DAY
	DRYWELL-TO-WETWELL LEAKAGE SOURCE BYPASSING SUPPRESSION POOL WATER	MAX 0.2 ft ²
	SERVICE WATER TEMPERATURE LIMITS	MAX NORMAL 95°F (TECH SPEC)

SAFETY RELIEF VALVE (3)	SET POINT (psig)	CAPACITY AT 103% OF SET POINT (lbm/hr)
1 (ADS)	1080	830,000
1	1090	838,000
2 (ONLY 1 ADS)	1100	844,000
2 (ADS)	1110	852,000

- NOTES: (1) INCLUDES FREE AIR VOLUME OF THE LOCA VENT SYSTEM.
 (2) DOES NOT INCLUDE FREE AIR VOLUME OF THE VENT SYSTEM.
 (3) ADS CONSISTS OF FOUR SAFETY RELIEF VALVES.

This section describes the acceptance criteria for the hydrodynamic loads and structural evaluations used in the plant unique analysis.

The acceptance criteria used in the PUA have been developed from the NRC review of the Long-Term Program Load Definition Report (LDR), the Plant Unique Analysis Applications Guide (PUAAG), and the supporting analytical and experimental programs conducted by the Mark I Owners Group. These criteria are documented in NUREG-0661 for both hydrodynamic load definition and structural applications. Sections 1 and 2 of NUREG-0661 give Introduction and Background; Section 3 presents a detailed discussion of the Hydrodynamic Load Evaluation; Section 4 presents the Structural and Mechanical Analyses and Acceptance Criteria, and Appendix A presents the Hydrodynamic Acceptance Criteria.

Appendix A of NUREG-0661 resulted from the NRC evaluation of the load definition procedures for suppression pool hydrodynamic loads which were proposed by the Mark I Owners Group for use in their plant-unique analyses. This NRC evaluation addressed only those events or event combinations which involve suppression pool hydrodynamic loads. Unless otherwise specified, all loading conditions or structural analysis techniques used in the plant unique analysis, but not addressed in NUREG-0661, are in accordance with the DAEC Final Safety Analysis Report (FSAR). The NRC hydrodynamic loads acceptance criteria are used with a coupled fluid-structure analytical model.

Wherever feasible, the conservative hydrodynamic acceptance criteria of NUREG-0661 were incorporated directly into the detailed plant unique load determinations and associated structural analyses. Where this simple, direct approach resulted in unrealistic hydrodynamic loads, more detailed plant unique analyses were performed. Many of these analyses have indicated that a specific interpretation of the generic rules was well founded. These specific

applications of the generic hydrodynamic acceptance criteria are identified in the following sections and are discussed in greater detail in Section 1-4.0.

1-3.1.1 LOCA-Related Load Applications

The hydrodynamic loads criteria are based on NRC review of and revision to experimentally-formulated hydrodynamic loads. Pool swell loads derived from plant unique quarter-scale two-dimensional tests are used to obtain net torus up-and-down loads and local pressure distributions. Vent system impact and drag loads resulting from pool swell effects are also based on experimental results, using analytical techniques where appropriate.

Condensation oscillation and chugging loads were derived from Full-Scale Test Facility (FSTF) results. Downcomer loads are based on test data, using comparisons of plant unique and FSTF dynamic load factors.

The acceleration drag volumes used in determining loads on submerged structures are calculated based upon the values in published technical literature rather than on the procedure which might be inferred from NUREG-0661, where the structure is idealized as a circumscribed circle for both velocity drag and for acceleration drag (see Section 1-4.1.5 and Table 1-4.1-1).

Condensation oscillation and post-chug torus shell and submerged structure loads are defined in terms of 50 harmonics. Random phasing of the loading harmonics is assumed, based on FSTF data and subsequent analysis (see Section 1-4.1.7.1).

NUREG-0661 states that the FSI effect on condensation oscillation and chugging submerged structure loads can be accounted for by adding the shell boundary accelerations to the local fluid acceleration. For DAEC, the FSI effect for a given structure is included by adding the pool fluid acceleration at the location of the structure, rather than the shell boundary acceleration (see Section 1-4.1.7.3).

The analysis techniques for SRV loads were developed to define T-quencher air clearing loads on the torus generically. However, a number of Mark I licensees have indicated that the generic load definition procedures are overly conservative for their plant design, especially when the procedures are coupled with conservative structural analysis techniques. To allow for these special cases, the NRC has stipulated requirements whereby in-plant tests could be used to derive the plant specific structural response to the SRV air clearing loads on the torus.

Because of the various phenomena associated with the air clearing phase of SRV discharge, an analysis procedure is necessary to extrapolate from test conditions to the design cases. Therefore, the NRC requirements are predicated on formulating a coupled fluid-structure analysis technique which is calibrated to the plant specific conditions for the simplest form of discharge (i.e., single valve, first actuation) and then applied to the design basis event conditions.

SRV torus shell loads are evaluated using the alternate approach of NUREG-0661, which allows the use of in-plant SRV tests to calibrate a coupled fluid-structure analytical model. This method utilizes shell pressure waveforms more characteristic of those observed in tests. A series of in-plant SRV tests were performed in June 1981 (Reference 4) to confirm that the computed loadings and predicted structural responses for SRV discharges are conservative (see Section 1-4.2.3).

For SRV bubble-induced drag loads on submerged structures, a bubble pressure multiplier is used which bounds the maximum peak positive bubble pressure and the maximum bubble pressure differential observed during the Monticello T-quencher tests (see Section 1-4.2.4).

As part of the PUA, each licensee is required to either demonstrate that previously submitted pool temperature response analyses are sufficient or provide plant-specific pool temperature response analyses to assure that SRV discharge transients will not exceed specified pool temperature limits. A suppression pool temperature monitoring system is also required to ensure that the suppression pool bulk temperature is within the allowable limits set forth in the plant technical specifications. Specific implementation of these considerations is discussed in Section 1-5.0.

Several loads are classified as secondary loads because of their inherent low magnitudes. These loads include: seismic slosh pressure loads, post-pool swell wave loads, asymmetric pool swell pressure loads, sonic and compression wave loads, and downcomer air clearing loads. These secondary loads are treated as negligible compared to other loads in the PUA, which is in accordance with Appendix A of NUREG-0661.

Section 4.0 of NUREG-0661 presents the NRC evaluation of the generic structural and mechanical acceptance criteria and of the general analysis techniques proposed by the Mark I Owners Group for use in the plant-unique analyses. Because most of the Mark I facilities were designed and constructed at different times, there are variations in the codes and standards to which they were constructed and subsequently licensed. For this reassessment of the suppression chamber, the criteria described in this subsection were developed to provide a consistent and uniform basis for acceptability. In this evaluation, references to "original design criteria" mean those specific criteria in the DAEC Final Safety Analysis Report (FSAR).

The structures described in Section 1-1.1 were categorized in accordance with their functions in order to assign the appropriate service limits. The general components of a Mark I suppression chamber have been classified in accordance with the American Society of Mechanical Engineers (ASME) Boiler and Pressure Vessel Code as specified in NUREG-0661. The classification of components is detailed in sections under Analysis Acceptance Criteria in Volumes 2 through 6.

1-3.2.2 Service Level Assignments

The criteria used in the plant-unique analyses to evaluate the acceptability of the existing Mark I containment designs or to provide the basis for any plant modifications generally follow Section III of the ASME Boiler and Pressure Vessel Code, 1977 Edition, with Addenda up to and including Winter 1978 (Reference 5). These criteria are equivalent to those of the ASME Code, 1977 Edition, with Addenda up to and including Summer 1977, with respect to the requirements of NUREG-0661.

Service Limits

The service limits are defined in terms of Levels A, B, C, D and E, which were first introduced into the ASME Code with Winter 1976 Addenda to NA-2140. The selection of specific service limits for each load combination was dependent on the functional requirements of the component analyzed and the nature of the applied load. Tables 1-3.2-1 and 1-3.2-2 give the assignments of service levels for each load combination. Details regarding service level assignments and other aspects of Tables 1-3.2-1 and 1-3.2-2 are described in Reference 2.

Table 1-3.2-1

EVENT COMBINATIONS AND SERVICE LEVELS FOR CLASS MC
COMPONENTS AND INTERNAL STRUCTURES

EVENT COMBINATIONS			SRV			SRV + EQ			SBA IBA		SBA + EQ IBA + EQ				SBA+SRV IBA+SRV		SBA + SRV + EQ IBA + SRV + EQ				DBA		DBA + EQ				DBA+SRV		DBA + EQ + SRV				
										CO, CH		CO, CH		CO, CH		CO, CH		PS (1)	CO, CH		PS		CO, CH		PS		CO, CH		PS		CO, CH		PS
TYPE OF EARTHQUAKE																																	
COMBINATION NUMBER			1	2	3	4	5	6	7	8	9	10	11	12	13	14	15	16	17	18	19	20	21	22	23	24	25	26	27				
LOADS	NORMAL (2)	N	X	X	X	X	X	X	X	X	X	X	X	X	X	X	X	X	X	X	X	X	X	X	X	X	X	X	X	X	X	X	
	EARTHQUAKE	EQ		X	X			X	X	X	X			X	X	X	X			X	X	X	X			X	X	X	X	X	X	X	
	SRV DISCHARGE	SRV	X	X	X							X	X	X	X	X	X							X	X(7)	X	X	X(7)	X(7)	X(7)	X(7)	X(7)	
	LOCA THERMAL	T _A				X	X	X	X	X	X	X	X	X	X	X	X	X	X	X	X	X	X	X	X	X	X	X	X	X	X	X	
	LOCA REACTIONS	R _A				X	X	X	X	X	X	X	X	X	X	X	X	X	X	X	X	X	X	X	X	X	X	X	X	X	X	X	
	LOCA QUASI-STATIC PRESSURE	P _A				X	X	X	X	X	X	X	X	X	X	X	X	X	X	X	X	X	X	X	X	X	X	X	X	X	X	X	
	LOCA POOL SWELL	P _{PS}																X		X	X			X		X	X						
	LOCA CONDENSATION OSCILLATION	P _{CO}					X			X	X		X			X	X		X			X	X		X				X	X			
LOCA CHUGGING	P _{CH}					X			X	X		X			X	X		X			X	X		X				X	X				
STRUCTURAL ELEMENT			ROW																														
EXTERNAL CLASS MC	TORUS, EXTERNAL VENT PIPE, BELLONS, DRYWELL (AT VENT), ATTACHMENT WELDS, TORUS SUPPORTS, SEISMIC RESTRAINTS	1	A	B	C	A	A	B	C	B	C	A	A	B	C	B	C	A	B	C	C	B	C	C	C	C	C	C	C	C	C	C	
INTERNAL VENT PIPE	GENERAL AND ATTACHMENT WELDS	2	A	B	C	A	A	B	C	B	C	A	A	B	C	B	C	A	B	C	C	B	C	C	C	C	C	C	C	C	C	C	
	AT PENETRATIONS (e.g., HEADER)	3	A	B	C	A	A	B	C	B	C	A	A	B	C	B	C	A	B	C	C	B	C	C	C	C	C	C	C	C	C	C	
VENT HEADER	GENERAL AND ATTACHMENT WELDS	4	A	B	C	A	A	B	C	B	C	A	A	B	C	B	C	A	B	C	C	B	C	C	C	C	C	C	C	C	C	C	
	AT PENETRATIONS (e.g., DOWNCOMERS)	5	A	B	C	A	A(4)	B	C	B(4)	C	A	A(4)	B	C	B(4)	C	A	B	C	C	B(4)	C	C	C	C	C	C	C	C	C	C	
DOWNCOMERS	GENERAL AND ATTACHMENT WELDS	6	A	B	C	A	A	B	C	B	C	A	A	B	C	B	C	A	B	C	C	B	C	C	C	C	C	C	C	C	C	C	
INTERNAL SUPPORTS			7	A	B	C	A	A	B	C	B	C	A	A	B	C	B	C	A	B	C	C	B	C	C	C	C	C	C	C	C	C	C
INTERNAL STRUCTURES	GENERAL	8	A	B	C	A	A	C	D	C	D	C	C	D	E	D	E	E	E	E	E	E	E	E	E	E	E	E	E	E	E	E	
	VENT DEFLECTOR	9	A	B	C	A	A	C	D	C	D	C	C	D	D	D	D	D	D	D	D	D	D	D	D	D	D	D	D	D	D	D	

NOTES TO TABLE 1-3.2-1

- (1) REFERENCE 2 STATES "WHERE THE DRYWELL-TO-WETWELL PRESSURE DIFFERENTIAL IS NORMALLY UTILIZED AS A LOAD MITIGATOR, AN ADDITIONAL EVALUATION SHALL BE PERFORMED WITHOUT SRV LOADINGS BUT ASSUMING LOSS OF THE PRESSURE DIFFERENTIAL. IN THE ADDITIONAL EVALUATION LEVEL D SERVICE LIMITS SHALL APPLY FOR ALL STRUCTURAL ELEMENTS EXCEPT ROW 8 INTERNAL STRUCTURES, WHICH NEED NOT BE EVALUATED. IF DRYWELL-TO-WETWELL PRESSURE DIFFERENTIAL IS NOT EMPLOYED AS A LOAD MITIGATOR, THE LISTED SERVICE LIMITS SHALL BE APPLICABLE". SINCE DAEC DOES NOT UTILIZE A DRYWELL-TO-WETWELL DIFFERENTIAL PRESSURE, THE LISTED SERVICE LIMITS ARE APPLIED.
- (2) NORMAL LOADS (N) CONSIST OF THE COMBINATION OF DEAD LOADS (D), LIVE LOADS (L), THERMAL EFFECTS DURING OPERATION (T_0) AND PIPE REACTIONS DURING OPERATION (R_0).
- (3) EVALUATION OF PRIMARY-PLUS-SECONDARY STRESS INTENSITY RANGE (NE-3221.4) AND OF FATIGUE (NE-3221.5) IS NOT REQUIRED.
- (4) WHEN CONSIDERING THE LIMITS ON LOCAL MEMBRANE STRESS INTENSITY (NE-3221.2) AND PRIMARY-MEMBRANE-PLUS-PRIMARY-BENDING STRESS (NE-3221.3), THE S_{mc} VALUE MAY BE REPLACED BY $1.3 S_{mc}$.

(NOTE: THE MODIFICATION TO THE LIMITS DOES NOT AFFECT THE NORMAL LIMITS ON PRIMARY-PLUS-SECONDARY STRESS INTENSITY RANGE (NE-3221.4 OR NE-3228.3) NOR THE NORMAL LIMITS ON FATIGUE EVALUATION (NE-3221.5(e) OR APPENDIX II-1500). THE MODIFICATION IS THAT THE LIMITS ON LOCAL MEMBRANE STRESS INTENSITY (NE-3221.2) AND ON PRIMARY-MEMBRANE-PLUS-PRIMARY BENDING STRESS INTENSITY (NE-3221.3) HAVE BEEN MODIFIED BY USING $1.3 S_{mc}$ IN PLACE OF THE NORMAL S_{mc} .

THIS MODIFICATION IS A CONSERVATIVE APPROXIMATION TO RESULTS FROM LIMIT ANALYSIS TESTING AS REPORTED IN REFERENCE 2 AND IS CONSISTENT WITH THE REQUIREMENTS OF NE-3228.2.
- (5) SERVICE LEVEL LIMITS SPECIFIED APPLY TO THE OVERALL STRUCTURAL RESPONSE OF THE VENT SYSTEM. AN ADDITIONAL EVALUATION WILL BE PERFORMED TO DEMONSTRATE THAT SHELL STRESSES DUE TO THE LOCAL POOL SWELL IMPINGEMENT PRESSURES DO NOT EXCEED SERVICE LEVEL C LIMITS.
- (6) FOR THE SUPPRESSION CHAMBER SHELL, THE S_{mc} VALUE MAY BE REPLACED BY $1.0 S_{mc}$ TIMES THE DYNAMIC LOAD FACTOR DERIVED FROM THE TORUS STRUCTURAL MODEL. AS AN ALTERNATIVE, THE 1.0 MULTIPLIER MAY BE REPLACED BY THE PLANT UNIQUE RATIO OF THE SUPPRESSION CHAMBER DYNAMIC FAILURE PRESSURE TO THE STATIC FAILURE PRESSURE.
- (7) SRV ACTUATION IS ASSUMED TO OCCUR COINCIDENT WITH THE POOL SWELL EVENT. ALTHOUGH SRV ACTUATION CAN OCCUR LATER IN THE DBA, THE RESULTING AIR LOADING ON THE SUPPRESSION CHAMBER SHELL IS NEGLIGIBLE SINCE THE AIR AND WATER INITIALLY IN THE LINE WILL BE CLEARED AS THE DRYWELL-TO-WETWELL ΔP INCREASES DURING THE DBA TRANSIENT.

Table 1-3.2-2

EVENT COMBINATIONS AND SERVICE LEVELS
FOR CLASS 2 AND 3 PIPING

EVENT COMBINATIONS			SRV		SRV + EQ		SBA IBA		SBA + EQ IBA + EQ				SBA+SRV IBA+SRV		SBA + SRV + EQ IBA + SRV + EQ				DBA		DBA + EQ				DBA+SRV		DBA + EQ + SRV			
								CO, CII		CO, CH		CO, CH		CO, CH	PS (1)	CO, CH	PS	CO, CH	PS	CO, CH	PS	CO, CH	PS	CO, CH						
TYPE OF EARTHQUAKE				0	S			0	S	0	S			0	S	0	S			0	S	0	S			0	S	0	S	
COMBINATION NUMBER			1	2	3	4	5	6	7	8	9	10	11	12	13	14	15	16	17	18	19	20	21	22	23	24	25	26	27	
LOADS	NORMAL (2)	N	X	X	X	X	X	X	X	X	X	X	X	X	X	X	X	X	X	X	X	X	X	X	X	X	X	X	X	
	EARTHQUAKE	EQ		X	X			X	X	X	X			X	X	X	X			X	X	X	X			X	X	X	X	
	SRV DISCHARGE	SRV	X	X	X							X	X	X	X	X	X							X	X(6)	X	X	X(6)	X(6)	
	THERMAL	T _A	X	X	X	X	X	X	X	X	X	X	X	X	X	X	X	X	X	X	X	X	X	X	X	X	X	X	X	
	PIPE PRESSURE	P _A	X	X	X	X	X	X	X	X	X	X	X	X	X	X	X	X	X	X	X	X	X	X	X	X	X	X	X	
	LOCA POOL SWELL	P _{PS}																X		X	X			X		X	X			
	LOCA CONDENSATION OSCILLATION	P _{CO}					X			X	X		X			X	X		X			X			X			X		
LOCA CHUGGING	P _{CII}					X			X	X		X			X	X		X			X	X		X			X	X		
STRUCTURAL ELEMENT			ROW																											
ESSENTIAL PIPING SYSTEMS	WITH IBA/DBA	10	B	B (3)	B (3)	B (4)	B (4)	B (4)	B (4)	B (4)	B (4)	B (4)	B (4)	B (4)	B (4)	B (4)	B (4)	B (4)	B (4)	B (4)	B (4)	B (4)	B (4)	B (4)	B (4)	B (4)	B (4)	B (4)	B (4)	
	WITH SBA	11				B (3)	B (3)	B (4)	B (4)	B (4)	B (4)	B (3)	B (3)	B (4)	B (4)	B (4)	B (4)	-	-	-	-	-	-	-	-	-	-	-	-	
NONESSENTIAL PIPING SYSTEMS	WITH IBA/DBA	12	B	C (5)	D (5)	D (5)	D (5)	D (5)	D (5)	D (5)	D (5)	D (5)	D (5)	D (5)	D (5)	D (5)	D (5)	D (5)	D (5)	D (5)	D (5)	D (5)	D (5)	D (5)	D (5)	D (5)	D (5)	D (5)	D (5)	
	WITH SBA	13				C (5)	C (5)	D (5)	D (5)	D (5)	D (5)	D (5)	D (5)	D (5)	D (5)	D (5)	D (5)	-	-	-	-	-	-	-	-	-	-	-	-	

NOTES TO TABLE 1-3.2-2

- (1) REFERENCE 2 STATES "WHERE A DRYWELL-TO-WETWELL PRESSURE DIFFERENTIAL IS NORMALLY UTILIZED AS A LOAD MITIGATOR, AN ADDITIONAL EVALUATION SHALL BE PERFORMED WITHOUT SRV LOADINGS BUT ASSUMING THE LOSS OF THE PRESSURE DIFFERENTIAL. SERVICE LEVEL D LIMITS SHALL APPLY FOR ALL STRUCTURAL ELEMENTS OF THE PIPING SYSTEM FOR THIS EVALUATION. THE ANALYSIS NEED ONLY BE ACCOMPLISHED TO THE EXTENT THAT INTEGRITY OF THE FIRST PRESSURE BOUNDARY ISOLATION VALUE IS DEMONSTRATED. IF THE NORMAL PLANT OPERATING CONDITION DOES NOT EMPLOY A DRYWELL-TO-WETWELL PRESSURE DIFFERENTIAL, THE LISTED SERVICE LEVEL ASSIGNMENTS SHALL BE APPLICABLE." SINCE DAEC DOES NOT UTILIZE A DRYWELL-TO-WETWELL DIFFERENTIAL PRESSURE, THE LISTED SERVICE LIMITS ARE APPLIED.
- (2) NORMAL LOADS (N) CONSIST OF DEAD LOADS (D).
- (3) AS AN ALTERNATIVE, THE $1.2 S_h$ LIMIT IN EQUATION 9 OF NC-3652.2 MAY BE REPLACED BY $1.8 S_h$, PROVIDED THAT ALL OTHER LIMITS ARE SATISFIED. FATIGUE REQUIREMENTS ARE APPLICABLE TO ALL COLUMNS, WITH THE EXCEPTION OF 16, 18, 19, 22, 24 AND 25.
- (4) FOOTNOTE 3 APPLIES EXCEPT THAT INSTEAD OF USING $1.8 S_h$ IN EQUATION 9 OF NC-3652.2, $2.4 S_h$ IS USED.
- (5) EQUATION 10 OF NC OR ND-3659 WILL BE SATISFIED, EXCEPT THE FATIGUE REQUIREMENTS ARE NOT APPLICABLE TO COLUMNS 16, 18, 19, 22, 24 AND 25 SINCE POOL SHELL LOADINGS OCCUR ONLY ONCE. IN ADDITION, IF OPERABILITY OF AN ACTIVE COMPONENT IS REQUIRED TO ENSURE CONTAINMENT INTEGRITY, OPERABILITY OF THAT COMPONENT MUST BE DEMONSTRATED.
- (6) SRV ACTUATION IS ASSUMED TO OCCUR COINCIDENT WITH THE POOL SWELL EVENT. ALTHOUGH SRV ACTUATION CAN OCCUR LATER IN THE DBA, THE RESULTING AIR LOADING ON THE SUPPRESSION CHAMBER SHELL IS NEGLIGIBLE SINCE THE AIR AND WATER INITIALLY IN THE LINE WILL BE CLEARED AS THE DRYWELL-TO-WETWELL ΔP INCREASES DURING THE DBA TRANSIENT.

The general structural analysis techniques proposed by the Mark I Owners Group are utilized with sufficient detail to account for all significant structural response modes and are consistent with the methods used to develop the loading functions defined in the LDR. For those loads considered in the original design but not redefined by the LDR, either the results of the original analysis are used or a new analysis is performed, based on the methods employed in the original plant design.

The damping values used in the analysis of dynamic loading events are those specified in Regulatory Guide 1.61, "Damping Values for Seismic Design of Nuclear Power Plants" (Reference 6) as required by NUREG-0661.

The structural responses resulting from two dynamic phenomena are combined by the absolute sum method. Time phasing of the two responses is such that the combined state of the stress results in the maximum stress intensity.

This section presents the load definition procedures used to develop the DAEC hydrodynamic loads and is organized in accordance with NUREG-0661, Section 3. Table 1-4.0-1 provides a cross-reference between the sections of this PUAR and the sections of Appendix A of NUREG-0661 where each load or event is addressed.

Table 1-4.0-1

PLANT UNIQUE ANALYSIS/NUREG-0661 LOAD SECTIONS
CROSS-REFERENCE

LOAD/EVENT	PUA SECTION	NUREG-0661 APPENDIX A SECTION
CONTAINMENT PRESSURE AND TEMPERATURE RESPONSE	1-4.1.1	2.0
VENT SYSTEM DISCHARGE LOADS	1-4.1.2	2.2
POOL SWELL LOADS ON TORUS SHELL	1-4.1.3	2.3 & 2.4
POOL SWELL LOADS ON ELEVATED STRUCTURES	1-4.1.4	2.6 - 2.10
POOL SWELL LOADS ON SUBMERGED STRUCTURES	1-4.1.5 & 1-4.1.6	2.14.1 & 2.14.2
CONDENSATION OSCILLATION LOADS ON TORUS SHELL	1-4.1.7.1	2.11.1
CONDENSATION OSCILLATION LOADS ON DOWNCOMERS AND VENT SYSTEM	1-4.1.7.2	2.11.2
CONDENSATION OSCILLATION LOADS ON SUBMERGED STRUCTURES	1-4.1.7.3	2.14.5
CHUGGING LOADS ON TORUS SHELL	1-4.1.8.1	2.12.1
CHUGGING LOADS ON DOWNCOMERS	1-4.1.8.2	2.12.2
CHUGGING LOADS ON SUBMERGED STRUCTURES	1-4.1.8.3	2.14.6
SRV ACTUATION CASES	1-4.2.1	2.13.7
SRV DISCHARGE LINE CLEARING LOADS	1-4.2.2	2.13.2 & 2.13.1
SRV LOADS ON TORUS SHELL	1-4.2.3	2.13.3
SRV LOADS ON SUBMERGED STRUCTURES	1-4.2.4	2.14.3 & 2.14.4
DESIGN BASIS ACCIDENT	1-4.3.1	3.2.1(1)
INTERMEDIATE BREAK ACCIDENT	1-4.3.2	3.2.1(1)
SMALL BREAK ACCIDENT	1-4.3.2	3.2.1(1)

(1) SECTIONS OF THE MAIN BODY OF NUREG-0661.

This subsection describes the procedures used to define the DAEC LOCA-related hydrodynamic loads. The sources of structural loads generated during a LOCA are primarily a result of the following conditions.

- o Pressures and temperatures within the drywell, vent system and wetwell,
- o Fluid flow through the vent system,
- o Initial LOCA bubble formation in the pool and the resulting displacement of water due to pool swell, and
- o Steam flow into the suppression pool (condensation oscillation and chugging).

For postulated pipe breaks inside the drywell, three LOCA categories are considered. These three categories, selected on the basis of break size, are referred to as the Design Basis Accident (DBA), Intermediate Break Accident (IBA) and Small Break Accident (SBA).

The DBA for the Mark I containment design is the instantaneous guillotine rupture of the largest pipe in the primary system (recirculation suction line). This LOCA leads to a specific combination of dynamic, quasi-static, and static loads. However, the DBA does not represent the limiting case for all loads and structural responses. Consequently, an IBA and an SBA are also evaluated. The IBA is evaluated as a 0.1 ft^2 instantaneous liquid line break in the primary system, and the SBA is evaluated as a 0.01 ft^2 instantaneous steam line break in the primary system.

The drywell and suppression chamber transient pressure and temperature responses are calculated using the General Electric Company Pressure Suppression Containment Analytical Model (Reference 7). This analytical model calculates the thermodynamic response of the drywell, vent system, and suppression chamber volumes to mass and energy released from the primary system following a postulated LOCA.

The containment pressure and temperature analyses are performed in accordance with Appendix A of NUREG-0661 and are documented in the PULD (Reference 8).

1-4.1.2 Vent System Discharge Loads

Of the three postulated LOCA categories, the DBA causes the most rapid pressurization of the containment system, the largest vent system mass flow rate, and therefore the most severe vent system thrust loads. The pressurization of the containment for the IBA and SBA is much less rapid than for the DBA. Thus, the resulting vent system thrust loads for the SBA and IBA are bounded by the DBA thrust loads. Consequently, vent system thrust loads are evaluated only for the DBA.

Reaction loads occur on the vent system (main vent, vent header, and downcomers) following a LOCA due to pressure imbalances between the vent system and the surrounding torus airspace, and due to forces resulting from changes in flow direction.

The LDR thrust equations consider these forces due to pressure distributions and momentum to define horizontal and vertical thrust forces. These equations are included in the analytical procedures applied to the main vents, vent header, and downcomer portions of the vent system.

Because main vents and downcomers are located symmetrically about the center of the vent system, the horizontal vent system thrust loads cancel each other, resulting in a zero effective horizontal vent system thrust load.

The bases, analytical procedures, and assumptions used to calculate thrust loads are described in the LDR. The DAEC plant unique DBA thrust loads for the main vent, the vent header, and the downcomers are based on a zero initial drywell-to-wetwell pressure differential. The thrust loads used in this PUA are documented in the PULD (Reference 8).

The analysis of the vent system is presented in Volume 3 of the PUAR. The vent system discharge loads are developed in accordance with Appendix A of NUREG-0661.

During the postulated LOCA, the air initially in the drywell and vent system is injected into the suppression pool, producing a downward reaction force on the suppression chamber followed by an upward reaction force. These vertical loads create a dynamic imbalance of forces on the suppression chamber, which acts in addition to the weight of the water applied to the suppression chamber. This dynamic force time history lasts for only a few seconds.

The bases, assumptions, and justifications for the pool swell loads on the suppression chamber shell due to the DBA are described in the LDR. The pool swell loads on the suppression chamber shell are based on a series of DAEC plant unique tests conducted in the Quarter-Scale Test Facility (QSTF) (Reference 9). The loads developed from these QSTF tests are documented in the PULD (Reference 8). The pool swell loads on the suppression chamber shell used in the PUA are based on the information in the PULD with the addition of the upload and download margins specified in Appendix A of NUREG-0661.

From the plant unique average submerged pressure and the suppression chamber air pressure time-histories, the local submerged pressure transients at different locations on the shell are calculated using the LDR methodology and the criteria given in NUREG-0661.

In order to perform pool swell analysis of the suppression chamber shell and supports, shell loads are divided into static and dynamic components. This is accomplished by subtracting the airspace pressures from the local submerged pressures.

Suppression chamber shell load development procedures, methodology, and assumptions are in accordance with Appendix A of NUREG-0661.

This subsection describes the load definition procedures used to define the following hydrodynamic loads on the main vent line, vent header, catwalk, and other structures initially above normal water level.

- Pool Swell Impact and Drag Load
- Froth Impingement Load, Region I
- Froth Impingement Load, Region II
- Pool Fallback Load
- Froth Fallback Load

The analysis of the effect of pool swell loads on elevated structures is presented in Volumes 3 and 4 of this PUAR.

1-4.1.4.1 Impact and Drag Loads on the Vent System

In the event of a postulated design basis LOCA, the pool surface rises during the pool swell phase and impacts structures in its path. The resulting loading condition of primary interest is the impact on the vent system. The impact phenomenon consists of two events: the impact of the pool on the structure and the drag on the structure as the pool flows past it following impact. The load definition includes both the impact and drag portions of the loading transient (Figures 1-4.1-1 and 1-4.1-2).

The vent system components which are potentially impacted during pool swell include the vent header (vent bay), the vent header deflector, and the vent lines. There are no vent header impact or drag loads in the non-vent bay and part of the vent bay due to the presence of the vent header deflector. This was determined from plant unique quarter-scale tests with a deflector in place (Reference 9).

The vent header deflector loads are developed on a plant unique basis. The bases, assumptions, and justifications for vent header deflector impact loads

are provided in the LDR. The PULD (Reference 8) presents the full-scale loads for the DAEC deflector. These loads are based on a zero initial drywell-to-wetwell pressure differential and include the load definition requirements specified in Appendix A of NUREG-0661.

Pool swell impact and drag loads on the main vent line are calculated using the procedure specified in Appendix A of NUREG-0661. The pool swell loads on the vent header and the vent header deflector are also calculated in accordance with Appendix A of NUREG-0661.

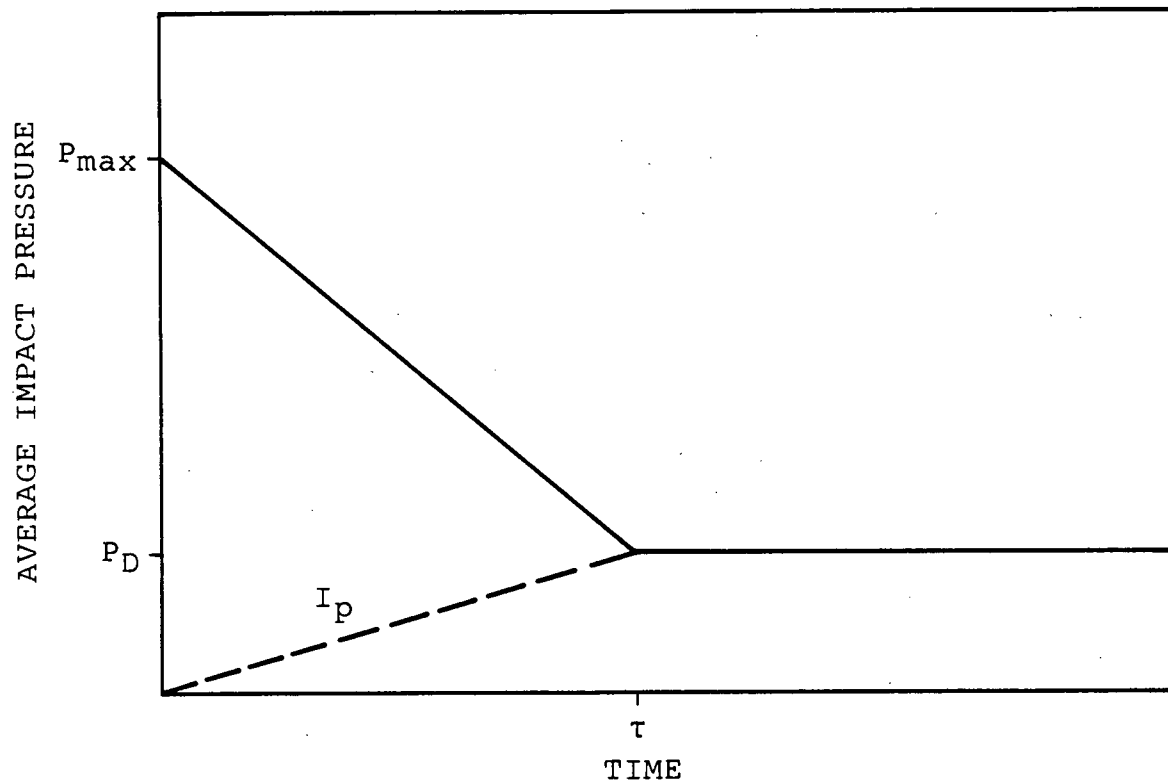


Figure 1-4.1-1

PULSE SHAPE FOR WATER IMPACT ON CYLINDRICAL TARGETS

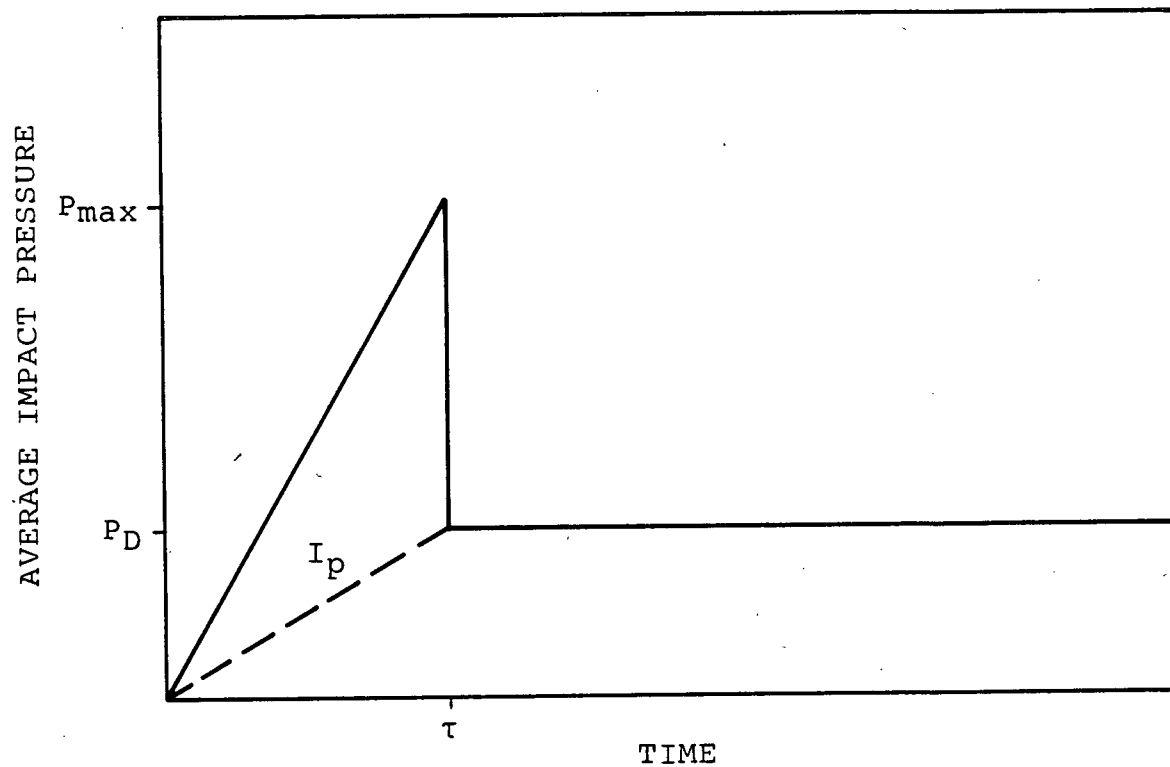


Figure 1-4.1-2

PULSE SHAPE FOR WATER IMPACT ON FLAT TARGETS

1-4.1.4.2 Impact and Drag Loads on Other Structures

As the pool surface rises due to the bubbles forming at the downcomer exits, it may impact structures located in the wetwell airspace. In the present context, "other structures" are defined as all structures located above the initial pool surface, exclusive of the vent system.

Section 4.3.4.6 of the LDR presents the bases, assumptions and methodology used in determining the pool swell impact and drag loads on structures located above the pool surface. These load specifications correspond to impact on "rigid" structures.

Impact and drag load development and application is in accordance with Appendix A of NUREG-0661.

1-4.1.4.3 Pool Swell Froth Impingement Loads

During the final stages of the pool swell phase of a DBA LOCA, the rising pool breaks up into a two-phase froth of air and water. This froth rises above the pool surface and may impinge on structures within the suppression chamber airspace. Subsequently, when the froth falls back, it creates froth fallback loads. There are two mechanisms by which froth may be generated.

Region I Froth

As the rising pool strikes the bottom of the vent header or the vent header deflector, a froth spray is formed, which travels upward and to both sides of the vent header. This is defined as the Region I froth impingement zone (Figure 1-4.1-3).

Region II Froth

A portion of the water above the expanding air bubble becomes detached from the bulk pool. This water is influenced only by its own inertia and gravity. The "bubble breakthrough" creates a froth which rises

into the airspace beyond the maximum bulk pool swell height. This is defined as the Region II froth impingement zone (Figure 1-4.1-4).

LDR methods are used to define the froth impingement loads for Region I. For the Region I froth formation, the LDR method assumes the froth density to be 20% of full water density for structures with maximum cross-section dimensions of less than 1 foot, and a proportionally lower density for structures greater than 1 foot. For the catwalk, the load is applied in the direction most critical to the structure within the region of load application as defined in the LDR. For the monorail, the direction of load application is as observed in the QSTF. The load is applied as a step function for a duration of 80 milliseconds for the catwalk and a duration of 10 milliseconds for the monorail.

The froth density of Region II is assumed to be 100% water density for structures or sections of structures with a maximum cross-sectional dimension less than or equal to 1 foot, 25% water density for structures greater than 1 foot, and 10% water density for structures located within the projected region

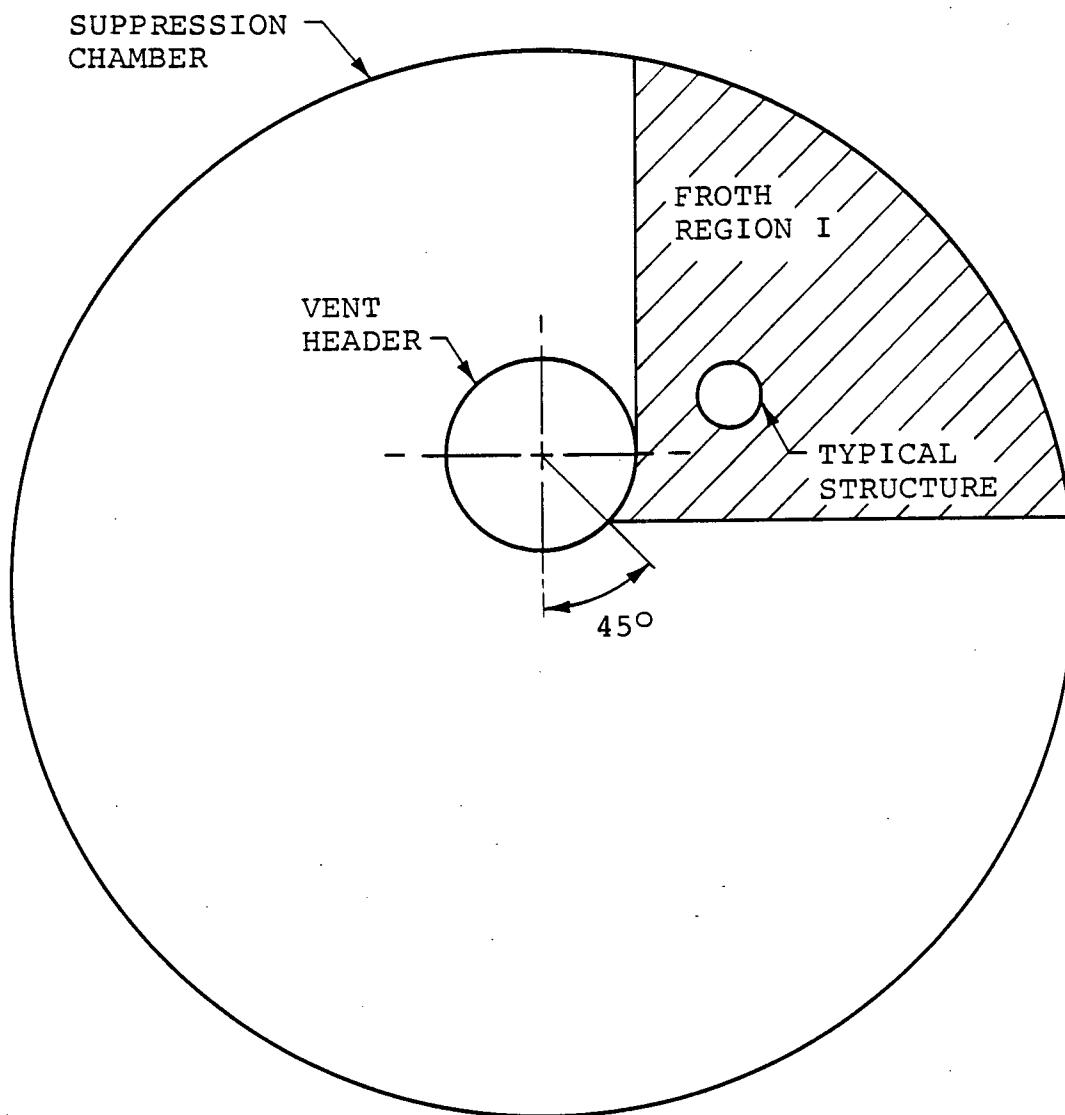
directly above the vent header. The load is applied in the direction most critical to the structure within the region of load application as defined in the LDR. The load is applied as a rectangular pulse with a duration of 100 milliseconds.

For some structures, the procedures described above result in unrealistically conservative loads. In these situations the alternate procedure outlined in Appendix A of NUREG-0661 is used. This procedure consists of calculating Region I froth loads from high-speed QSTF movies. In this case, the froth source velocity, mean jet angle, froth duration, and froth density in Region I are derived from a detailed analysis of the QSTF plant specific high-speed films.

With either methodology for Region I, the vertical component of the source velocity is decelerated to the elevation of the target structure to obtain the froth impingement velocity. The load is applied in the direction most critical to the structure within the sector obtained from QSTF movies. The QSTF movies were used to check if a structure was impinged by Region I froth. Uncertainty limits for each parameter are applied to assure a conservative load specification.

The froth fallback pressure is based on the conservative assumption that all of the froth fallback momentum is transferred to the structure. The froth velocity is calculated by allowing the froth to fall freely from the height of the upper suppression chamber shell directly above the subject structure. The froth fallback pressure is applied uniformly to the upper projected area of the structure being analyzed in the direction most critical to the behavior of the structure. The froth fallback is specified to start when the froth impingement load ends and lasts for 1.0 second. The range of direction of application is directed downward ± 45 degrees from the vertical.

The pool swell froth impingement and froth fallback loads used in the PUA are in accordance with Appendix A of NUREG-0661.



1. REGION IS SYMMETRIC ON BOTH SIDES OF VENT HEADER.

Figure 1-4.1-3

FROTH IMPINGEMENT ZONE - REGION I

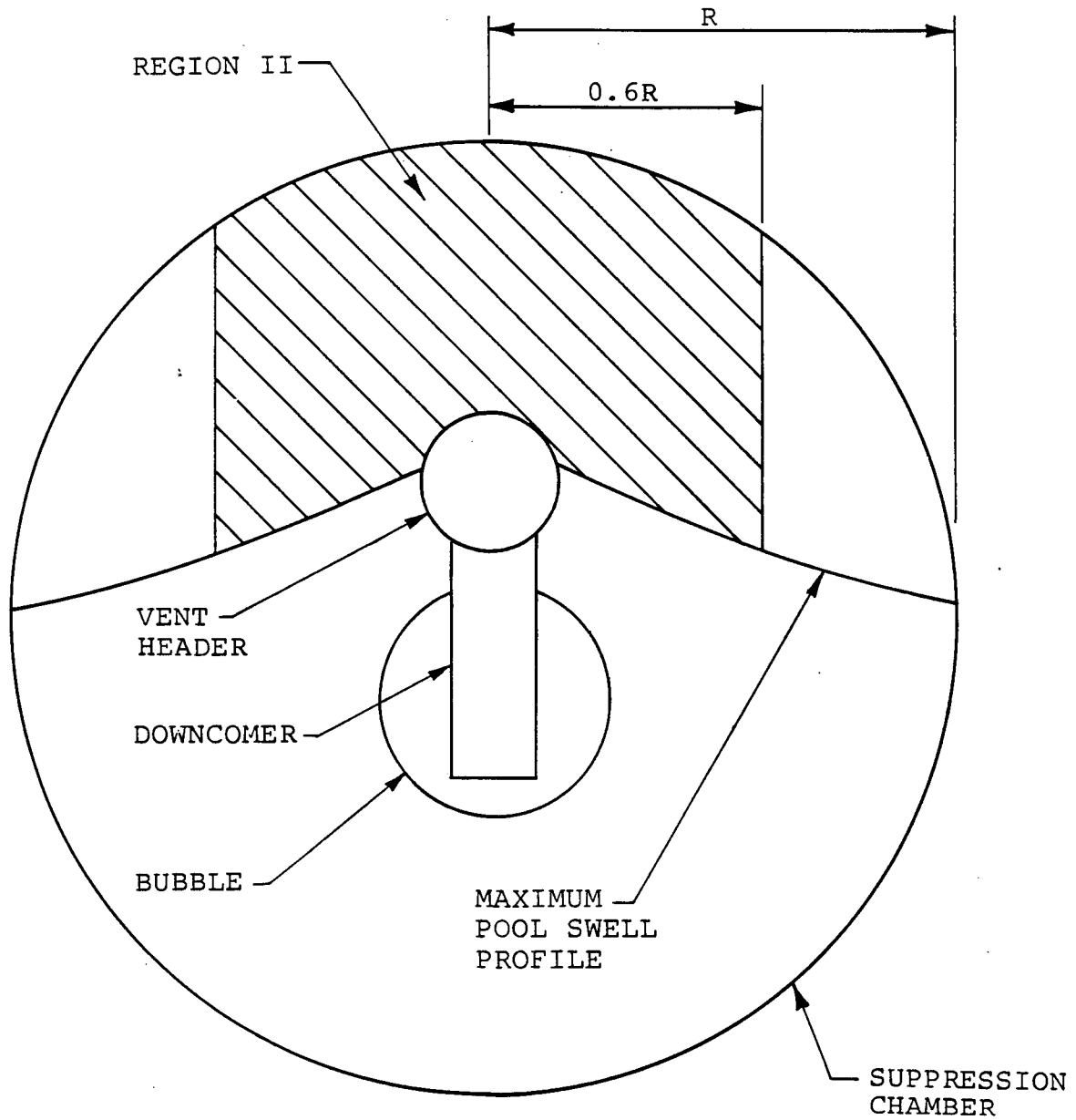


Figure 1-4.1-4
FROTH IMPINGEMENT ZONE - REGION II

1-4.1.4.4 Pool Fallback Loads

This subsection describes pool fallback loads which apply to structures within the suppression chamber that are below the upper surface of the pool at its maximum height and above the downcomer exit level. After the pool surface has reached maximum height as a result of pool swell, it falls back under the influence of gravity and creates drag loads on structures inside the suppression chamber. The structures affected are between the maximum bulk pool swell height and the downcomer exit level, or immersed in an air bubble extending beneath the downcomer exit level.

For structures immersed in the pool, the drag force during fallback (as described in the LDR) is the sum of standard drag (proportional to velocity squared) and acceleration drag (proportional to acceleration). For structures which are beneath the upper surface of the pool but within the air bubble, there is an initial load associated with resubmergence of the structure by either an irregular impact with the bubble-pool interface or a process similar to froth fallback. This initial load is bounded by the

standard drag because conservative assumptions are made in calculating the standard drag.

The load calculation procedure, as described in the LDR, requires determination of the maximum pool swell height above the height of the top surface of the structure. Freefall of the bulk fluid from this height is assumed and this produces both standard drag and acceleration drag, with the total drag given by the sum.

The LDR procedure results in a conservative calculation of the velocity since it is unlikely that any appreciable amount of pool fluid will be in freefall through this entire distance. The maximum pool swell height is determined from the QSTF plant unique tests (References 9 and 10).

The procedures outlined in Appendix A of NUREG-0661 are used to account for interference effects associated with both standard and acceleration drag forces.

Structures which may be enveloped by the LOCA bubble are evaluated for potential fallback loads as a

result of bubble collapse to ensure that such loads are not larger than the LOCA bubble drag loads (Section 1-4.1.6).

The fallback load is applied uniformly over the upper projected surface of the structure in the direction most critical to the behavior of the structure. The range of ± 45 degrees from the vertical is applied to both the radial and longitudinal planes of the suppression chamber.

The procedures used in the PUA to determine pool fallback loads are in accordance with Appendix A of NUREG-0661.

As the drywell pressurizes during a postulated DBA LOCA, the water slug initially standing in the submerged portion of the downcomer vents is accelerated downward into the suppression pool. As the water slug enters the pool, it forms a jet which could potentially load structures which are intercepted by the discharge. Forces due to the pool acceleration and velocity induced by the advancing jet front are also created.

LOCA water jet loads affect structures which are enclosed by the jet boundaries and last from the time that the jet first reaches the structure until the time when the last particle of the water slug passes the structure. Pool motion can create loads on structures which are within the region of motion for the duration of the water jet. The assumptions included in the methodology are presented in the LDR.

The calculation procedure used to obtain LOCA jet loads is based on experimental data obtained from tests performed at the Quarter-Scale Test Facility (Reference 10) and on the analytical model described

in Reference 1. Figure 1-4.1-5 shows plant unique downcomer clearing information, obtained experimentally during the QSTF testing in the form of LOCA jet fluid velocity and acceleration time-histories.

As the jet travels through the pool, the particles at the rear of the water slug, which were discharged from the downcomer at higher velocities, catch up with particles at the front of the water slug, which were discharged at lower velocities. When this "overtaking" occurs both particles are assumed to continue on at the higher velocity. As the rear particles catch up to the particles in front, the jet becomes shorter and wider. When the last fluid particle leaving the downcomer catches up to the front of the jet, the jet dissipates.

Forces due to pool motion induced by the advancing jet are calculated for structures that are within four downcomer diameters below the downcomer exit elevation. The flow field, standard drag and acceleration drag are calculated using the equations in the LDR.

Structures that are within four downcomer diameters below the downcomer exit elevation will sustain a loading, first from the flow field induced by the jet, then from the jet itself if it is within the cross-section of the jet. Forces resulting from the flow field are due to standard drag and acceleration drag. The force from the jet is due to standard drag only, since particles within the jet travel at constant discharge velocity (i.e., there is no acceleration).

The standard drag force on the submerged structure is computed based on the normal velocity component of the jet intercepting the structure, the projected area of the structure intercepted by the normal velocity component of the jet, and the jet or flow field area.

For LOCA water jet loads, downcomers are modeled as jet sources for submerged structures based on the location of the structure.

Structures are divided into several sections following the procedure given in the LDR and the criteria given in NUREG-0661. For each section, the

location, acceleration drag volume, drag coefficient and orientation are inputs into the LOCA jet model.

The LOCA water jet loads on circular cross-section structures due to standard and acceleration drag are developed in accordance with Appendix A of NUREG-0661. For structures with sharp corners, these drag loads are calculated considering forces on an equivalent cylinder of diameter $D_{eq} = 2^{1/2} L_{max}$, where L_{max} is the maximum transverse dimension. For acceleration drag, this technique results in unrealistic loads on some structures such as I-beams due to the significant increase in the acceleration drag volume. In these cases, the acceleration drag volumes in Table 1-4.1-1 are used in the acceleration drag load calculation. A literature search concluded that these acceleration drag volumes are appropriate in this application. References 11 and 12 show that the values in Table 1-4.1-1 are applicable for the cases evaluated in this analysis. The LOCA water jet load is a transient load and therefore is applied dynamically.

Table 1-4.1-1

HYDRODYNAMIC MASS AND ACCELERATION DRAG VOLUMES
FOR TWO-DIMENSIONAL STRUCTURAL COMPONENTS
(LENGTH L FOR ALL STRUCTURES)

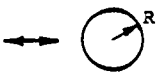
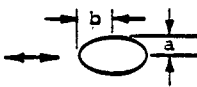
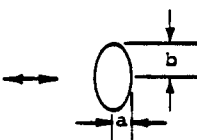
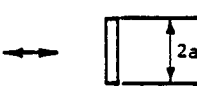

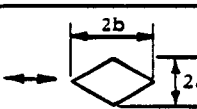
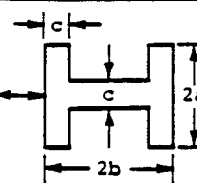
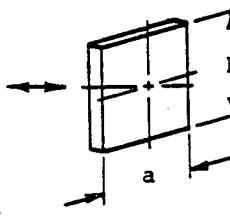
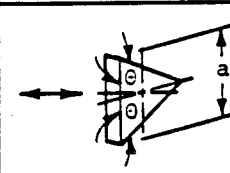
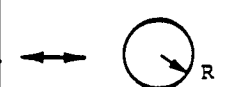
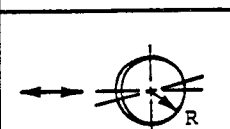
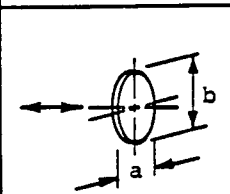
BODY	SECTION THROUGH BODY AND UNIFORM FLOW DIRECTION	HYDRODYNAMIC MASS	ACCELERATION DRAG VOLUME V_A																																			
CIRCLE		$\rho \pi R^2 L$	$2 \pi R^2 L$																																			
ELLIPSE		$\rho \pi a^2 L$	$\pi a(a+b) L$																																			
ELLIPSE		$\rho \pi b^2 L$	$\pi b(a+b) L$																																			
PLATE		$\rho \pi a^2 L$	$\pi a^2 L$																																			
RECTANGLE		<table><tr><td colspan="3"><u>a/b</u></td></tr><tr><td></td><td></td><td>$\rho \pi a^2 L$</td></tr><tr><td>10</td><td>1.14</td><td>$\rho \pi a^2 L$</td></tr><tr><td>5</td><td>1.21</td><td>$\rho \pi a^2 L$</td></tr><tr><td>2</td><td>1.36</td><td>$\rho \pi a^2 L$</td></tr><tr><td>1</td><td>1.51</td><td>$\rho \pi a^2 L$</td></tr><tr><td>1/2</td><td>1.70</td><td>$\rho \pi a^2 L$</td></tr><tr><td>1/5</td><td>1.98</td><td>$\rho \pi a^2 L$</td></tr><tr><td>1/10</td><td>2.23</td><td>$\rho \pi a^2 L$</td></tr></table>	<u>a/b</u>					$\rho \pi a^2 L$	10	1.14	$\rho \pi a^2 L$	5	1.21	$\rho \pi a^2 L$	2	1.36	$\rho \pi a^2 L$	1	1.51	$\rho \pi a^2 L$	1/2	1.70	$\rho \pi a^2 L$	1/5	1.98	$\rho \pi a^2 L$	1/10	2.23	$\rho \pi a^2 L$	<table><tr><td>$aL(4b+a)$</td></tr><tr><td>$aL(4b+1.14\pi a)$</td></tr><tr><td>$aL(4b+1.21\pi a)$</td></tr><tr><td>$aL(4b+1.36\pi a)$</td></tr><tr><td>$aL(4b+1.51\pi a)$</td></tr><tr><td>$aL(4b+1.70\pi a)$</td></tr><tr><td>$aL(4b+1.98\pi a)$</td></tr><tr><td>$aL(4b+2.23\pi a)$</td></tr></table>	$aL(4b+a)$	$aL(4b+1.14\pi a)$	$aL(4b+1.21\pi a)$	$aL(4b+1.36\pi a)$	$aL(4b+1.51\pi a)$	$aL(4b+1.70\pi a)$	$aL(4b+1.98\pi a)$	$aL(4b+2.23\pi a)$
<u>a/b</u>																																						
		$\rho \pi a^2 L$																																				
10	1.14	$\rho \pi a^2 L$																																				
5	1.21	$\rho \pi a^2 L$																																				
2	1.36	$\rho \pi a^2 L$																																				
1	1.51	$\rho \pi a^2 L$																																				
1/2	1.70	$\rho \pi a^2 L$																																				
1/5	1.98	$\rho \pi a^2 L$																																				
1/10	2.23	$\rho \pi a^2 L$																																				
$aL(4b+a)$																																						
$aL(4b+1.14\pi a)$																																						
$aL(4b+1.21\pi a)$																																						
$aL(4b+1.36\pi a)$																																						
$aL(4b+1.51\pi a)$																																						
$aL(4b+1.70\pi a)$																																						
$aL(4b+1.98\pi a)$																																						
$aL(4b+2.23\pi a)$																																						
DIAMOND		<table><tr><td colspan="3"><u>a/b</u></td></tr><tr><td>2</td><td>0.85</td><td>$\rho \pi a^2 L$</td></tr><tr><td>1</td><td>0.76</td><td>$\rho \pi a^2 L$</td></tr><tr><td>1/2</td><td>0.67</td><td>$\rho \pi a^2 L$</td></tr><tr><td>1/5</td><td>0.61</td><td>$\rho \pi a^2 L$</td></tr></table>	<u>a/b</u>			2	0.85	$\rho \pi a^2 L$	1	0.76	$\rho \pi a^2 L$	1/2	0.67	$\rho \pi a^2 L$	1/5	0.61	$\rho \pi a^2 L$	<table><tr><td>$aL(2b+0.85\pi a)$</td></tr><tr><td>$aL(2b+0.76\pi a)$</td></tr><tr><td>$aL(2b+0.67\pi a)$</td></tr><tr><td>$aL(2b+0.61\pi a)$</td></tr></table>	$aL(2b+0.85\pi a)$	$aL(2b+0.76\pi a)$	$aL(2b+0.67\pi a)$	$aL(2b+0.61\pi a)$																
<u>a/b</u>																																						
2	0.85	$\rho \pi a^2 L$																																				
1	0.76	$\rho \pi a^2 L$																																				
1/2	0.67	$\rho \pi a^2 L$																																				
1/5	0.61	$\rho \pi a^2 L$																																				
$aL(2b+0.85\pi a)$																																						
$aL(2b+0.76\pi a)$																																						
$aL(2b+0.67\pi a)$																																						
$aL(2b+0.61\pi a)$																																						
I-BEAM		<table><tr><td colspan="3">$\frac{a}{c} = 2.6 \quad \frac{b}{c} = 3.6$</td></tr><tr><td colspan="3">$2.11 \rho \pi a^2 L$</td></tr></table>	$\frac{a}{c} = 2.6 \quad \frac{b}{c} = 3.6$			$2.11 \rho \pi a^2 L$			$(2.11\pi a^2 + 2c(2a+b-c)) L$																													
$\frac{a}{c} = 2.6 \quad \frac{b}{c} = 3.6$																																						
$2.11 \rho \pi a^2 L$																																						

Table 1-4.1-1

HYDRODYNAMIC MASS AND ACCELERATION DRAG VOLUMES
FOR TWO-DIMENSIONAL STRUCTURAL COMPONENTS

(LENGTH L FOR ALL STRUCTURES)

(Concluded)

BODY	BODY AND FLOW DIRECTION	HYDRODYNAMIC MASS	ACCELERATION DRAG VOLUME V_A
RECTANGULAR PLATE		$\frac{b/a}{\begin{array}{ll} 1 & 0.478 \rho \pi / 4a^2 b \\ 1.5 & 0.680 \rho \pi / 4a^2 b \\ 2 & 0.840 \rho \pi / 4a^2 b \\ 2.5 & 0.953 \rho \pi / 4a^2 b \\ 3 & \rho \pi / 4a^2 b \\ \infty & \rho \pi / 4a^2 b \end{array}}$	$\begin{array}{l} 0.478 \pi / 4a^2 b \\ 0.680 \pi / 4a^2 b \\ 0.840 \pi / 4a^2 b \\ 0.953 \pi / 4a^2 b \\ \pi / 4a^2 b \\ \pi / 4a^2 b \end{array}$
TRIANGULAR PLATE		$\frac{\rho a^3 (\tan \theta)^{3/2}}{3\pi}$	$\frac{a^3 (\tan \theta)^{3/2}}{3\pi}$
SPHERE		$\rho 2\pi R^3 / 3$	$2\pi R^3 / 3$
CIRCULAR DISK		$\rho 8R^3 / 3$	$8R^3 / 3$
ELLIPTICAL DISK		$\frac{b/a}{\begin{array}{ll} \infty & \rho \pi / 6ba^2 \\ 3 & 0.9 \rho \pi / 6ba^2 \\ 2 & 0.826 \rho \pi / 6ba^2 \\ 1.5 & 0.748 \rho \pi / 6ba^2 \\ 1.0 & 0.637 \rho \pi / 6ba^2 \end{array}}$	$\begin{array}{l} \pi / 6ba^2 \\ 0.9 \pi / 6ba^2 \\ 0.826 \pi / 6ba^2 \\ 0.748 \pi / 6ba^2 \\ 0.637 \pi / 6ba^2 \end{array}$

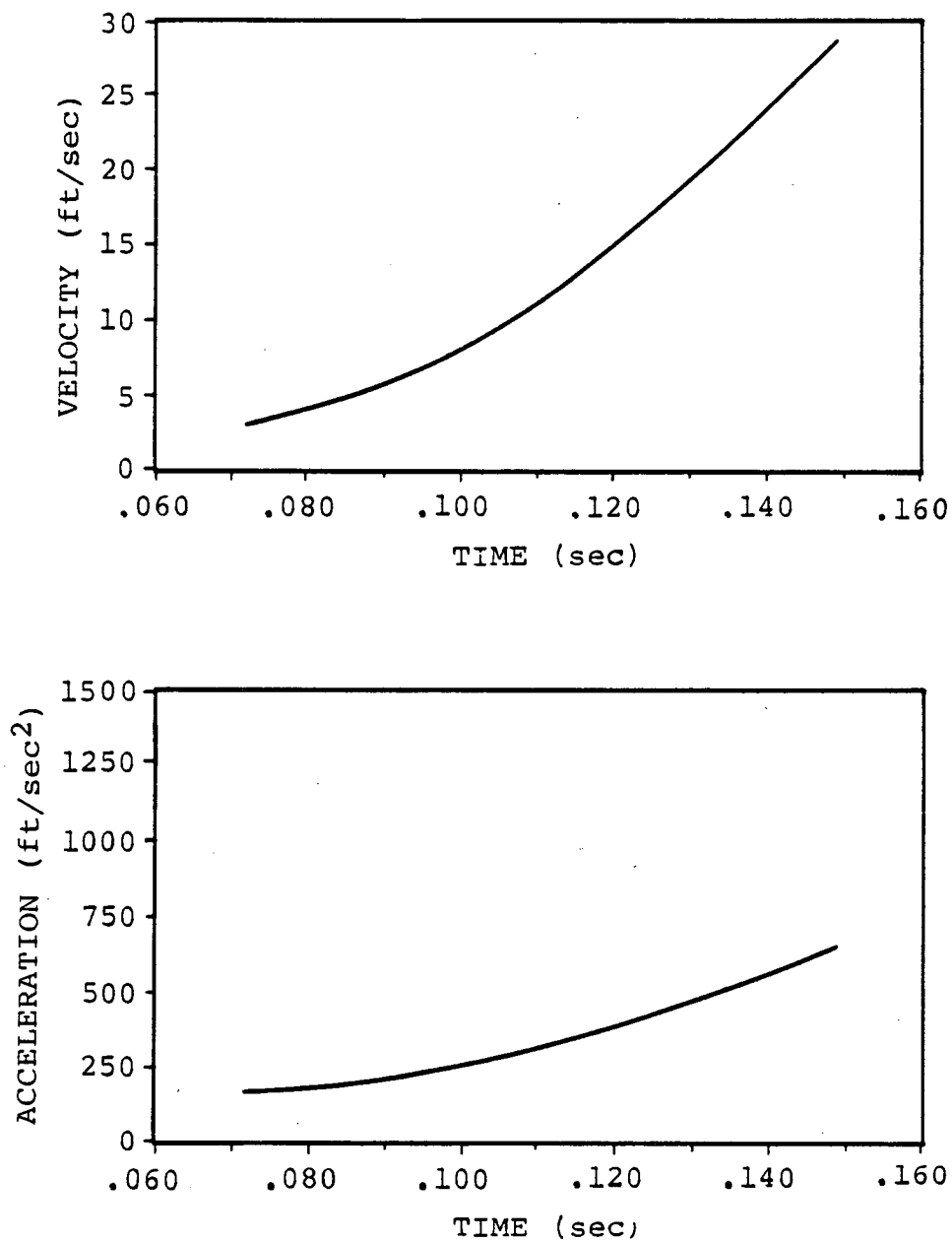


Figure 1-4.1-5
QUARTER-SCALE DOWNCOMER WATER
SLUG EJECTION, TEST 8

During the initial phase of the DBA, pressurized drywell air is purged into the suppression pool through the submerged downcomers. After the vent clearing phase of a DBA, a single bubble is formed around each downcomer. During the bubble growth period, unsteady fluid motion is created within the suppression pool. During this period, all submerged structures below the pool surface will be exposed to transient hydrodynamic loads.

The bases of the flow model and load evaluation for the definition of LOCA bubble-induced loads on submerged structures are presented in Section 4.3.8 of the LDR.

For the phase after contact between bubbles of adjacent downcomers, the pool swell flow field above the downcomer exit elevation is derived from QSTF plant unique tests (Reference 10). After bubble contact, the load will act only vertically. This pool swell drag load is computed using the method described in Section 1-4.1.4.2.

The parameters which affect load determination are torus geometry, downcomer locations, and thermodynamic properties. Table 1-4.1-2 presents these plant specific data. Figure 1-4.1-6 presents the DBA plant unique transient drywell pressure time-history, which is an input into the model.

The torus is modeled as a rectangular cell with dimensions as given in Table 1-4.1-2. The structures are divided into sections and the loads on each section are calculated following the procedure given in the LDR and the criteria given in NUREG-0661.

The procedure used for calculating drag loads on structures with circular and sharp-cornered cross-sections is in accordance with Appendix A of NUREG-0661. For some structures with sharp corners such as I-beams, the acceleration drag volumes are calculated using the information in Table 1-4.1-1. The LOCA bubble loads are transient loads and are therefore applied dynamically.

Table 1-4.1-2

PLANT UNIQUE PARAMETERS
FOR LOCA BUBBLE DRAG LOAD DEVELOPMENT

PARAMETER		VALUE
NUMBER OF DOWNCOMERS PER 1/16 SEGMENT		3
WATER DEPTH IN SUPPRESSION CHAMBER (ft)		10.416
CELL	WIDTH (ft)	25.207
	LENGTH (ft)	19.626
VERTICAL DISTANCE FROM DOWNCOMER EXIT TO TORUS SUPPRESSION CHAMBER CENTERLINE (ft)		5.749
DOWNCOMER	INSIDE RADIUS (ft)	0.979
	SUBMERGENCE (ft)	3.333
UNDISTURBED PRESSURE AT BUBBLE CENTER ELEVATION BEFORE THE BUBBLE APPEARS (psia)		16.568
INITIAL DRYWELL	PRESSURE BEFORE LOCA (psia)	14.7
	TEMPERATURE BEFORE LOCA (°F)	135
OVERALL VENT PIPE FRICTION FACTOR (f _l /d)		4.0
INITIAL LOCA BUBBLE WALL VELOCITY (ft/sec)		12.965

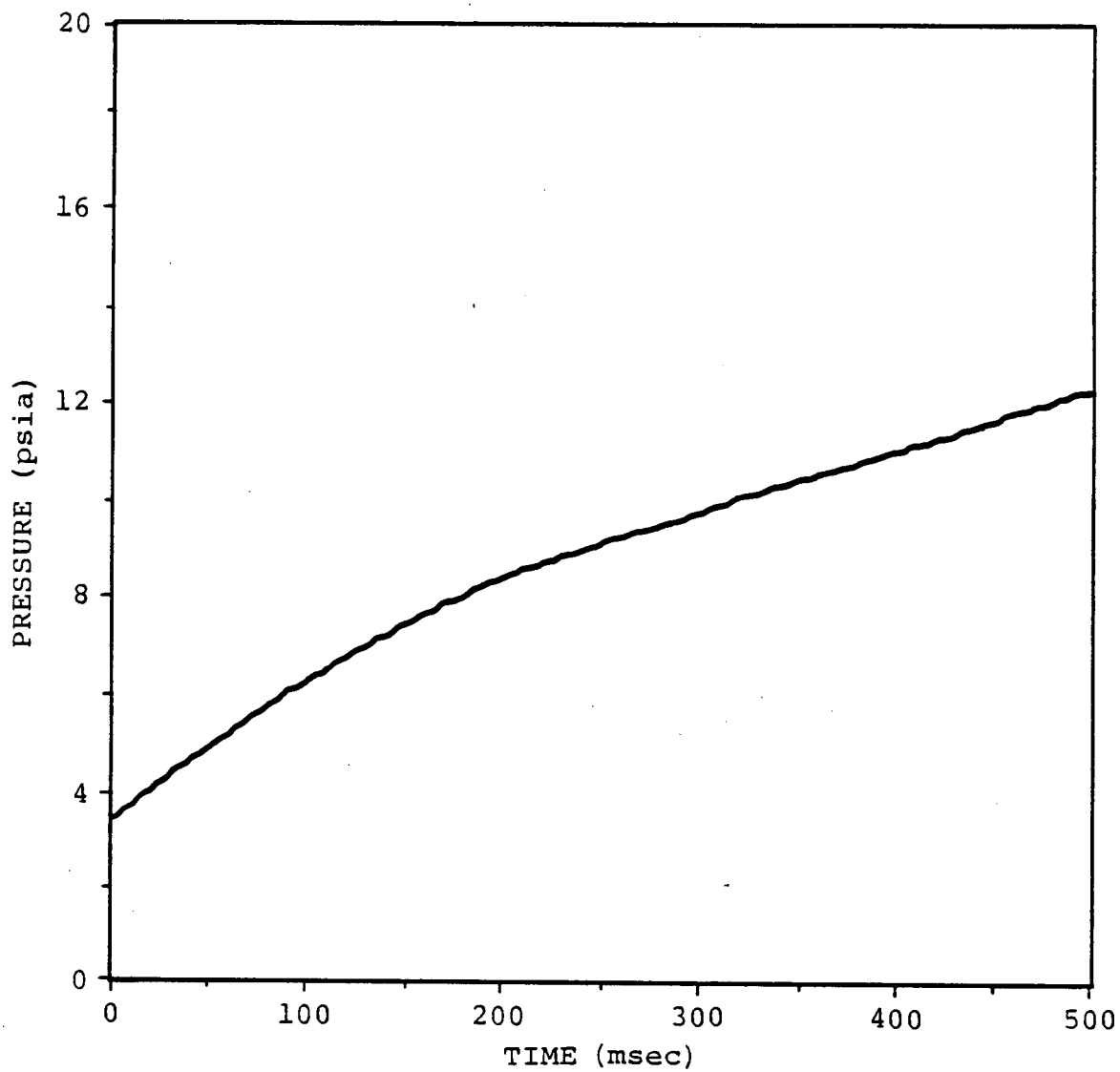


Figure 1-4.1-6

QUARTER-SCALE DRYWELL PRESSURE
TIME-HISTORY

IOW-40-199-1
Revision 0

1-4.35

1-4.1.7 Condensation Oscillation Loads

This subsection describes the condensation oscillation loads on the various structures and components in the suppression chamber.

Following the pool swell transient of a postulated LOCA, there is a period during which condensation oscillations occur at the downcomer exit. Condensation oscillations are associated with the pulsating movement of the steam-water interface caused by variations in the condensation rate at the downcomer exit. These condensation oscillations cause periodic pressure oscillations on the torus shell, on submerged structures and in the vent system. The loads specified for condensation oscillation are based on the Full-Scale Test Facility (FSTF) tests (References 13, 14, and 15). The LDR and NUREG-0661 discuss the bases, assumptions and methodology for computation of the condensation oscillation loads.

1-4.1.7.1 CO Loads on the Suppression Chamber Shell

Loads on the submerged portion of the suppression chamber shell during the condensation oscillation phenomenon consist of pressure oscillations superimposed on the prevailing local static pressures.

The condensation oscillation load on the suppression chamber shell is a rigid wall load specified in terms of the pressure at the suppression chamber bottom dead center. It is used in conjunction with a flexible wall coupled fluid-structural model of the torus. The LDR load definition for condensation oscillation consists of 50 harmonic loadings with amplitudes which vary with frequency. Three alternate rigid wall pressure amplitude variations with frequency are specified in the LDR. A fourth alternate load case is also considered based on the results of Test M12 from the supplemental test series conducted at the FSTF (References 14 and 15). The rigid wall pressure amplitude variation with frequency is given in Table 1-4.1-3 and Figure 1-4.1-7. The alternate frequency spectrum which produces the maximum total response is used for design.

The effects of all harmonics must be summed to obtain the total response of the structure. Random phasing of the loading harmonics is assumed, based on experimental observations and subsequent analysis.

The implementation of the random phasing approach is accomplished by multiplying the absolute sum of the responses of all 50 harmonics by a scale factor. This scale factor is calculated using cumulative distribution function (CDF) curves of the responses at 14 locations on the FSTF suppression chamber shell. Each of the CDF curves is generated using 200 sets of random phase angles. Using this approach, a scale factor of 0.65 is developed which results in a non-exceedance probability of 84% at a confidence level of 90%. This scale factor is applied to the absolute sum of the responses of all 50 harmonics for all DAEC suppression chamber shell locations evaluated.

Table 1-4.1-4 compares measured and calculated FSTF response to CO loads. The calculated FSTF response in Table 1-4.1-4 is determined using CO load Alternates 1, 2, and 3 and the random phasing approach described above. In all cases the calculated

response is greater than the measured response, demonstrating the conservatism of this approach. Although not shown in Table 1-4.1-4, CO load Alternate 4 adds approximately 20% to the calculated shell response. Thus using Alternate 4 in the DAEC analysis contributes additional conservatism to the comparison shown in Table 1-4.1-4.

Table 1-4.1-5 lists the onset times and durations for condensation oscillation. Test results indicate that for the postulated IBA, condensation oscillation loads are bounded by chugging loads. Test results also indicate that for the postulated SBA, condensation oscillation loads are not significant; therefore, none are specified.

The longitudinal condensation oscillation pressure distribution along the suppression chamber centerline is uniform. The cross-sectional variation of the suppression chamber wall pressure varies linearly with elevation from zero at the water surface to a maximum at the suppression chamber bottom (Figure 1-4.1-8).

Since suppression chamber dimensions and the number of downcomers vary, the magnitude of the condensation oscillation load differs for each Mark I plant. A multiplication factor was developed to account for the effect of the pool-to-vent area ratio. This factor is 0.825 for DAEC (Figure 1-4.1-9) and was developed using the method described in the LDR. The DAEC unique condensation oscillation load is determined by multiplying the amplitude of the baseline rigid wall load (Table 1-4.1-3) by this factor.

Table 1-4.1-3

DBA CONDENSATION OSCILLATION TORUS
SHELL PRESSURE AMPLITUDES

FREQUENCY INTERVALS (Hz)	MAXIMUM PRESSURE AMPLITUDE (psi)			
	ALTERNATE 1	ALTERNATE 2	ALTERNATE 3	ALTERNATE 4
0-1	0.29	0.29	0.29	0.25
1-2	0.25	0.25	0.25	0.28
2-3	0.32	0.32	0.32	0.33
3-4	0.48	0.48	0.48	0.56
4-5	1.86	1.20	0.24	2.71
5-6	1.05	2.73	0.48	1.17
6-7	0.49	0.42	0.99	0.97
7-8	0.59	0.38	0.30	0.47
8-9	0.59	0.38	0.30	0.34
9-10	0.59	0.38	0.30	0.47
10-11	0.34	0.79	0.18	0.49
11-12	0.15	0.45	0.12	0.38
12-13	0.17	0.12	0.11	0.20
13-14	0.12	0.08	0.08	0.10
14-15	0.06	0.07	0.03	0.11
15-16	0.10	0.10	0.02	0.08
16-17	0.04	0.04	0.04	0.04
17-18	0.04	0.04	0.04	0.05
18-19	0.04	0.04	0.04	0.03
19-20	0.27	0.27	0.27	0.34
20-21	0.20	0.20	0.20	0.23
21-22	0.30	0.30	0.30	0.49
22-23	0.34	0.34	0.34	0.37
23-24	0.33	0.33	0.33	0.31
24-25	0.16	0.16	0.16	0.22

Table 1-4.1-3

DBA CONDENSATION OSCILLATION TORUS
SHELL PRESSURE AMPLITUDES
 (Concluded)

FREQUENCY INTERVALS (Hz)	MAXIMUM PRESSURE AMPLITUDE (psi)			
	ALTERNATE 1	ALTERNATE 2	ALTERNATE 3	ALTERNATE 4
25-26	0.25	0.25	0.25	0.50
26-27	0.58	0.58	0.58	0.51
27-28	0.13	0.13	0.13	0.39
28-29	0.19	0.19	0.19	0.27
29-30	0.14	0.14	0.14	0.09
30-31	0.08	0.08	0.08	0.08
31-32	0.03	0.03	0.03	0.07
32-33	0.03	0.03	0.03	0.05
33-34	0.03	0.03	0.03	0.04
34-35	0.05	0.05	0.05	0.04
35-36	0.08	0.08	0.08	0.07
36-37	0.10	0.10	0.10	0.11
37-38	0.07	0.07	0.07	0.06
38-39	0.06	0.06	0.06	0.05
39-40	0.09	0.09	0.09	0.03
40-41	0.33	0.33	0.33	0.08
41-42	0.33	0.33	0.33	0.19
42-43	0.33	0.33	0.33	0.19
43-44	0.33	0.33	0.33	0.13
44-45	0.33	0.33	0.33	0.18
45-46	0.33	0.33	0.33	0.30
46-47	0.33	0.33	0.33	0.18
47-48	0.33	0.33	0.33	0.19
48-49	0.33	0.33	0.33	0.17
49-50	0.33	0.33	0.33	0.21

IOW-40-199-1
 Revision 0

1-4.42

Table 1-4.1-4

FSTF RESPONSE TO CONDENSATION OSCILLATION

RESPONSE QUANTITY	CALCULATED FSTF RESPONSE AT 84% NEP ⁽¹⁾	MAXIMUM MEASURED FSTF RESPONSE		
		M8	M11B	M12
BOTTOM DEAD CENTER AXIAL STRESS (ksi)	3.0	2.3	1.6	2.7
BOTTOM DEAD CENTER HOOP STRESS (ksi)	3.7	2.6	1.4	2.9
BOTTOM DEAD CENTER DISPLACEMENT (in.)	0.17	0.11	0.08	0.14
INSIDE COLUMN FORCE (kips)	184	93	68	109
OUTSIDE COLUMN FORCE (kips)	208	110	81	141

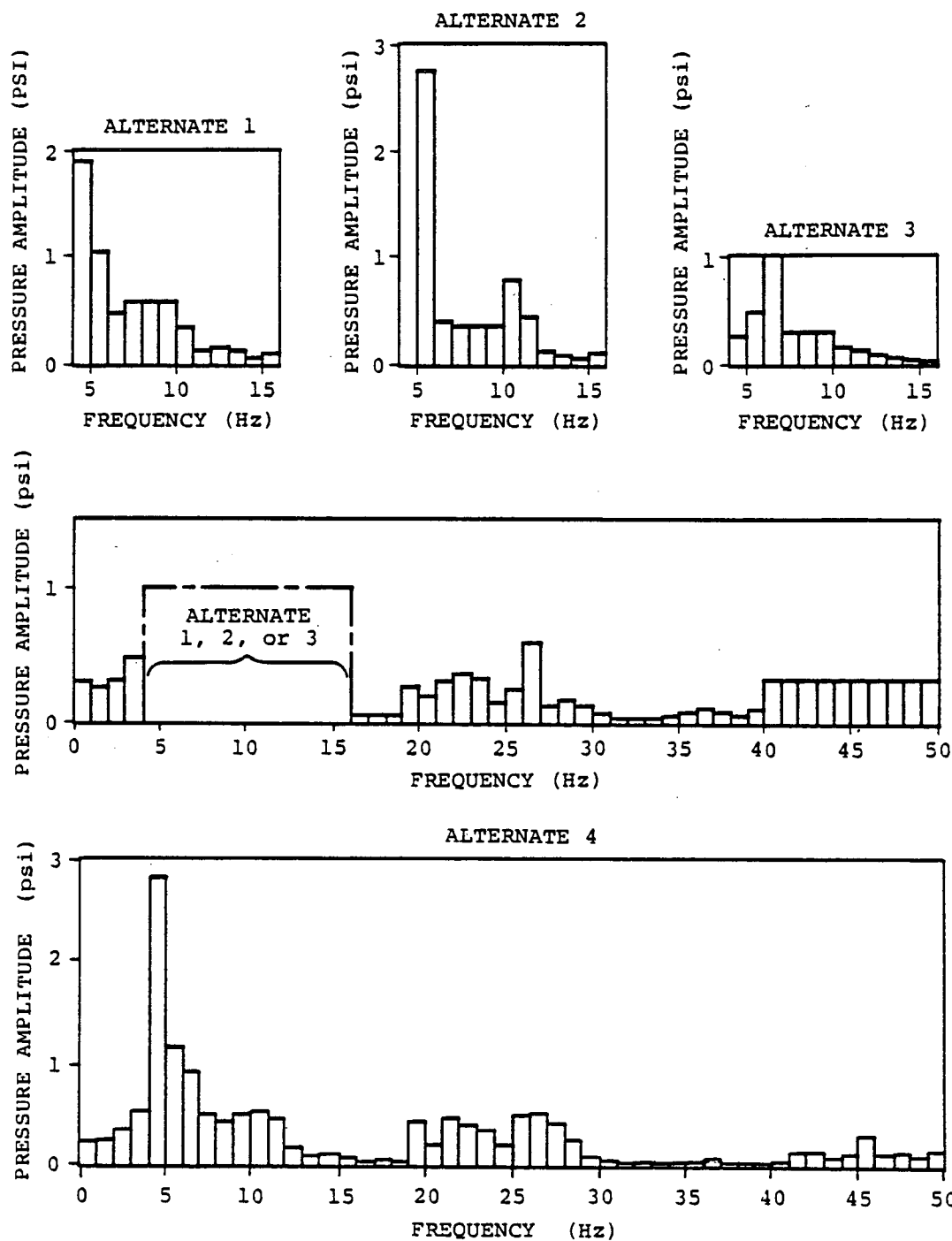
(1) USING CO LOAD ALTERNATES 1, 2 AND 3.

Table 1-4.1-5

CONDENSATION OSCILLATION ONSET AND DURATION

BREAK SIZE	ONSET TIME AFTER BREAK	DURATION AFTER ONSET
DBA	5 SECONDS	30 SECONDS
IBA	5 SECONDS ⁽¹⁾	900 SECONDS ⁽¹⁾
SBA	NOT APPLICABLE	NOT APPLICABLE

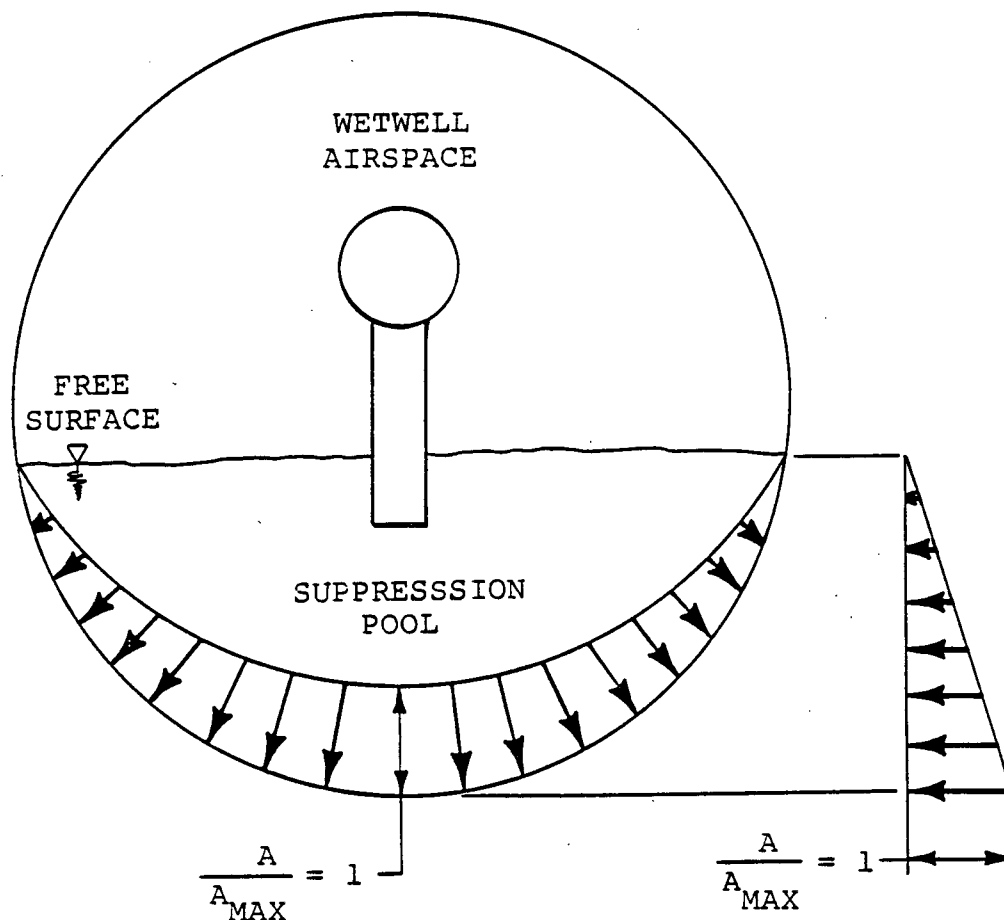
(1) FOR THE IBA, CHUGGING LOADS AS DEFINED IN SECTION 1-4.1.8.2. ARE USED.



1. ALL AMPLITUDES REPRESENT ONE-HALF OF THE PEAK-TO-PEAK AMPLITUDE.

Figure 1-4.1-7

CONDENSATION OSCILLATION BASELINE RIGID WALL PRESSURE
AMPLITUDES ON TORUS SHELL BOTTOM DEAD CENTER



1. A = LOCAL PRESSURE OSCILLATION AMPLITUDE.
2. A_{MAX} = MAXIMUM PRESSURE OSCILLATION AMPLITUDE
(AT TORUS BOTTOM DEAD CENTER).

Figure 1-4.1-8

MARK I CONDENSATION OSCILLATION - TORUS VERTICAL
CROSS-SECTIONAL DISTRIBUTION FOR PRESSURE OSCILLATION AMPLITUDE

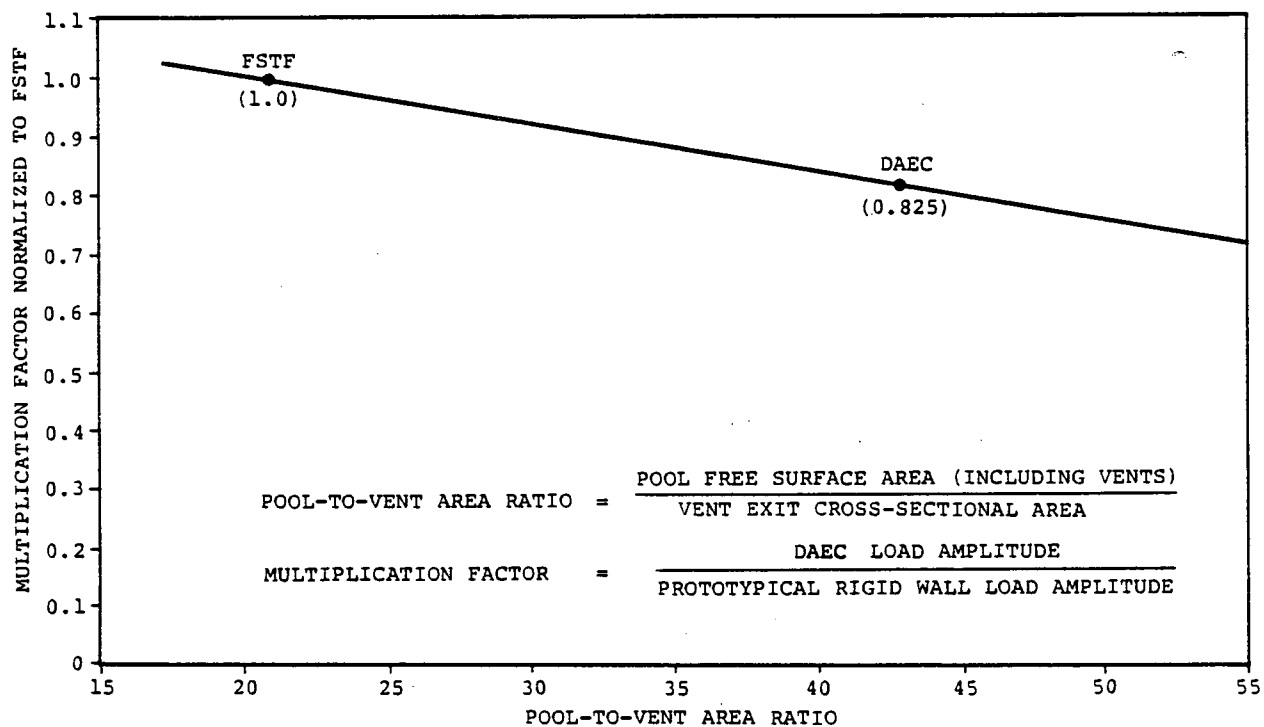


Figure 1-4.1- 9

MARK I CONDENSATION OSCILLATION - MULTIPLICATION FACTOR TO
ACCOUNT FOR THE EFFECT OF THE POOL-TO-VENT AREA RATIO

IOW-40-199-1
 Revision 0

1-4.47

1-4.1.7.2 CO Loads on the Downcomers and Vent System

Downcomer Dynamic Loads

The downcomers experience loading during the condensation oscillation phase of the blowdown. The procedure for defining the dynamic portion of this loading for both a DBA and an IBA is presented in this section. Condensation oscillation loads do not occur for the SBA. The bases, assumptions, and loading definition details are presented in the LDR.

The downcomer dynamic load is due to the internal pressure in each downcomer. The downcomer internal pressure load results in vertical dynamic loading. There is no net lateral loading on the downcomers or the vent header due to condensation oscillation, since DAEC has single vertical downcomers located symmetrically beneath the vent header. The internal pressure load has three frequency bands over which it is applied.

Table 1-4.1-6 lists the downcomer internal pressure loads for the DBA CO period. Figure 1-4.1-10 shows the internal pressure load and the three frequency

bands over which it is applied. The downcomer breathing frequency was determined from an eigen value analysis which resulted in a very low frequency ratio. Consequently, the pressure magnitudes associated with each frequency band were summed and applied statically (See Volume 3).

Table 1-4.1-7 provides the downcomer internal pressure loads for the IBA CO period. Figure 1-4.1-11 shows these downcomer internal pressure load values and the range of application. The procedure used to evaluate the IBA CO downcomer loads is the same as that used for the DBA CO downcomer loads.

Vent System Loads

Loads on the vent system during the condensation oscillation phenomenon result from harmonic pressure oscillations superimposed on the prevailing local static pressures in the vent system.

Condensation oscillation loads are specified for all three components of the vent system: the main vents, the vent header, and the downcomers (Table 1-4.1-8).

These loads, as determined from FSTF data, are generic and are thus directly applicable to all Mark I plants.

IOW-40-199-1
Revision 0

1-4.50

nutech
ENGINEERS

Table 1-4.1-6

DOWNCOMER INTERNAL PRESSURE LOADS
FOR DBA CONDENSATION OSCILLATION

FREQUENCY	PRESSURE (psi)	APPLIED FREQUENCY RANGE (Hz)
DOMINANT	3.6	4-8
SECOND HARMONIC	1.3	8-16
THIRD HARMONIC	0.6	12-24

Table 1-4.1-7

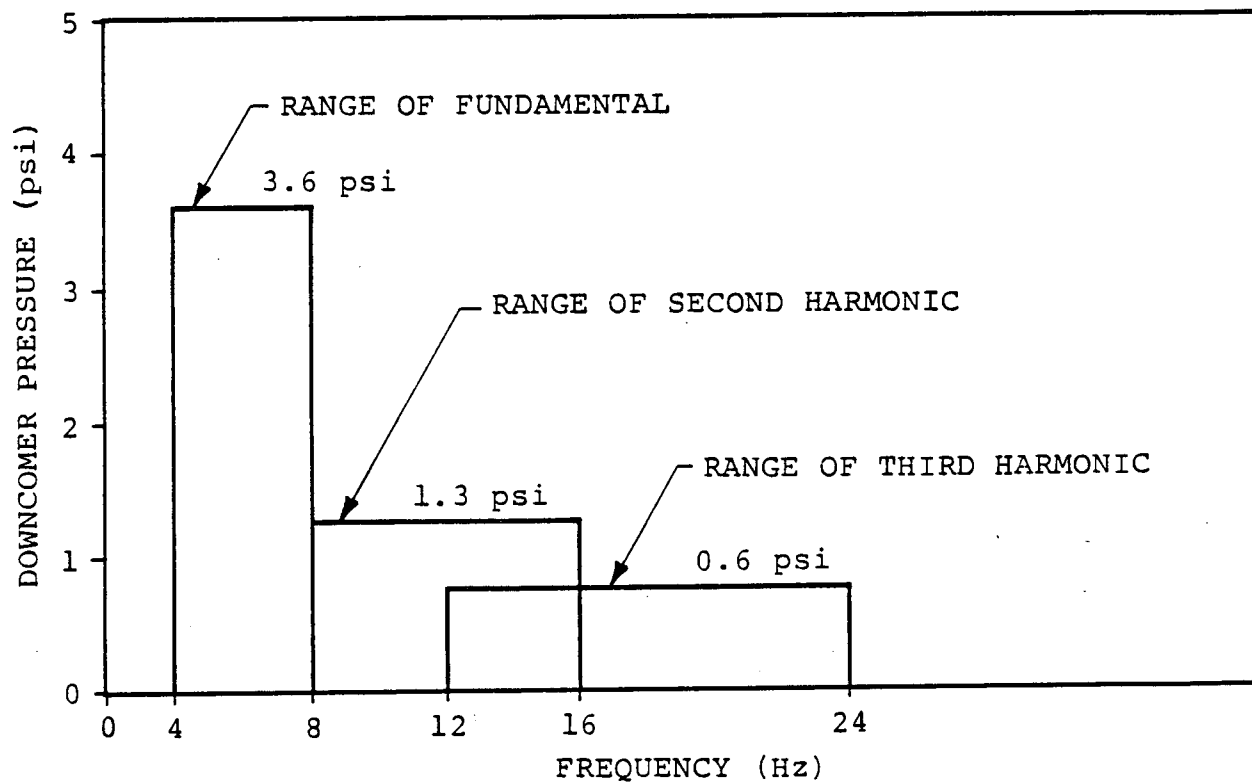
DOWNCOMER INTERNAL PRESSURE LOADS
FOR IBA CONDENSATION OSCILLATION

FREQUENCY	PRESSURE (psi)	APPLIED FREQUENCY RANGE (Hz)
DOMINANT	1.1	6-10
SECOND HARMONIC	0.8	12-20
THIRD HARMONIC	0.2	18-30

Table 1-4.1-8

CONDENSATION OSCILLATION LOADS
ON THE VENT SYSTEM

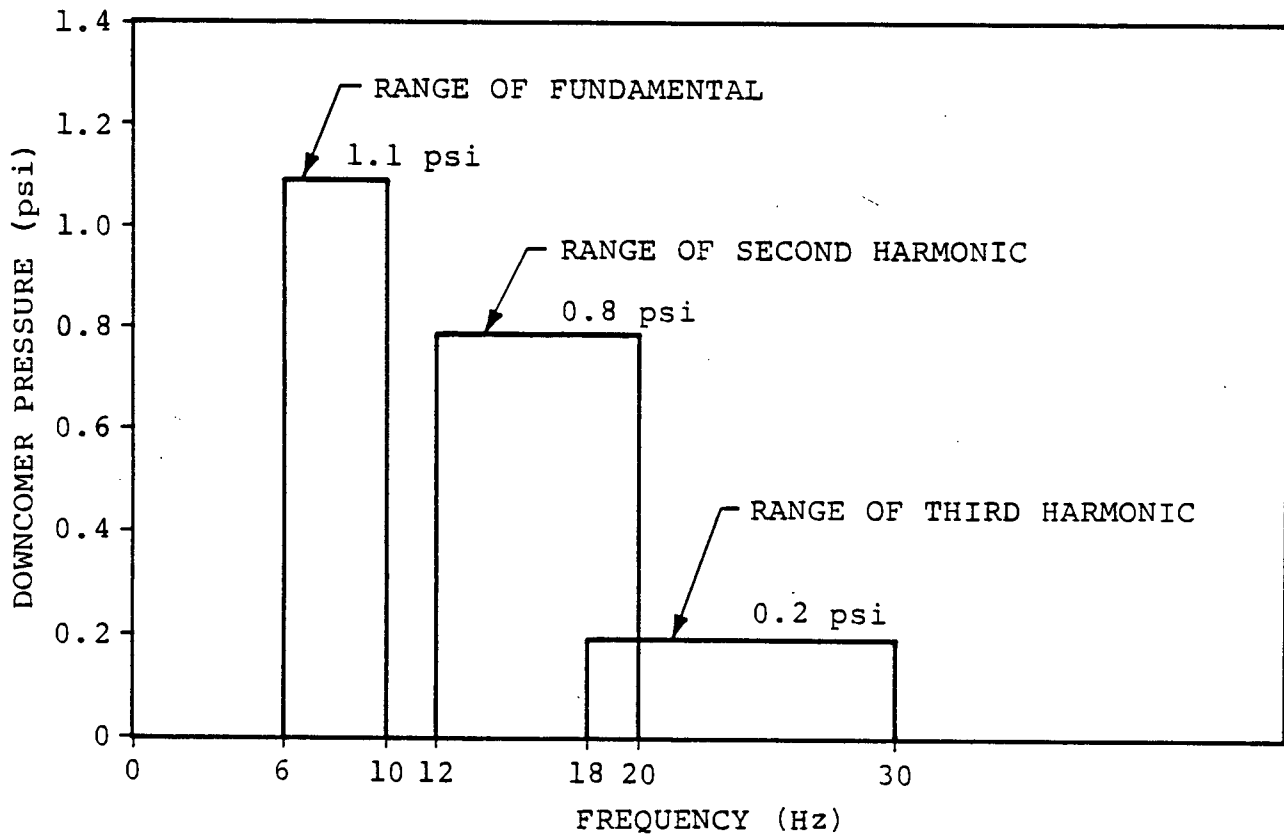
COMPONENTS		DBA	IBA
MAIN VENT AND VENT HEADER	AMPLITUDE	<u>+2.5</u> psi	<u>+2.5</u> psi
	FREQUENCY RANGE	AT FREQUENCY OF MAXIMUM RESPONSE IN 4-8 Hz RANGE	AT FREQUENCY OF MAXIMUM RESPONSE IN 6-10 Hz RANGE
	FORCING FUNCTION	SINUSOIDAL	SINUSOIDAL
	SPATIAL DISTRIBUTION	UNIFORM	UNIFORM
DOWNCOMERS	AMPLITUDE	<u>+5.5</u> psi	<u>+2.1</u> psi
	FREQUENCY RANGE	AT FREQUENCY OF MAXIMUM RESPONSE IN 4-8 Hz RANGE	AT FREQUENCY OF MAXIMUM RESPONSE IN 6-10 Hz RANGE
	FORCING FUNCTION	SINUSOIDAL	SINUSOIDAL
	SPATIAL DISTRIBUTION	UNIFORM	UNIFORM



1. THE AMPLITUDES SHOWN ARE HALF-RANGE
(ONE-HALF OF THE PEAK-TO-PEAK VALUE).

Figure 1-4.1-10

DOWNCOMER INTERNAL PRESSURE LOADING FOR DBA CO



1. THE AMPLITUDES SHOWN ARE HALF-RANGE
(ONE-HALF OF THE PEAK-TO-PEAK VALUE).

Figure 1-4.1-11

DOWNCOMER INTERNAL PRESSURE LOADING FOR IBA CO

1-4.1.7.3 CO Loads on Submerged Structures

The condensation oscillation phase of the postulated LOCA induces bulk pool motion, creating drag loads on structures submerged in the pool. The basis of the flow model used to determine condensation oscillation loads on submerged structures is presented in the LDR.

Condensation oscillations are described by fluid sources located at downcomer vent exits. The average source strengths are determined from wall load measurements. By using potential flow theory and the method of images to account for the effects of solid walls and the free surface, the velocity and acceleration flow fields within the suppression chamber are established. For each structure, the loads are computed using both the average source strength applied at all downcomers and the maximum source strength applied at the nearest downcomer.

The fluid-structure interaction (FSI) effects are included when the local fluid acceleration is less than twice the boundary acceleration. Pool fluid accelerations are computed within the suppression

chamber using frequency decomposed radial shell accelerations obtained from the suppression chamber analysis described in Volume 2. The FSI effects for a given structure are computed using the pool fluid accelerations at the actual location of the structure.

Drag forces on submerged structures can be separated into two components, standard drag, and acceleration drag. The sum of these two effects gives the total drag load on a submerged structure. The calculations for condensation oscillation submerged structure loads use the same procedure as used for calculating LOCA bubble-induced drag loads on submerged structures. Acceleration drag volumes for some structures with sharp corners (e.g., I-beams) are calculated using equations from Table 1-4.1-1 instead of volumes derived by circumscribed cylinders, as noted in Section 1-4.1.5.

The source amplitudes used for condensation oscillation submerged structure loads are in accordance with NUREG-0661 and are presented in Table 1-4.1-9. The source forcing function has the form of a sinusoidal wave characterized by the appropriate amplitude and

frequency taken from Table 1-4.1-9. The LDR defines the total drag force as the summation of the resulting responses from all 50 harmonics. As described in Section 1-4.1.7.1, the summation is performed to achieve a minimum non-exceedance probability of 84%.

Table 1-4.1-9

AMPLITUDES AT VARIOUS FREQUENCIES FOR CONDENSATION OSCILLATION
SOURCE FUNCTION FOR LOADS ON SUBMERGED STRUCTURES

FREQUENCY (Hz)	AMPLITUDE (ft ³ /sec ²)	FREQUENCY (Hz)	AMPLITUDE (ft ³ /sec ²)
0-1	28.38	26-27	56.75
1-2	24.46	27-28	12.72
2-3	31.31	28-29	18.59
3-4	46.97	29-30	13.70
4-5	182.00	30-31	7.93
5-6	267.13	31-34	2.94
6-7	96.87	34-35	4.89
7-10	57.73	35-36	7.83
10-11	77.30	36-37	9.79
11-12	44.03	37-38	6.85
12-13	16.63	38-39	5.87
13-14	11.74	39-40	8.81
14-15	6.85	40-41	32.29
15-16	9.79	41-42	32.29
16-19	3.91	42-43	32.29
19-20	26.42	43-44	32.29
20-21	19.57	44-45	32.29
21-22	29.36	45-46	32.29
22-23	33.27	46-47	32.29
23-24	32.29	47-48	32.29
24-25	15.66	48-49	32.29
25-26	24.46	49-50	32.29

This subsection describes the chugging loads on the various structures and components in the DAEC suppression chamber.

Chugging occurs during a postulated LOCA when the steam flow through the vent system falls below the rate necessary to maintain steady condensation at the downcomer exits. The corresponding flow rates for chugging are less than those of the condensation oscillation phenomenon. During chugging, steam bubbles form at the downcomer exits, oscillate as they grow to a critical size (approximately downcomer diameter), and begin to collapse independently in time. The resulting load on the suppression chamber shell due to a chugging cycle consists of a low frequency oscillation (pre-chug) which corresponds to the oscillating bubbles at the downcomer exit as they grow, followed by a higher frequency "ring-out" of the suppression chamber shell-pool water system (post-chug) in response to the collapsing bubbles (Figure 1-4.1-12).

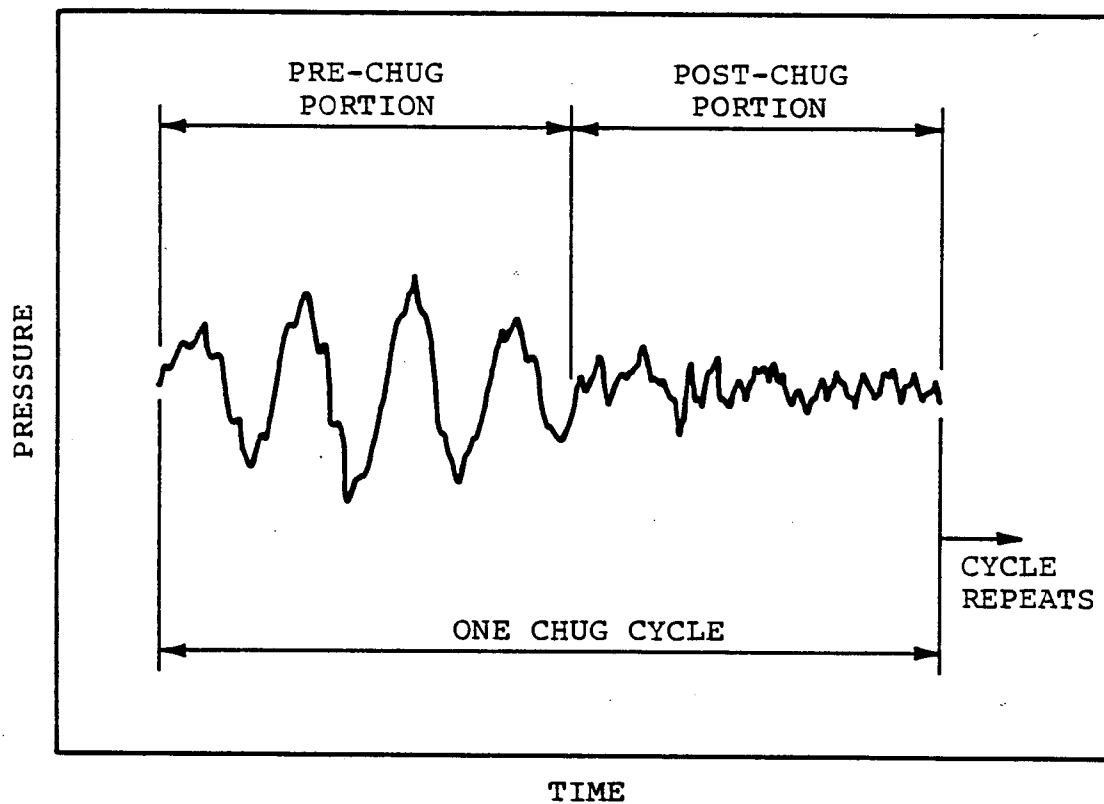


Figure 1-4.1-12
TYPICAL CHUG CYCLE AVERAGE PRESSURE
TRACE ON THE TORUS SHELL

1-4.1.8.1 Chugging Loads on the Suppression Chamber Shell

During the chugging regime of a postulated LOCA, the chugging loads on the suppression chamber shell occur as a series of chugging cycles. The chugging load cycles are divided into pre-chug and post-chug portions. The bases for pre-chug and post-chug rigid wall load definitions are presented in the LDR.

For the pre-chug portion of the chugging cycle, both symmetric and asymmetric loading conditions are used to conservatively account for any randomness in the chugging phenomenon. The asymmetric loading is based on both low and high amplitude chugging data conservatively distributed around the suppression chamber in order to maximize the asymmetric loading.

In order to bound the post-chug portion of the chugging cycle, symmetric loads are used. Asymmetric loads are not specified, since any azimuthal response would be governed by the asymmetric pre-chug low frequency load specification.

The chugging onset times and durations for the DBA, IBA, and SBA are in accordance with the LDR and are

presented in Table 1-4.1-10. DAEC utilizes motor driven feedwater pumps and the IBA scenario for this configuration is described in Section 2.2 of the LDR. For the IBA, the ADS is assumed to be initiated 900 seconds after the break and the reactor is assumed to be depressurized 200 seconds after ADS initiation, at which time chugging ends. For the SBA, the reactor is assumed to be depressurized 600 seconds after ADS initiation, at which time chugging ends.

a. Pre-Chug Load

The symmetric pre-chug suppression chamber shell pressure load is specified as ± 2.0 psi applied uniformly along the suppression chamber longitudinal axis. Figure 1-4.1-13 shows the longitudinal distribution of the asymmetric pre-chug pressure load, which varies from ± 0.4 to ± 2.0 psi. The pre-chug cross-sectional distribution for both symmetric and asymmetric cases (Figure 1-4.1-14) is the same as for condensation oscillation. The pre-chug loads are applied at the single frequency producing the maximum response in the range of 6.9 to 9.5

Hz. The pre-chug load of 0.5 second duration is applied at 1.4 second intervals for the appropriate total chugging duration (Table 1-4.1-10).

b. Post-Chug Load

Table 1-4.1-11 and Figure 1-4.1-15 define the amplitude versus frequency variation for the post-chug suppression chamber shell pressure load. The load is applied uniformly along the suppression chamber longitudinal axis. The cross-sectional variation is the same for the condensation oscillation and pre-chug loads (Figure 1-4.1-14). The steady-state responses from the application of the pressure amplitudes at each frequency are summed (Figure 1-4.1-15). The summation is performed as described in Section 1-4.1.7.3 for the condensation oscillation load. The post-chug load of 0.5 second duration is applied at 1.4 second intervals for the appropriate total duration (Table 1-4.1-10).

Table 1-4.1-10

CHUGGING ONSET AND DURATION

BREAK SIZE	ONSET TIME AFTER BREAK	DURATION AFTER ONSET
DBA	35 SECONDS	30 SECONDS
IBA	905 SECONDS	200 SECONDS
SBA	300 SECONDS	900 SECONDS

Table 1-4.1-11

POST-CHUG RIGID WALL PRESSURE AMPLITUDES
ON TORUS SHELL BOTTOM DEAD CENTER

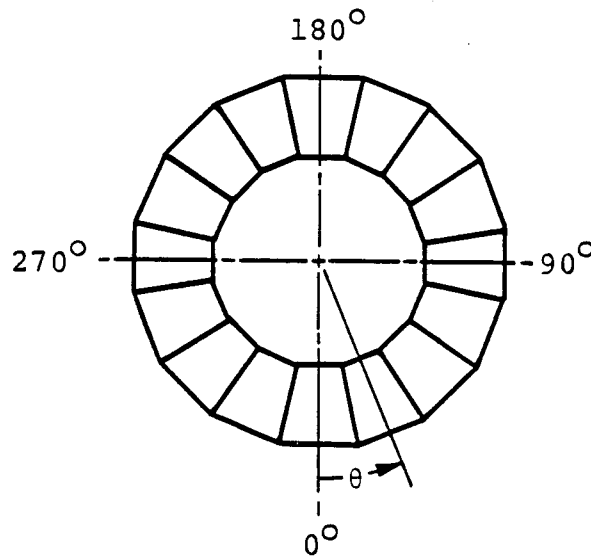
FREQUENCY RANGE (1) (Hz)	PRESSURE (psi)	FREQUENCY RANGE (1) (Hz)	PRESSURE (psi)
0-1	0.04	25-26	0.04
1-2	0.04	26-27	0.28
2-3	0.05	27-28	0.18
3-4	0.05	28-29	0.12
4-5	0.06	29-30	0.09
5-6	0.05	30-31	0.03
6-7	0.10	31-32	0.02
7-8	0.10	32-33	0.02
8-9	0.10	33-34	0.02
9-10	0.10	34-35	0.02
10-11	0.06	35-36	0.03
11-12	0.05	36-37	0.05
12-13	0.03	37-38	0.03
13-14	0.03	38-39	0.04
14-15	0.02	39-40	0.04
15-16	0.02	40-41	0.15
16-17	0.01	41-42	0.15
17-18	0.01	42-43	0.15
18-19	0.01	43-44	0.15
19-20	0.04	44-45	0.15
20-21	0.03	45-46	0.15
21-22	0.05	46-47	0.15
22-23	0.05	47-48	0.15
23-24	0.05	48-49	0.15
24-25	0.04	49-50	0.15

(1) A HALF-RANGE EQUALS ONE-HALF OF THE PEAK-TO-PEAK
AMPLITUDE

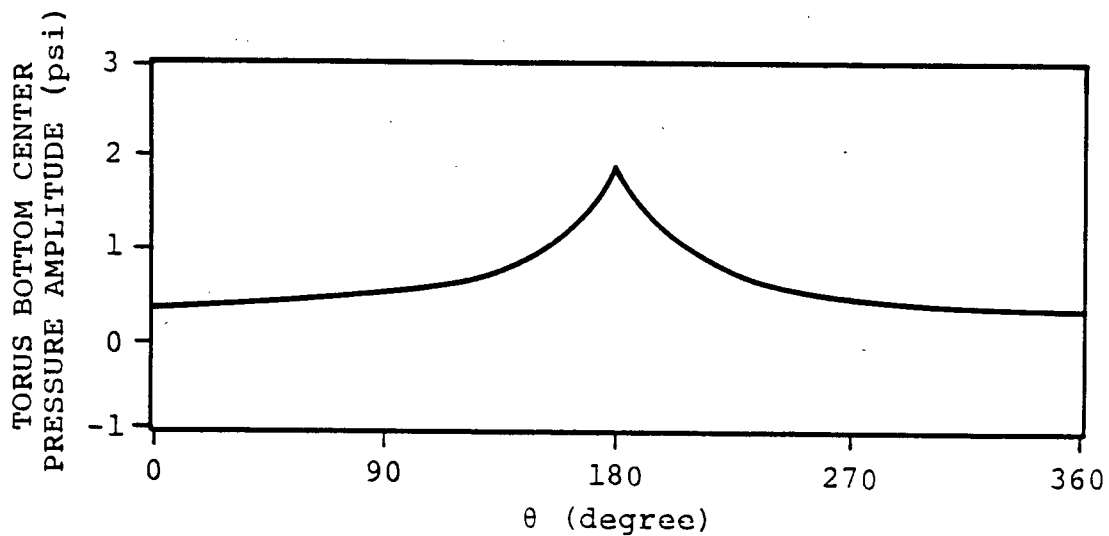
IOW-40-199-1

Revision 0

1-4.66



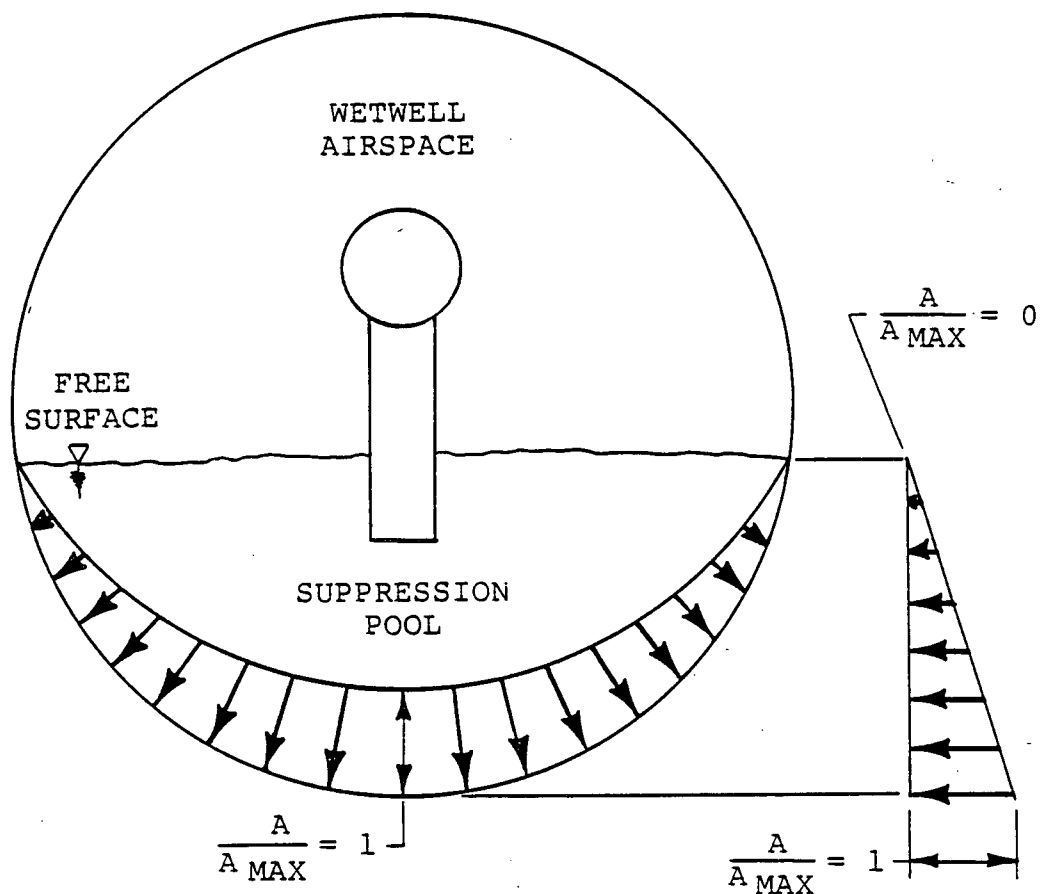
PLAN VIEW OF TORUS



1. THE AMPLITUDE SHOWN HERE REPRESENTS ONE-HALF OF THE PEAK-TO-PEAK AMPLITUDE.
2. HIGHEST VALUE IN BAY APPLIED OVER THE ENTIRE BAY.

Figure 1-4.1-13

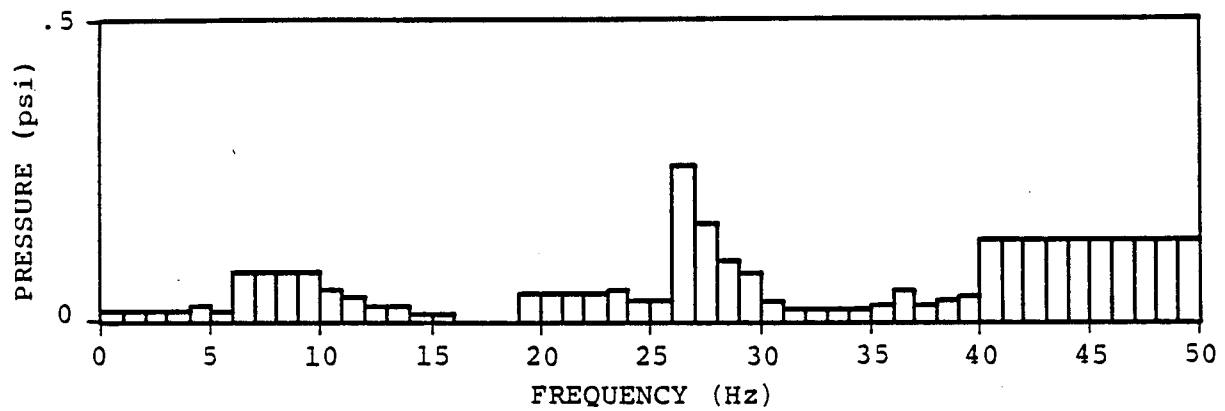
MARK I CHUGGING - TORUS ASYMMETRIC LONGITUDINAL
DISTRIBUTION FOR PRESSURE AMPLITUDE



1. A = LOCAL PRESSURES OSCILLATION AMPLITUDE
2. A_{MAX} = MAXIMUM PRESSURE OSCILLATION AMPLITUDE
(AT TORUS BOTTOM DEAD CENTER)

Figure 1-4.1-14

MARK I CHUGGING - TORUS VERTICAL CROSS-SECTIONAL
DISTRIBUTION FOR PRESSURE AMPLITUDE



THE AMPLITUDE SHOWN HERE REPRESENTS
ONE-HALF OF THE PEAK-TO-PEAK AMPLITUDE.

Figure 1-4.1-15
POST-CHUG RIGID WALL PRESSURE AMPLITUDES
ON TORUS SHELL BOTTOM DEAD CENTER

IOW-40-199-1
Revision 0

1-4.69

1-4.1.8.2 Chugging Downcomer Lateral Loads

During the chugging phase of a postulated LOCA, vapor bubbles which form at the downcomer exit collapse suddenly and intermittently to produce lateral loads on the downcomer. The procedure for defining the dynamic portion of this loading for a DBA, IBA, and SBA is presented in this section.

The basis for the chugging lateral load definition is the data obtained from the instrumented downcomers of the Mark I Full-Scale Test Facility. The chugging downcomer lateral load definition was developed for Mark I downcomer pairs which are untied. In this untied configuration, the downcomers in a pair respond independently to chugging lateral loads, as observed at the FSTF. Therefore, the LDR chugging downcomer lateral loads are directly applicable to the DAEC configuration with a single downcomer.

The FSTF downcomer lateral loads are defined as Resultant-Static-Equivalent Loads (RSEL) which when applied statically to the end of the downcomer, reproduce the measured bending response near the downcomer/vent header (DC/VH) junction at any given time.

The loads associated with chugging obtained from the FSTF data are scaled to determine plant-specific loads for DAEC. The maximum downcomer design load, histograms of load reversals, and the maximum vent system loading produced by synchronous chugging of the downcomers are determined from the FSTF loads.

For fatigue evaluation of the downcomers, the required stress reversals at the downcomer/vent header junction are obtained from the FSTF, RSEL reversal histograms. The plant unique junction stress reversals are obtained by scaling the FSTF, RSEL reversals by the ratio of the chugging duration specified for DAEC to that of the FSTF. Table 1-4.1-10 lists chugging durations for the DBA, IBA, and SBA.

1-4.1.8.3 Chugging Loads on Submerged Structures

Chugging at the downcomer exits induces bulk water motion and therefore creates drag loads on structures submerged in the pool. The submerged structure load definition method for chugging follows that used to predict drag forces caused by condensation oscillations (see Section 1-4.1.7.3), except that the source strength for chugging is proportional to the wall load measurement corresponding to the chugging regime.

The bases and assumptions of the flow model for the chugging load definition are presented in the LDR. Table 1-4.1-12 presents the source amplitudes for pre-chug and post-chug regimes.

The load development procedure for chugging loads on submerged structures is the same as presented in Section 1-4.1.7.3 for condensation oscillation and is in accordance with NUREG-0661. The responses from the 50 harmonics are summed as described in Section 1-4.1.7.1. Acceleration drag volumes for structures with sharp corners (e.g., I-beams) are calculated

using equations from Table 1-4.1-1. Fluid-structure interaction effects are included as described in Section 1-4.1.7.3.

Table 1-4.1-12
AMPLITUDES AT VARIOUS FREQUENCIES FOR
CHUGGING SOURCE FUNCTION
FOR LOADS ON SUBMERGED STRUCTURES

CHUGGING	FREQUENCY (Hz)	AMPLITUDE (ft ³ /sec ²)
PRE	6.9 - 9.5	195.70
POST	0-2	11.98
	2-3	10.36
	3-4	9.87
	4-5	17.40
	5-6	17.00
	6-10	18.88
	10-11	87.90
	11-12	76.18
	12-13	41.01
	13-14	35.89
	14-15	6.82
	15-16	6.20
	16-17	3.14
	17-18	4.18
	18-19	2.94
	19-20	16.82
	20-21	17.53
	21-22	30.67

Table 1-4.1-12
AMPLITUDES AT VARIOUS FREQUENCIES FOR
CHUGGING SOURCE FUNCTION
FOR LOADS ON SUBMERGED STRUCTURES
(Concluded)

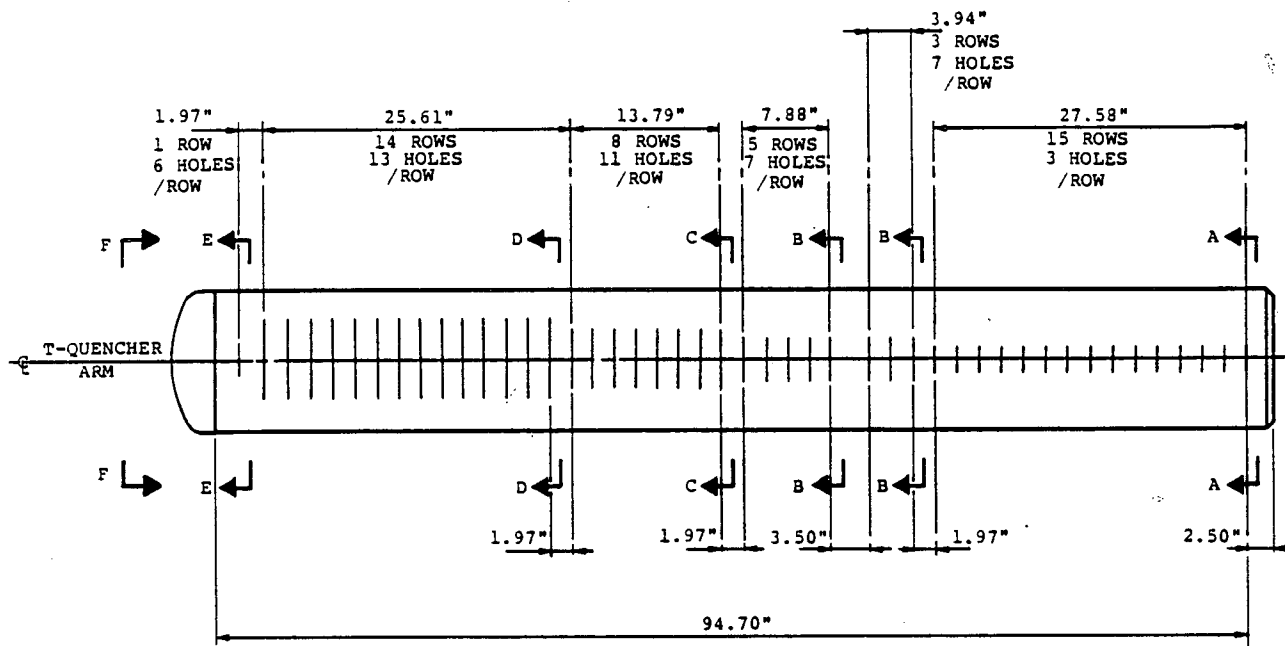
CHUGGING	FREQUENCY (Hz)	AMPLITUDE (ft ³ /sec ²)
POST	22-24	92.39
	24-25	134.50
	25-26	313.84
	26-27	377.83
	27-28	251.89
	28-29	163.32
	29-30	116.66
	30-31	43.14
	31-32	21.57
	32-33	37.91
	33-34	50.54
	34-35	42.54
	35-36	61.87
	36-37	41.95
	37-38	20.97
	38-39	24.47
	39-40	29.37
	40-50	224.90

This section discusses the procedures used to determine loads created when one or more SRV's are actuated.

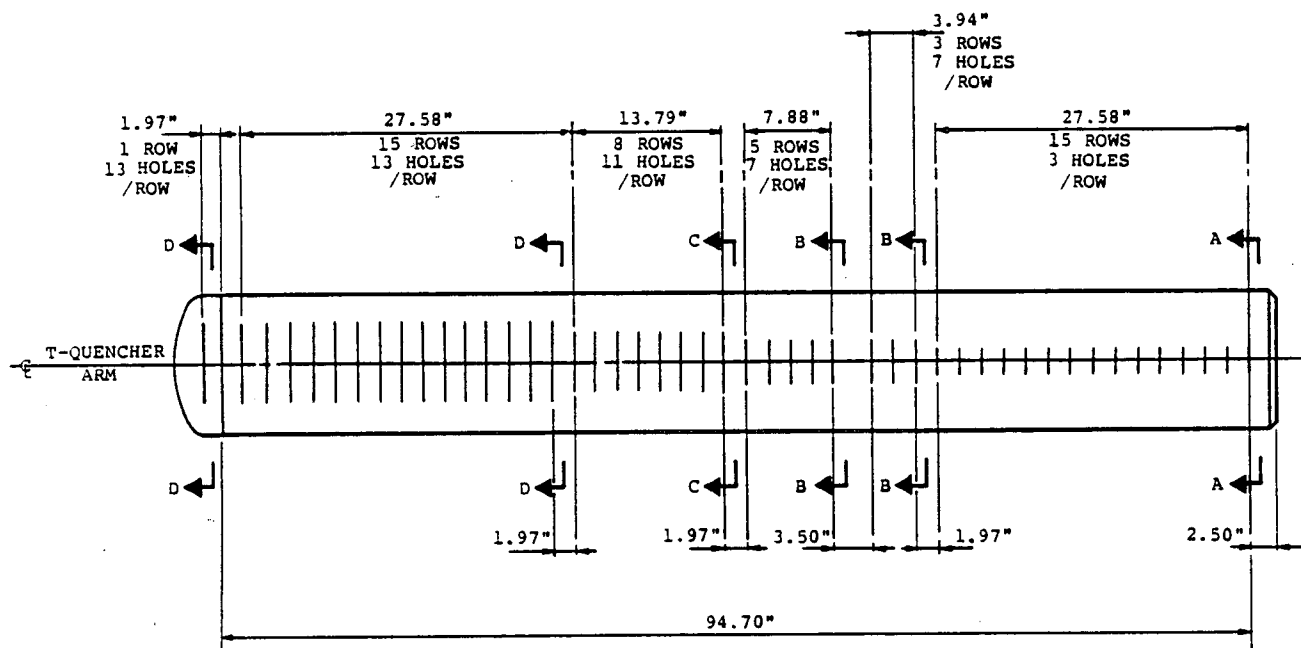
When an SRV actuates, pressure and thrust loads are exerted on the SRVDL piping and the T-quencher discharge device. In addition, the expulsion of water followed by air into the suppression pool through the T-quencher results in pressure loads on the submerged portion of the suppression chamber shell and drag loads on submerged structures.

The T-quencher utilized in the DAEC is the standard Mark I T-quencher as described in the LDR. The DAEC T-quencher has 12" diameter arms which are connected to the ramshead. The T-quencher is located coincident with both the azimuthal and radial center lines of the bay. The SRV discharge line is slanted from the vertical going into the ramshead. Figures 1-4.2-1 and 1-4.2-2 show the details of the hole distribution along the arm. Figure 1-4.2-3 illustrates the connection of the SRVDL to the T-quencher. Volume 5 of this PUAR provides a detailed description of the T-quencher and its support structure.

As allowed in Section 2.13.9 of Appendix A of NUREG-0661, plant unique SRV testing at DAEC has been performed to confirm that the computed loadings and predicted structural responses for SRV discharges are conservative.



LEFT T-QUENCHER ARM



RIGHT T-QUENCHER ARM

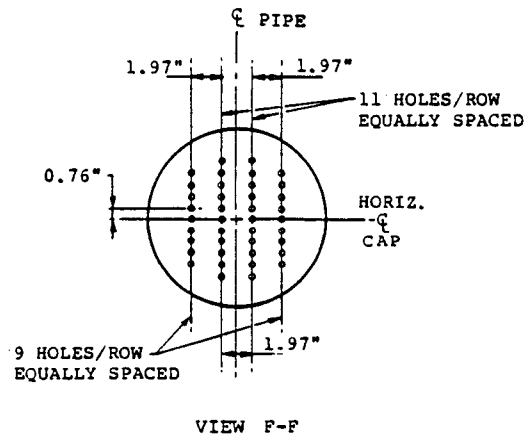
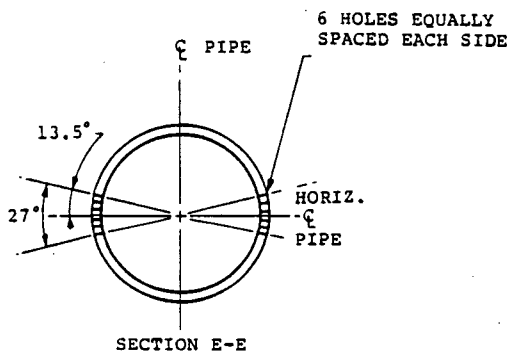
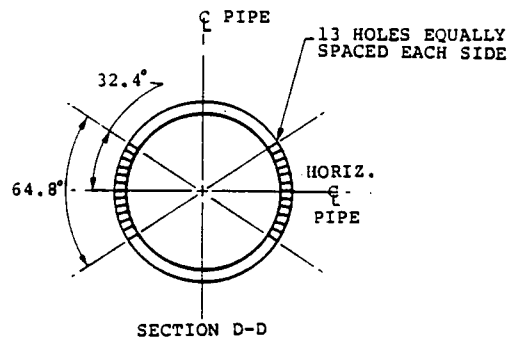
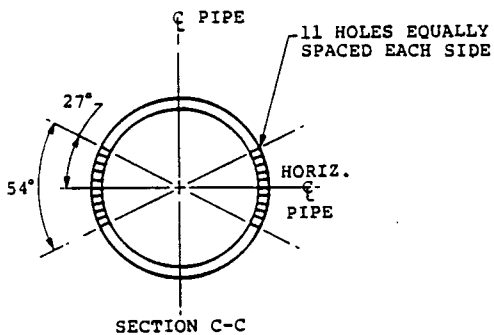
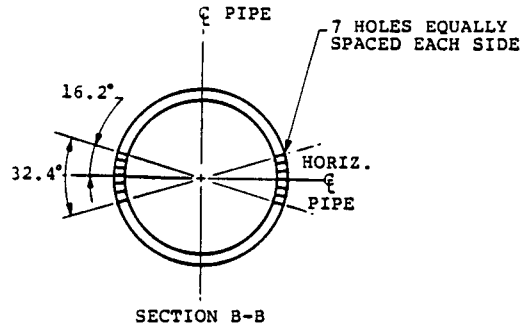
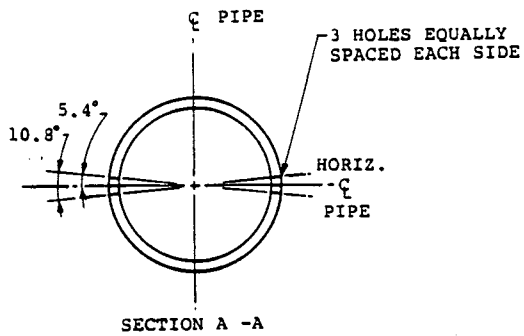
1. SEE FIGURE 1-4.2-2 FOR SECTIONS AND VIEWS.
2. SEE FIGURE 1-4.2-3 FOR DEFINITION OF ARMS.

Figure 1-4.2-1

T-QUENCHER ARM HOLE PATTERN-ELEVATION VIEWS

IOW-40-199-1
Revision 0

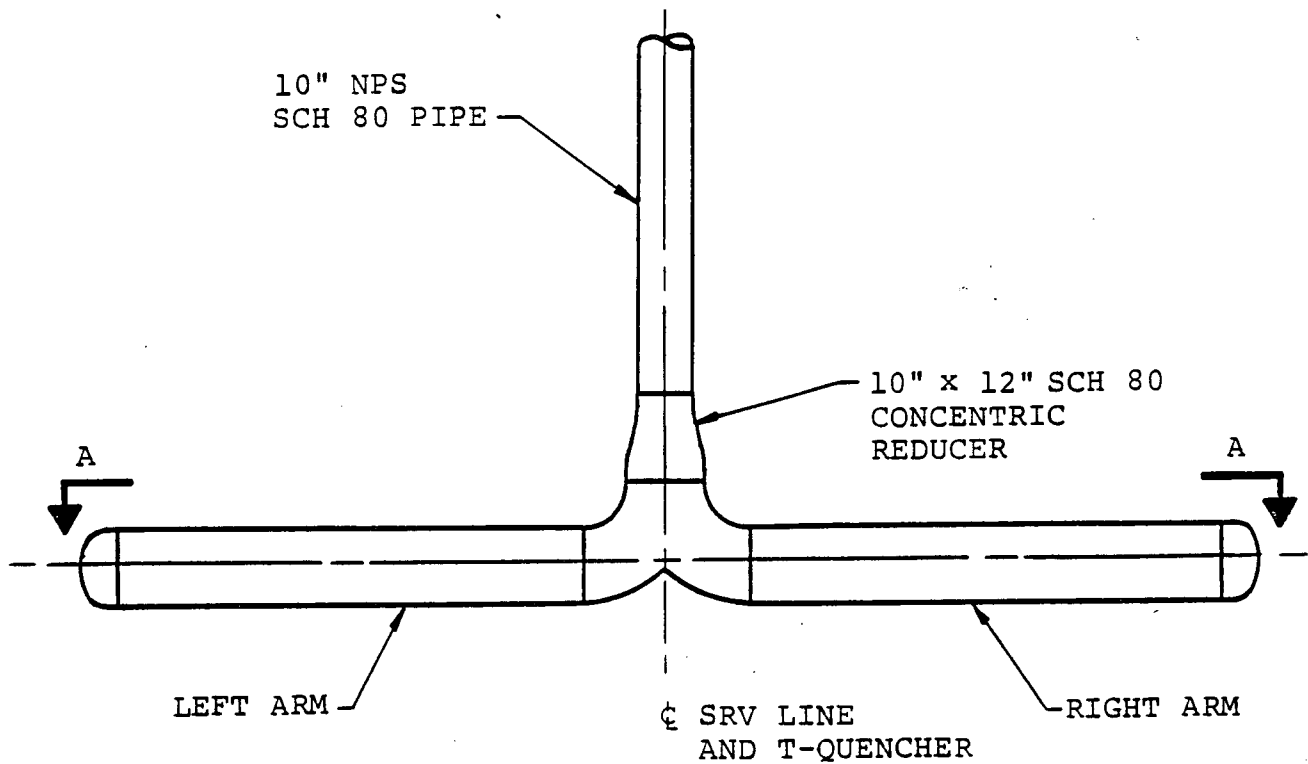
1-4.78



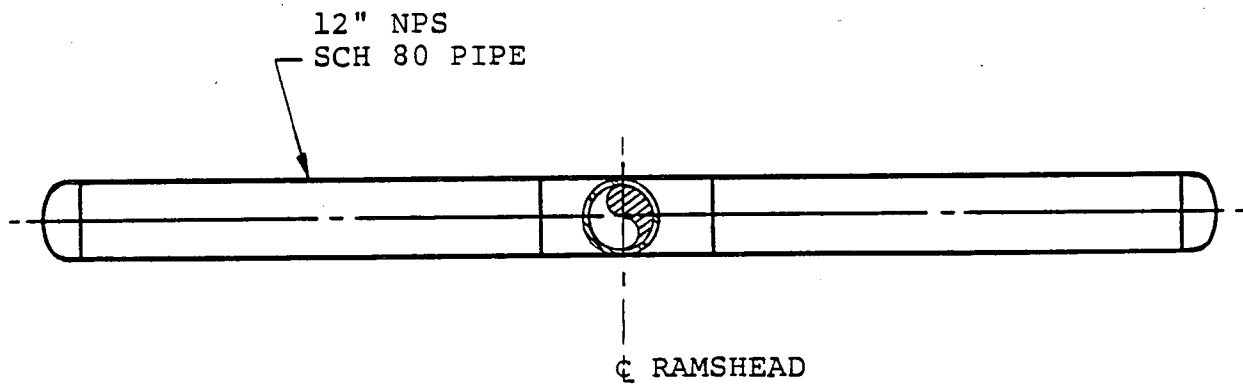
1. SECTIONS AND VIEWS TAKEN FROM FIGURE 1-4.2-1

Figure 1-4.2-2

T-QUENCHER ARM HOLE PATTERN-SECTION VIEWS



PLAN VIEW



VIEW A-A

Figure 1-4.2-3
T-QUENCHER AND SRV LINE

1-4.2.1 SRV Actuation Cases

This section provides a discussion on the selection of SRV discharge cases which are considered for design load evaluations. The load cases summarized in Table 1-4.2-1 are described as follows.

Load Case Al.1 (Normal Operating Condition (NOC), First Actuation)

A first actuation of a SRV may occur under normal operating conditions. That is, the SRVDL is cold, there is air in the drywell, and the water in the SRVDL is at its normal operating level.

Load Case Al.2 (SBA/IBA, First Actuation)

First actuation of SRV(s) is assumed to occur at the predicted time of ADS actuation. At this time the SRVDL is full of air at the pressure corresponding to the drywell pressure minus the vacuum breaker set point. The water level inside the line is depressed below the normal operating level because the drywell

pressure is higher than the wetwell pressure by a pressure differential equal to the downcomer submergence.

Load Case A1.3 (DBA, First Actuation)

The assumptions used are the same as for Case A1.1, except for SRV flowrate. This load case is bounded by Case A1.1.

Load Case B (NOC, First Actuation, Leaking SRV)

SRV first actuation may occur under NOC for leaking SRV's. For T-quenchers, Load Case A1.1 bounds the leaking SRV load.

Load Case C3.1 (NOC, Subsequent Actuation, Second Peak Water Leg)

After the SRV is closed following a first actuation (Case A1.1), the steam in the line is condensed, causing a rapid pressure drop which draws water back into the line. At the same time, the vacuum breaker allows air from the drywell to enter the discharge line. The air

repressurizes the line and the water refloods to a point which is higher than its equilibrium height, and oscillates back to its equilibrium point. A subsequent actuation is assumed to occur at the time that the water level is at its second peak. This assumption provides loads which bound those obtained when analyzing for normal water level.

Load Case C3.2 (SBA/IBA, Subsequent Actuation)

Following SRV closure after the SBA/IBA first actuation (Case A1.2), the water will reflood back into the line while air from the drywell flows through the vacuum breaker into the SRVDL. The SRV is assumed to actuate after the water level oscillations are damped out and the level stabilized at a point determined by the drywell-to-wetwell ΔP minus the vacuum breaker set point.

Load Case C3.3 (SBA/IBA, Subsequent Actuation, Steam in SRVDL)

This case differs from the previous case in that during the reflood transient, steam,

instead of air, flows through the vacuum breaker. Thus, the line contains very little air, and the loading imposed on the suppression chamber shell from this subsequent SRV actuation is bounded by Case C3.2.

The SRVDL water leg is assumed at its equilibrium height for load case C3.2 and at its second peak for load case C3.1. The time at which the equilibrium height is reestablished after first valve actuation closure is calculated using the LDR SRV discharge line reflood model. DAEC primary system transient analyses are used to confirm that more than the minimum required time is available for the SRVDL water leg to return to the equilibrium position. For steam-in-the-drywell conditions, a steam-water convective heat transfer coefficient of 2×10^5 BTU/hr-ft²-°F is used. This conservative coefficient is based on the results of a literature survey on chugging and the downcomer water column rise characteristics during chugging in the Mark I Full-Scale Test Facility.

The number of SRV's predicted to actuate for each of the above conditions is maximized in performing the

DAEC structural evaluations documented in the remaining PUAR volumes. Section 1-4.3 identifies the other hydrodynamic loads which must be combined with SRV loads.

Table 1-4.2-1

SRV LOAD CASE/INITIAL CONDITIONS

DESIGN INITIAL CONDITION, LOAD CASE	ANY ONE VALVE	ADS VALVES	MULTIPLE VALVES (1)
NOC, FIRST ACTUATION	A1.1		A3.1
SBA/IBA, FIRST ACTUATION	A1.2	A2.2	A3.2
DBA, FIRST ACTUATION ⁽²⁾	A1.3		
NOC, LEAKING SRV ⁽³⁾			B3.1 ⁽⁴⁾
NOC, SUBSEQUENT ACTUATION			C3.1
SBA/IBA, SUBSEQUENT ACTUATION, AIR IN SRVDL			C3.2
SBA/IBA, SUBSEQUENT ACTUATION, STEAM IN SRVDL			C3.3

- (1) THE NUMBER (ONE OR MORE) AND LOCATION OF VALVES ASSUMED TO ACTUATE ARE DETERMINED BY PLANT UNIQUE ANALYSIS.
- (2) THIS ACTUATION IS ASSUMED TO OCCUR COINCIDENT WITH THE POOL SWELL EVENT. ALTHOUGH SRV ACTUATION CAN OCCUR LATER IN THE DBA, THE RESULTING AIR LOADING ON THE SUPPRESSION CHAMBER IS NEGLIGIBLE SINCE THE AIR AND WATER INITIALLY IN THE LINE WILL BE CLEARED AS THE DRYWELL-TO-WETWELL ΔP INCREASES DURING THE DBA TRANSIENT.
- (3) THIS IS APPLICABLE TO RAMSHEAD DISCHARGE ONLY.
- (4) ONLY ONE VALVE OF THE MULTIPLE GROUP IS ASSUMED TO LEAK.

The flow of high pressure steam into the discharge line when an SRV opens results in the development of a pressure wave at the entrance of the line. During the early portion of this transient, a substantial pressure differential exists across the pressure wave. This pressure differential, plus momentum effects from steam (or water in initially submerged pipe runs) flowing around elbows in the line, results in transient thrust loads on the SRV discharge pipe segments. These loads are considered in the design of SRV pipe restraints, SRV penetrations in the vent lines, and T-quencher supports.

The bases, assumptions, and descriptions of the SRV discharge line clearing analytical model are presented in the LDR. The parameters affecting SRVDL clearing load development are the SRVDL geometry, plant specific initial conditions for the SRV actuation cases, and the SRV mass flow rate. Table 1-4.2-2 presents plant specific initial conditions for various actuation cases. Table 1-4.2-3 presents common SRVDL analysis input parameters (case-independent). All input calculation procedures for the SRVDL clearing model are consistent with the LDR.

The line clearing model is used to obtain transient values for the following parameters or loads for each SRV actuation case for each SRVDL.

- SRVDL Pressures and Temperatures
- Thrust Loads on SRVDL Pipe Segments
- T-quencher Internal Discharge Pressure and Temperature
- Water Slug Mass Flow Rate
- Water Clearing Time, Velocity and Acceleration

The values obtained for T-quencher discharge pressure and water clearing time are used as input to evaluate the suppression chamber shell loads (Section 1-4.2.3) and SRV air bubble drag loads (Section 1-4.2.4) on submerged structures. The water slug mass flowrate and acceleration are used as input to calculations of SRV water jet loads on submerged structures (see Section 1-4.2.4).

The water clearing thrust load along the axis of the T-quencher (due to the uneven split flow through the ramshead), and the thrust load perpendicular to the T-quencher arms (due to a skewed air/water interface) are calculated as specified in the LDR.

The SRV water and air clearing thrust and all other SRV water clearing load calculation procedures, load definitions, and applications are in accordance with the LDR and Appendix A of NUREG-0661.

Table 1-4.2-2
PLANT UNIQUE INITIAL
CONDITIONS FOR ACTUATION CASES
USED FOR SRVDL CLEARING TRANSIENT LOAD DEVELOPMENT

PARAMETER	CASE A1.1	CASE A1.2	CASE C3.1	CASE C3.2
PRESSURE IN THE WETWELL (psia)	14.7	43.0	14.7	43.0
PRESSURE IN THE DRYWELL (psia)	14.7	44.4	14.7	44.4
ΔP VACUUM BREAKER (psid)	0.3	0.3	0.3	0.3
INITIAL PIPE WALL TEMPERATURE IN THE WETWELL AIRSPACE (°F)	115	340	350	350
INITIAL PIPE WALL TEMPERATURE IN THE SUPPRESSION POOL (°F)	95	154	95	154
PRESSURE IN THE POOL (psia)	14.4	44.1	14.4	44.1
INITIAL AIR PRESSURE IN SRVDL (psia)	14.4	44.1	14.4	44.1
INITIAL AIR DENSITY IN SRVDL (lbm/ft ³)	0.068	0.149	0.040	0.147
INITIAL WATER VOLUME IN SRVDL AND T-QUENCHER (ft ³)	14.917	13.257	15.674	13.257

Table 1-4.2-3

SRVDL ANALYSIS PARAMETERS

PARAMETER	VALUE
DESIGN SRV FLOW RATE (lbm/sec)	290.3
STEAM LINE PRESSURE (psia)	1158.0
STEAM DENSITY IN THE STEAM LINE (lbm/ft ³)	2.65
RATIO OF AREAS OF DISCHARGE DEVICE EXIT TO TOTAL T-QUENCHER ARM	0.94

Following SRV actuation, the air mass in the SRVDL is expelled into the suppression pool, forming many small air bubbles. These bubbles then coalesce into four larger bubbles which expand and contract as they rise and break through the pool surface. The positive and negative dynamic pressures developed within these bubbles result in an oscillatory, attenuated pressure loading on the suppression chamber shell.

To account for the variations in the hydrodynamic characteristics of the SRV discharge line configurations, loads are generated for the shortest and the longest SRV line and the higher of the two loads is used in the analysis. This approach conservatively bounds the loads. The analytical model which is used to predict air bubble and suppression chamber shell boundary pressures resulting from SRV discharge is similar to that described in Reference 16. The analytical model in Reference 16 was modified slightly to more closely bound the magnitudes and time characteristics of pressures observed in the Monticello test. Figure 1-4.2-4 shows a comparison

of the shell pressure time-history measured during the Monticello test to the shell pressure time-history computed using the revised analytical model. The comparison is shown for shell pressures at the bottom of the suppression chamber beneath the quencher, where the highest shell pressures were observed. Figure 1-4.2-4 shows that the predicted shell pressures envelop those observed in the Monticello test.

The pressure time-history generated using the analytical model discussed above is used to perform a forced vibration analysis of the suppression chamber. The phenomena associated with SRV discharge into the suppression pool are characteristic of an initial value or free vibration condition rather than a forced vibration condition. Correction factors are applied to convert the forced vibration response to a free vibration response.

The correction factors are developed using simple one degree-of-freedom analogs. The factors vary with the ratio of load frequency to structural frequency and are applied to the response (displacement, velocity, and acceleration) associated with each structural

mode. Figure 1-4.2-5 shows the modal correction factors used in the suppression chamber evaluation.

The pressure magnitudes produced by the analytical model discussed previously were calibrated to envelop the maximum local shell pressures observed in the DAEC test. This results in an overly conservative prediction of net vertical loads, as discussed in Section 3.10.2.9 of NUREG-0661. A net vertical load correction factor was developed by comparing net vertical pressure loads measured in the DAEC test with those predicted during test conditions. The factor was determined to be 0.73 for upward and downward loads. This correction factor is applied to forces acting on the suppression chamber supports.

Table 1-4.2-4 shows a comparison of shell membrane stresses and column forces observed in the Monticello test with those values predicted using the analytical methods and correction factors described above. This table shows that predicted forces and stresses conservatively bound the measured values at all locations. A series of in-plant tests were performed at DAEC in June 1981. These tests provided additional confirmation that the computed loadings and predicted structure response due to SRV discharge

are conservative. A comparison of shell membrane stresses and column forces observed in the DAEC test with those values predicted using the analytical methods described above is shown in Table 1-4.2-5.

The torus shell pressures are generated following NUREG-0661. For instance, the water leg is limited to 13.5 feet, the frequency is adjusted accordingly ($\pm 25\%$ for first actuations, $\pm 40\%$ for subsequent actuations), and the pressure amplitude for first actuation is used with the frequency of the subsequent actuation, for subsequent actuations.

Table 1-4.2-4

COMPARISON OF ANALYSIS AND MONTICELLO TEST RESULTS

QUANTITY	LOCATION	ANALYSIS	TEST	<u>ANALYSIS</u> <u>TEST</u>
SUPPRESSION CHAMBER SHELL MEMBRANE STRESSES (ksi)	MIDBAY 90° FROM BDC REACTOR SIDE	2.8	0.6	4.7
	MIDBAY 52.5° FROM BDC REACTOR SIDE	2.3	1.1	2.1
	MIDBAY 12.4° FROM BDC REACTOR SIDE	2.2	1.7	1.3
	MIDBAY 12.4° FROM BDC OPPOSITE REACTOR	2.1	1.4	1.5
	MIDBAY 52.5° FROM BDC OPPOSITE REACTOR	2.5	1.1	2.3
	1/4 BAY 12.4° FROM BDC OPPOSITE REACTOR	2.2	1.4	1.6
TORUS COLUMN UPLIFT LOADS (kips)	INSIDE COLUMN	123.9	49.0	2.5
	OUTSIDE COLUMN	157.8	52.5	3.0
TORUS COLUMN DOWN LOADS (kips)	INSIDE COLUMN	152.9	64.5	2.4
	OUTSIDE COLUMN	178.2	78.5	2.3

Table 1-4.2-5

COMPARISON OF ANALYSIS AND DAEC TEST RESULTS

QUANTITY	LOCATION	ANALYSIS	TEST	<u>ANALYSIS</u> <u>TEST</u>
SUPPRESSION CHAMBER SHELL MEMBRANE STRESSES (ksi)	MIDBAY 12° FROM BDC REACTOR SIDE	3.3	2.6	1.3
	MIDBAY 12° FROM BDC OPPOSITE REACTOR	3.6	2.1	1.7
	MIDBAY 45° FROM BDC OPPOSITE REACTOR	2.9	1.3	2.2
	1/4 BAY 12° FROM BDC OPPOSITE REACTOR	3.5	3.1	1.1
TORUS COLUMN UPLIFT LOADS (kips)	INSIDE COLUMN	110.7	36.5	3.0
	OUTSIDE COLUMN	124.7	38.8	3.2
TORUS COLUMN DOWN LOADS (kips)	INSIDE COLUMN	51.2	24.3	2.1
	OUTSIDE COLUMN	54.0	50.2	1.1

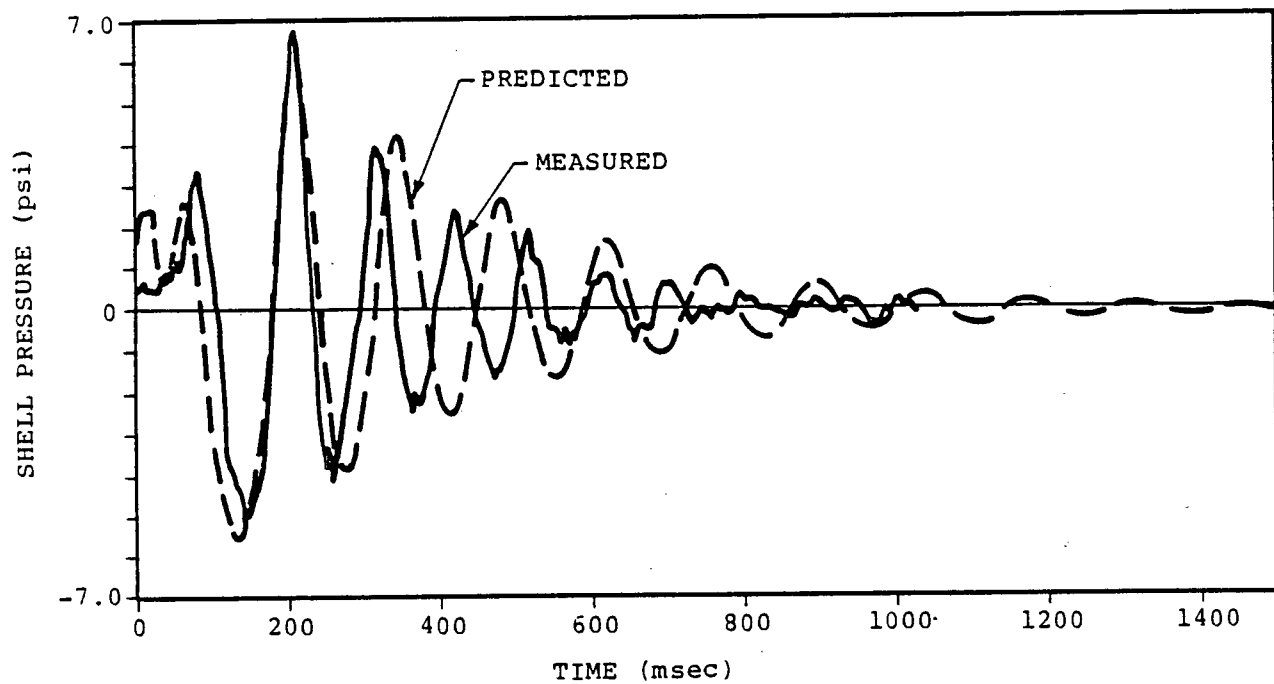


Figure 1-4.2-4

COMPARISON OF PREDICTED AND MEASURED SHELL PRESSURE
TIME-HISTORIES FOR MONTICELLO TEST 801

IOW-40-199-1
Revision 0

1-4.98

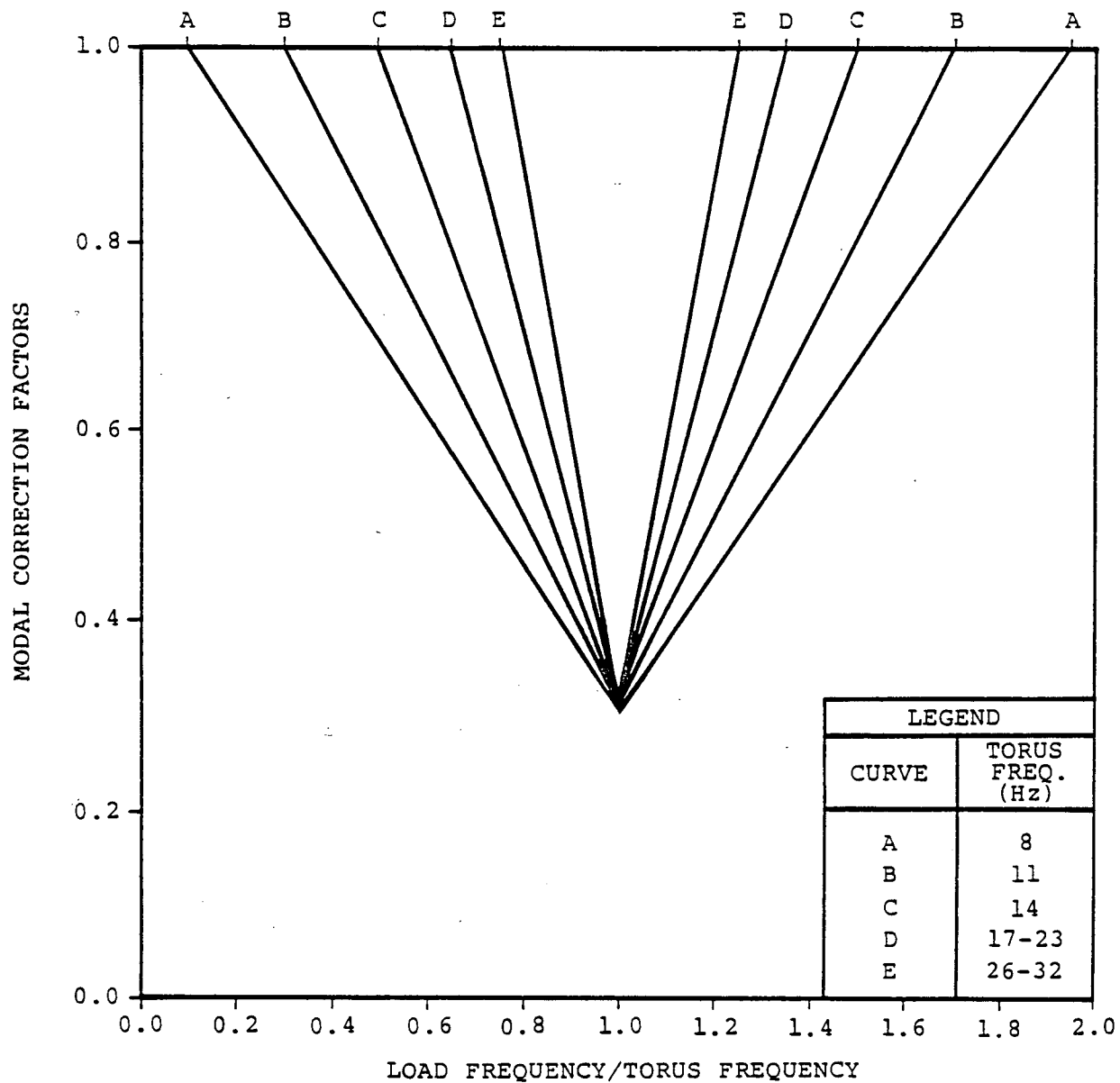


Figure 1-4.2-5

MODAL CORRECTION FACTORS FOR ANALYSIS
OF SRV DISCHARGE TORUS SHELL LOADS

IOW-40-199-1
Revision 0

1-4.99

1-4.2.4 SRV Loads on Submerged Structures

This section addresses the load definition procedures for determining SRV loads on submerged structures due to T-quencher water jets and bubbles.

When an SRV is actuated, water initially contained in the submerged portion of the SRVDL is forced out of the T-quencher through holes in the arms, forming orifice jets. Some distance downstream, the orifice jets merge to form column jets. Further downstream, the column jets merge to form the quencher arm jets. As soon as the water flow through the arm hole ceases, the quencher arm jet velocity decreases rapidly and the jet penetrates a limited distance into the pool. The T-quencher water jets create drag loads on nearby submerged structures which are within the jet path.

Oscillating bubbles resulting from a SRV actuation create an unsteady three-dimensional flow field and therefore induce acceleration and standard drag forces on the submerged structures in the suppression pool.

a. T-quencher Water Jet Loads

The T-quencher water jet model conservatively models the T-quencher water jet test data. The bases, justification, and assumptions for the Mark I T-quencher model are presented in Reference 1. The SRV T-quencher water jet analytical model calculation procedure and application are in accordance with Mark I LDR techniques, and satisfies NUREG-0661 requirements (References 3 and 20).

b. SRV Bubble-Induced Drag Loads

The SRV bubble drag load development methodology, load definition, and application for the DAEC plant unique analysis are performed utilizing the DAEC T-quencher geometry (Figure 1-4.2-1). The techniques utilized in developing the DAEC loads are in accordance with the LDR and Appendix A of NUREG-0661. Dynamic load factors are derived from DAEC in-plant SRV test data.

A bubble pressure bounding factor based on Monticello test data is utilized for DAEC SRV load development in place of the LDR value of 2.5. A value of 1.75 produces results which bound the peak positive bubble pressure and maximum bubble pressure differential from the Monticello T-quencher test data. The calculated values using 1.75 are 9.9 psid and 18.1 psid, respectively. The predicted values correspond to single valve actuation at normal water level of the cold pop case listed in Table 3-3 of Reference 16. The measured values shown in Table 3-3 of Reference 16 are 9.3 psid and -8.1 psid for the peak maximum and minimum bubbles pressures, respectively.

The bubble pressure bounding factor of 1.75 derived from the Monticello test data and used to generate loads for DAEC was subsequently verified against the DAEC SRV test data. The peak maximum and minimum bubble pressures were 16.2 psid and -7.4 psid, respectively, measured at DAEC during a cold pop, single valve actuation at normal water level. The predicted bubble pressures using a value of 1.75 are 16.31 psid and -7.58 psid for the maximum and

minimum bubble pressures, respectively. The comparison clearly shows that the value of 1.75 produces results which are bounding for DAEC as well.

For submerged structures with sharp corners such as T-beams, I-beams, etc., the acceleration drag volumes are calculated using the methodology in Section 1-4.1.5.

The model described in Section 1-4.2.3 is used to determine drag loads on downcomers due to SRV bubble oscillation.

Calibration factors developed from the in-plant tests conducted at DAEC in June 1981 were used to determine drag loads on SRV lines, elbow support beams, T-quenchers and their supports, and vent header support columns.

For the SRVDL piping and piping supports in the wetwell, the SRVDL-related loads such as rams-head thrust, air bubble drag and uneven clearing thrust loads were developed for actuations occurring under the in-plant test conditions.

Subsequently, the piping and piping support response due to these analytically derived loads was calculated. The calculated stresses were then compared with the peak piping and piping support response detected by the in-plant test. A calibration factor is generated based on the ratio of the stress response from the actual test and the analytically derived stress for the test conditions.

For the vent header support columns, loads were developed for actuations occurring under in-plant test conditions. Subsequently, the vent header column response due to these analytically derived loads was calculated. The calculated stresses were then compared with the peak column responses detected during the SRV in-plant test. A calibration factor is generated based upon the ratio of the responses from the actual test and the analytically derived stress for the test conditions.

Not all of the suppression pool hydrodynamic loads discussed in this evaluation can occur at the same time. In addition, the load magnitudes and timing vary, depending on the accident scenario being considered. Therefore, it is necessary to construct a series of event combinations to describe the circumstances under which individual loads might combine.

Tables 1-3.2-1 and 1-3.2-2 show the event combinations used in the plant unique analysis. The combinations of load cases were determined from typical plant primary system and containment response analyses, with considerations for automatic actuation, manual actuation, and single active failures of the various systems in each event. This section describes the event sequences for the following postulated LOCA's.

- Design Basis Accident
- Intermediate Break Accident
- Small Break Accident

Table 1-4.3-1 identifies the SRV and LOCA loads which potentially affect structural components and identifies the appropriate section of this report defining the loads. For SRV piping and other structures within the wetwell, the locations of the structural components are considered to determine if any of the identified conditions affect the structures.

Table 1-4.3-1

SRV AND LOCA STRUCTURAL LOADS

LOADS	STRUCTURES						OTHER WETWELL INTERIOR STRUCTURES		
	TORUS SHELL	TORUS SUPPORT SYSTEM	MAIN VENTS	VENT HEADER	DOWNCOMERS	SRV PIPING	ABOVE NORMAL WATER LEVEL	ABOVE BOTTOM OF DOWNCOMERS AND BELOW NORMAL WATER LEVEL	BELOW BOTTOM OF DOWNCOMERS
1-4.1.1 CONTAINMENT PRESSURE AND TEMPERATURE RESPONSE	X	X	X	X	X	X	X	X	X
1-4.1.2 VENT SYSTEM DISCHARGE LOADS			X	X	X				
1-4.1.3 POOL SWELL LOADS ON THE TORUS SHELL	X	X							
1-4.1.4 POOL SWELL LOADS ON ELEVATED STRUCTURES									
1-4.1.4.1 IMPACT AND DRAG LOADS ON THE VENT SYSTEM			X	X	X				
1-4.1.4.2 IMPACT AND DRAG LOADS ON OTHER STRUCTURES			X			X	X		
1-4.1.4.3 POOL SWELL FROTH IMPINGEMENT LOADS			X				X		
1-4.1.4.4 POOL FALLBACK LOADS						X	X	X	
1-4.1.5 LOCA WATERJET LOADS ON SUBMERGED STRUCTURES						X			X
1-4.1.6 LOCA BUBBLE-INDUCED LOADS ON SUBMERGED STRUCTURES						X			X
1-4.1.7 CONDENSATION OSCILLATION LOADS									
1-4.1.7.1 CO LOADS ON THE TORUS SHELL	X	X							
1-4.1.7.2 CO LOADS ON THE DOWNCOMERS AND VENT SYSTEM			X	X	X				
1-4.1.7.3 CO LOADS ON SUBMERGED STRUCTURES						X		X	X
1-4.1.8 CHUGGING LOADS									
1-4.1.8.1 CHUGGING LOADS ON THE TORUS SHELL	X	X							
1-4.1.8.2 CHUGGING DOWNCOMER LATERAL LOADS				X	X				
1-4.1.8.3 CHUGGING LOADS ON SUBMERGED STRUCTURES						X		X	X
1-4.2 SAFETY RELIEF VALVE DISCHARGE LOADS									
1-4.2.2 SRV DISCHARGE LINE CLEARING LOADS						X			
1-4.2.3 SRV LOADS ON THE TORUS SHELL	X	X							
1-4.2.4 SRV LOADS ON SUBMERGED STRUCTURES					X	X		X	X

The DBA for the Mark I containment design is the instantaneous guillotine rupture of the largest pipe in the primary system (the recirculation line). Figures 1-4.3-1 through 1-4.3-3 present the load combinations for the DBA. Table 1-4.3-2 presents the nomenclature for these figures. The bar charts for the DBA show the loading condition combination for postulated breaks large enough to produce significant pool swell. The length of the bars in the figures indicates the time periods during which the loading conditions may occur. Loads are considered to act simultaneously on a structure at a specific time if the loading condition bars overlap at that time. For SRV discharge, the loads may occur at any time during the indicated time period. The assumption of combining a SRV discharge with the DBA is beyond the design basis of the DAEC. Therefore, the DBA and SRV load combination is evaluated only to demonstrate containment structural capability. Table 1-4.3-3 shows the SRV discharge loading conditions.

Table 1-4.3-2

EVENT TIMING NOMENCLATURE

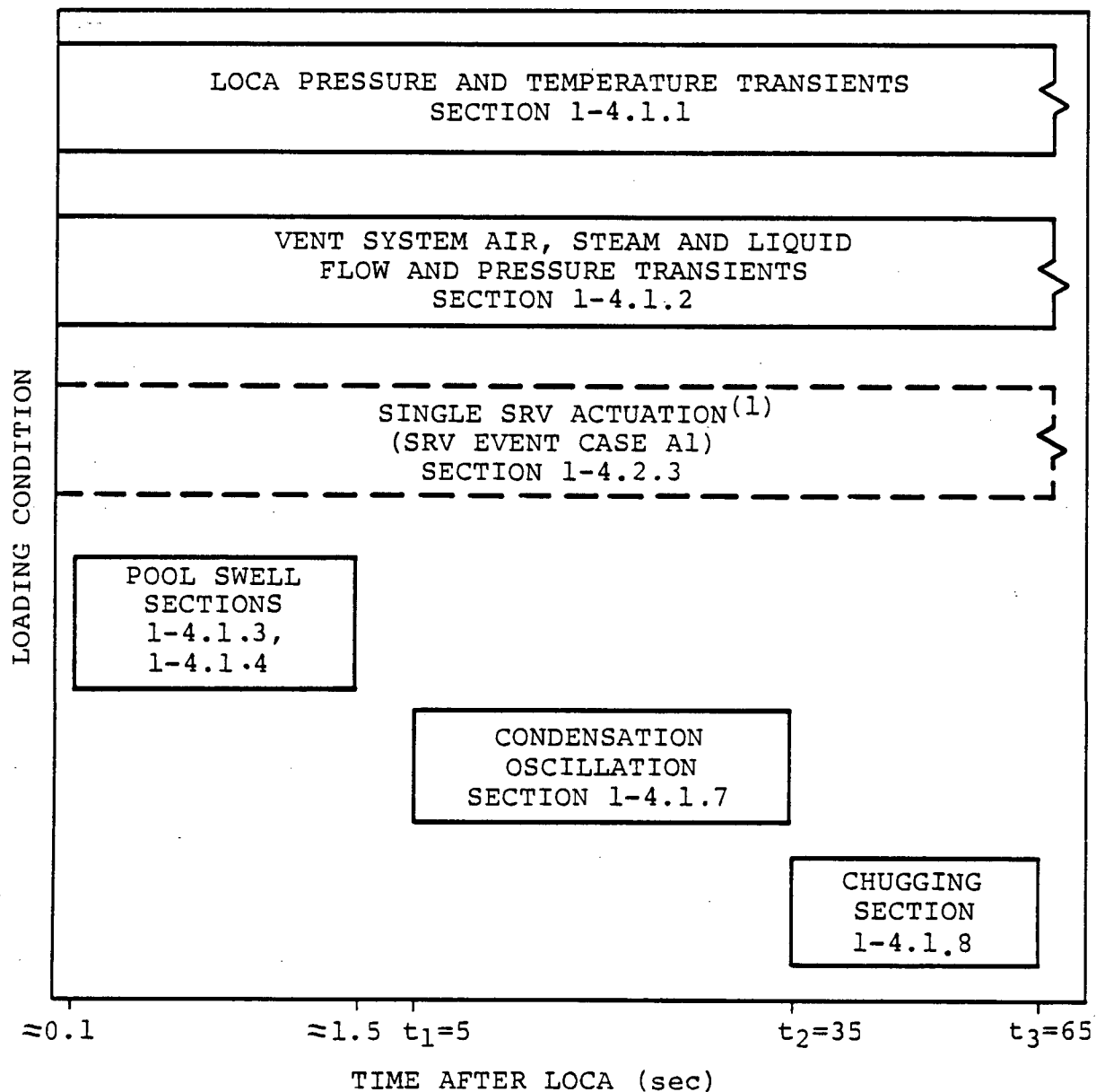
TIME	DESCRIPTION
t_1	THE ONSET OF CONDENSATION OSCILLATION
t_2	THE BEGINNING OF CHUGGING
t_3	THE END OF CHUGGING
t_4	TIME OF COMPLETE REACTOR DEPRESSURIZATION
t_{ADS}	ADS ACTUATION ON HIGH DRYWELL PRESSURE AND LOW REACTOR WATER LEVEL. THE ADS IS ASSUMED TO BE ACTUATED BY THE OPERATOR FOR THE SBA.

Table 1-4.3-3

SRV DISCHARGE LOAD CASES
FOR MARK I STRUCTURAL ANALYSIS

INITIAL CONDITIONS	ANY ONE VALVE	ADS VALVES	MULTIPLE VALVES (1)
FIRST ACTUATION	A 1	A 2	A 3
FIRST ACTUATION, LEAKING SRV(2)			B 3
SUBSEQUENT ACTUATION			C 3

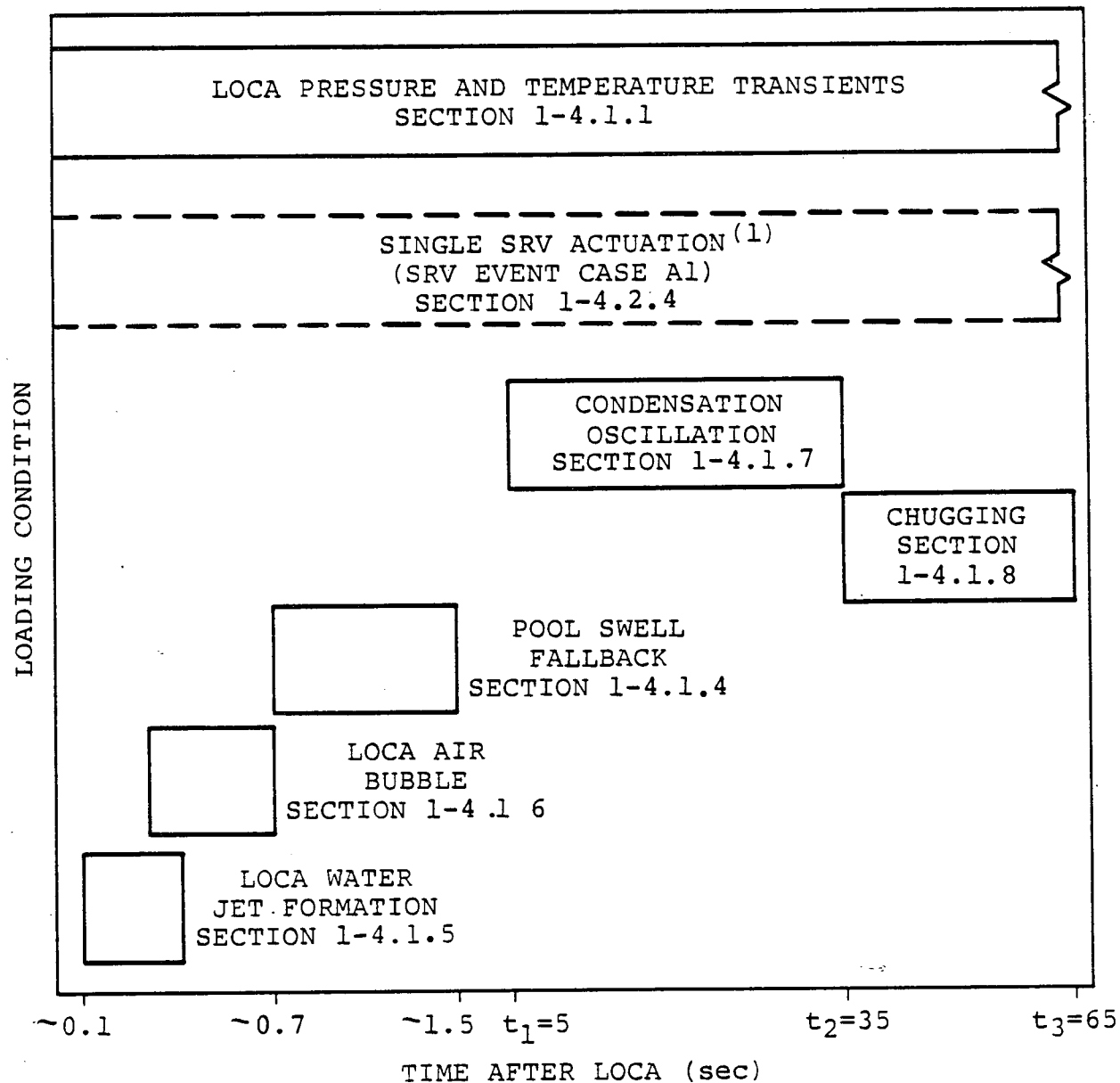
- (1) THE NUMBER (ONE OR MORE) AND LOCATION OF SRV's ASSUMED TO ACTUATE ARE DETERMINED BY PLANT UNIQUE ANALYSES.
- (2) THE LOADS FOR T-QUENCHER DISCHARGE DEVICES ARE NOT AFFECTED BY LEAKING SRV's. NO SRV's ARE CONSIDERED TO LEAK PRIOR TO A LOCA.



- (1) THIS ACTUATION IS ASSUMED TO OCCUR COINCIDENT WITH THE POOL SWELL EVENT. ALTHOUGH SRV ACTUATION CAN OCCUR LATER IN THE DBA, THE RESULTING AIR LOADING ON THE TORUS SHELL IS NEGLIGIBLE SINCE THE AIR AND WATER INITIALLY IN THE LINE WILL BE CLEARED AS THE DRYWELL-TO-WETWELL ΔP INCREASES DURING THE DBA TRANSIENT.

Figure 1-4.3-1

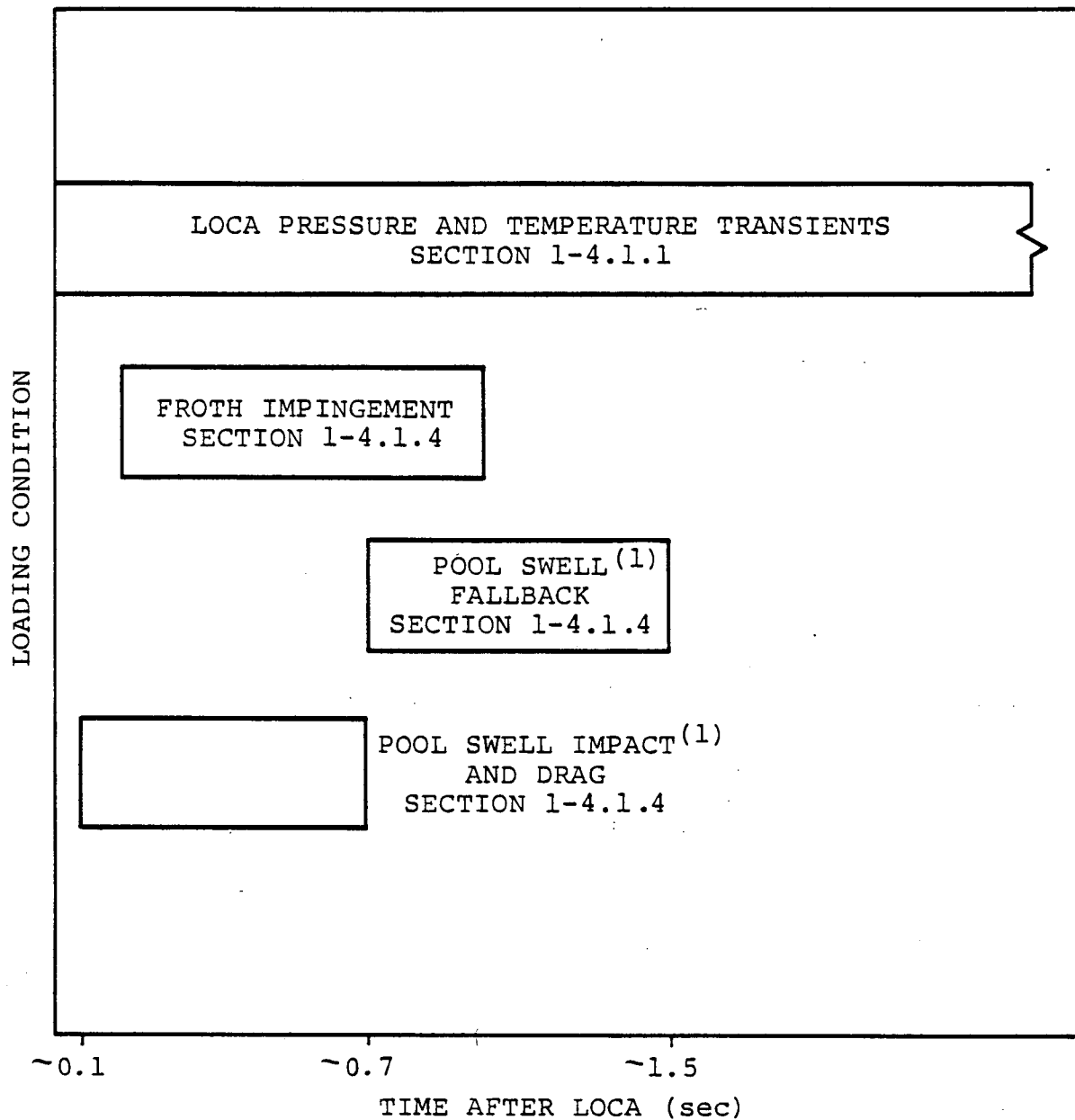
LOADING CONDITION COMBINATIONS FOR THE VENT HEADER,
MAIN VENTS, DOWNCOMERS, AND TORUS SHELL DURING A DBA



- (1) THIS ACTUATION IS ASSUMED TO OCCUR COINCIDENT WITH THE POOL SWELL EVENT. ALTHOUGH SRV ACTUATION CAN OCCUR LATER IN THE DBA, THE RESULTING AIR LOADING ON THE TORUS SHELL IS NEGLIGIBLE SINCE THE AIR AND WATER INITIALLY IN THE LINE WILL BE CLEARED AS THE DRYWELL-TO-WETWELL ΔP INCREASES DURING THE DBA TRANSIENT.

Figure 1-4.3-2

LOADING CONDITION COMBINATIONS FOR SUBMERGED
STRUCTURES DURING A DBA



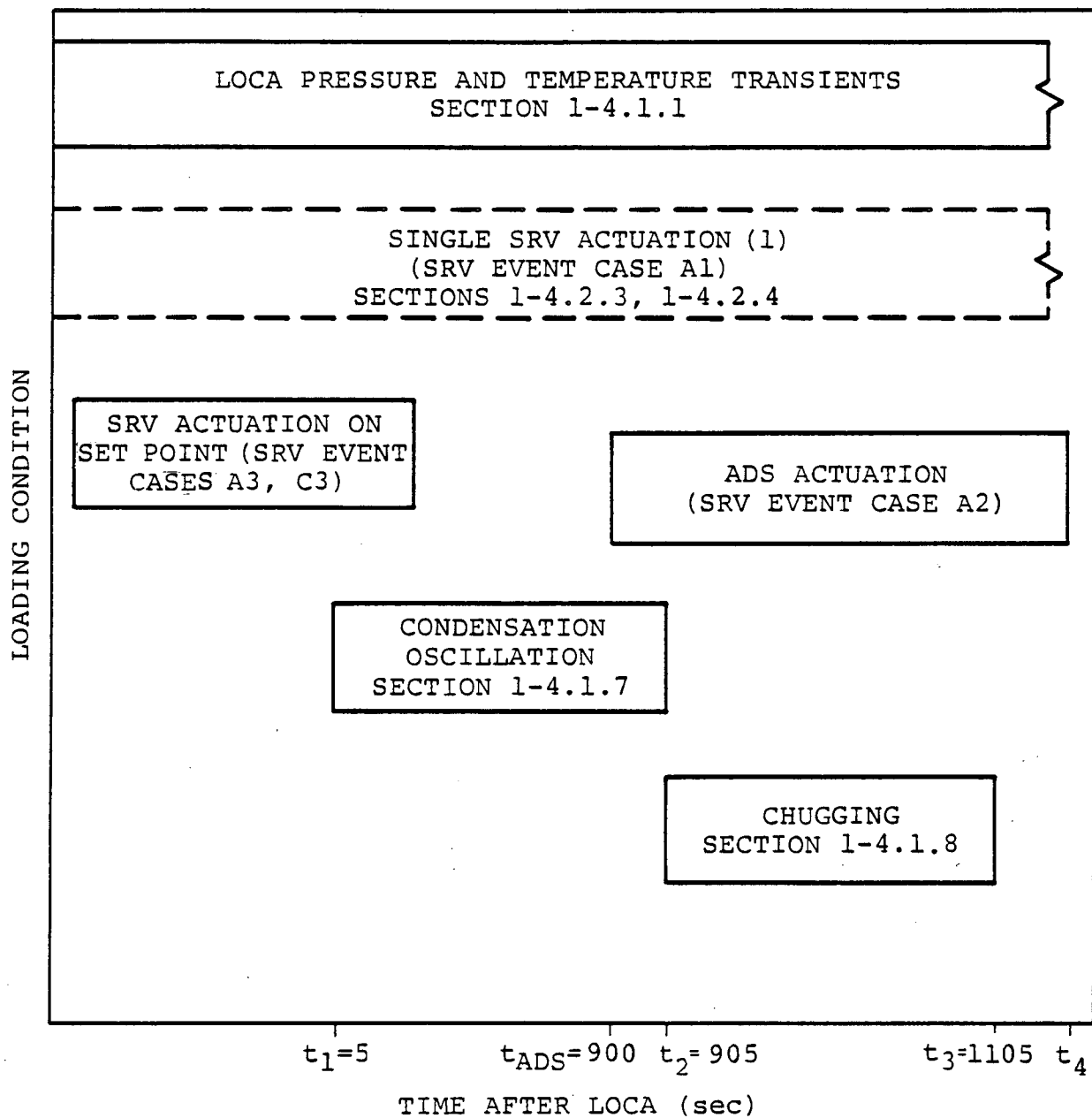
(1) STRUCTURES BELOW MAXIMUM POOL SWELL HEIGHT.

Figure 1-4.3-3

LOADING CONDITION COMBINATIONS FOR SMALL
STRUCTURES ABOVE SUPPRESSION POOL DURING A DBA

1-4.3.2 Intermediate Break Accident

The bar chart (Figure 1-4.3-4) shows conditions for a break size large enough such that the HPCI system cannot prevent ADS actuation on low-water level, but, for smaller break sizes which would produce significant pool swell loads. A break size of 0.1 ft^2 is assumed for an IBA. Table 1-4.3-3 shows SRV discharge loading conditions. The IBA break is too small to cause significant pool swell.



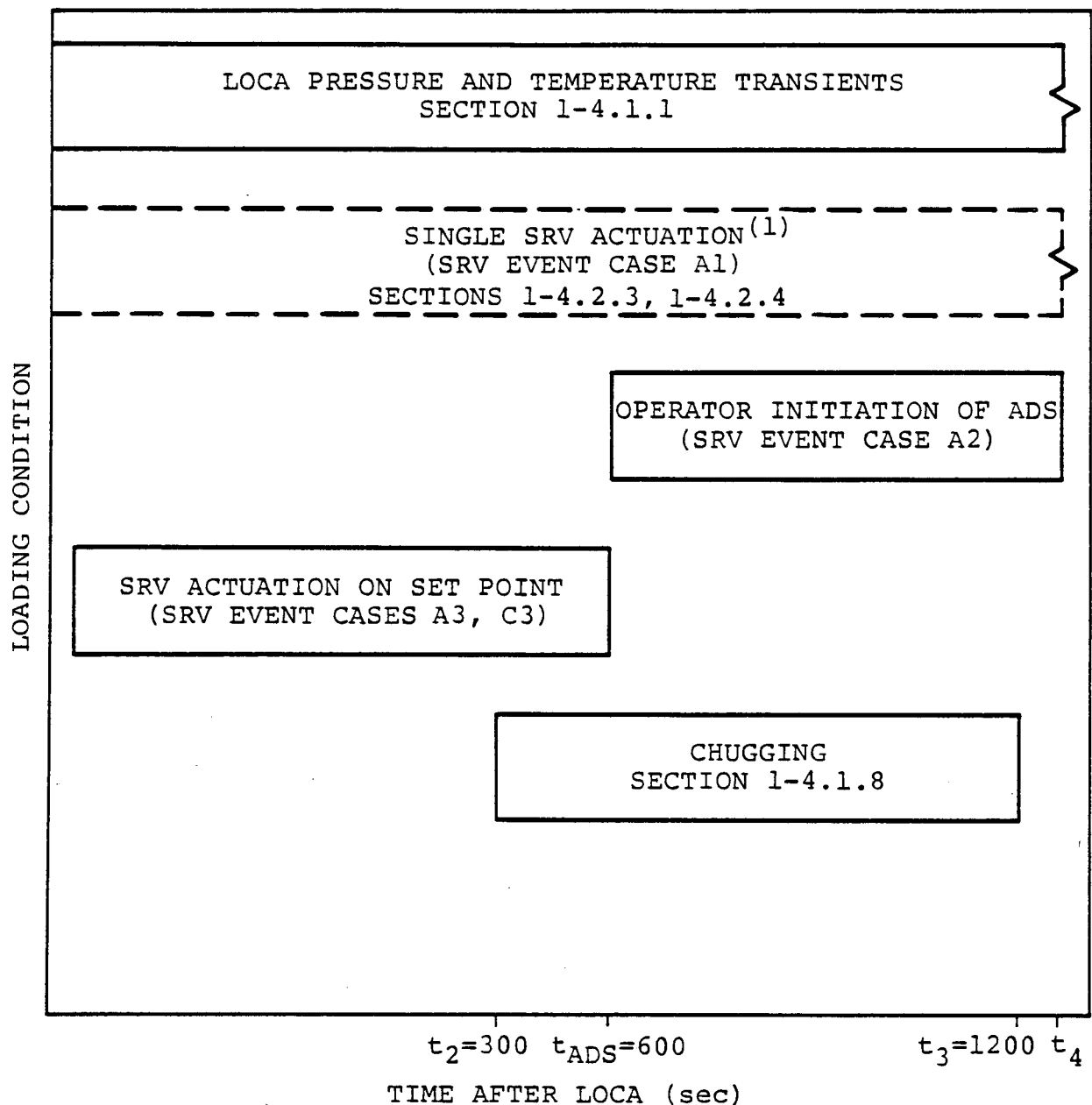
(1) LOADING NOT COMBINED WITH OTHER SRV CASES.

Figure 1-4.3-4

LOADING CONDITION COMBINATIONS FOR THE
VENT HEADER, MAIN VENTS, DOWNCOMERS, TORUS SHELL,
AND SUBMERGED STRUCTURES DURING AN IBA

1-4.3.3 Small Break Accident

The bar chart (Figure 1-4.3-5) for the SBA shows conditions for a break size equal to 0.01 ft^2 . For a SBA, the HPCI system would be able to maintain the water level and the reactor would be depressurized by means of operator initiation of the ADS. Table 1-4.3-3 identifies the SRV discharge loading conditions. The SBA break is too small to cause significant pool swell and condensation oscillation does not occur during an SBA. The ADS is assumed to be initiated by the operator 10 minutes after the SBA begins. With the concurrence of the NRC (Reference 17), the procedures which the operator will use to perform this action are being developed as part of the Emergency Procedures Guidelines.



(1) LOADING NOT COMBINED WITH OTHER SRV CASES.

Figure 1-4.3-5
LOADING CONDITION COMBINATIONS FOR THE VENT HEADER,
MAIN VENTS, DOWNCOMERS, TORUS SHELL, AND
SUBMERGED STRUCTURES DURING A SBA

1-5.0

SUPPRESSION POOL TEMPERATURE MONITORING SYSTEM

This section describes the DAEC suppression pool temperature response to SRV transients and the design of the Suppression Pool Temperature Monitoring System (SPTMS).

IOW-40-199-1
Revision 0

1-5.1

The DAEC takes advantage of the large thermal capacitance of the suppression pool during plant transients requiring safety relief valve actuation. Steam is discharged through the SRV's into the suppression pool where it is condensed, resulting in an increase in the temperature of the suppression pool water. Although stable steam condensation is expected at all pool temperatures, Reference 16 imposes a local temperature limit (Figure 1-5.1-1) in the vicinity of the DAEC T-quencher discharge devices.

To demonstrate that the local pool temperature limit is satisfied, seven limiting transients involving SRV discharges are analyzed. Table 1-5.1-1 provides a summary of the transients analyzed and the corresponding pool temperature results. Three of the transients conservatively assume the failure of one Residual Heat Removal (RHR) loop in addition to the single equipment malfunction or operator error which initiated the event. This conservative assumption exceeds the current licensing basis for anticipated operational transients.

Each of the SRV discharge transients are analyzed assuming an initial pool temperature of 95°F, which is the Technical Specification pool temperature limit for normal power operation. The notes to Table 1-5.1-1 list other initial conditions and assumptions included in these analyses.

The analysis of Case 2C, normal depressurization at isolated hot shutdown, shows a maximum local pool temperature of 187°F. This demonstrates that with no system failures and in the event of a non-mechanistic scram, depressurizing the reactor pressure vessel (RPV) with SRV's at 100°F/hr results in local pool temperatures that are well below the condensation stability limit shown (Figure 1-5.1-1).

Case 1B, SORV at power and spurious isolation with RHR loops available, and Case 2A, reactor rapid depressurization after isolation with one RHR loop available, result in a maximum local pool temperature of 193°F, which is below the condensation stability limit of 200.2°F. High local temperatures are predicted in these cases because of reduced mixing when the available RHR pool cooling system is switched to the shutdown cooling mode.

The maximum local pool temperature of all other cases also remains below the condensation stability limit throughout the transient. In general, local-to-bulk temperature differences at the time of maximum temperatures are about 10°F for cases where two RHR loops are assumed available and about 26°F for cases where one RHR loop is assumed available. Thus, bulk pool circulation induced by the RHR loops leads to good thermal mixing, which effectively lowers the local pool temperatures in the vicinity of quencher devices.

Table 1-5.1-1 shows the two events which produce the highest maximum local pool temperature, Cases 1B and 2A. These two cases were also analyzed at 102% of 105% of rated turbine throttle steam flow (1691 MWT). Table 1-5.1-2 shows the results as Cases 1BX and 2AX. Cases 1B and 2A were also analyzed with an RHR heat exchanger service water flow rate of 4080 gpm, which is a 15% decrease in flow rate. Table 1-5.1-2 shows these results as Cases 1BY and 2AY. The additional SRV transients were analyzed to bound Cases 1B and 2A. The results show that the effects on the maximum bulk and local pool temperatures are

negligible. In particular, the maximum local pool temperature increased to 194°F, which is well below the condensation stability limit shown (Figure 1-5.1-1).

Table 1-5.1-1

SUMMARY OF DAEC POOL TEMPERATURE RESPONSE TO SRV TRANSIENTS

CASE NUMBER	EVENT	NUMBER OF SRV's MANUALLY OPENED	MAXIMUM COOLDOWN RATE (°F/hr)	MAXIMUM BULK POOL TEMPERATURE (°F)	MAXIMUM LOCAL POOL TEMPERATURE (°F)
1A	SORV AT POWER, 1 RHR LOOP	0	790	156	186
1B	SORV AT POWER, SPURIOUS ISOLATION, 2 RHR LOOPS	0	1110 ⁽¹⁾	181	193
2A	RAPID DEPRESSURIZATION AT ISOLATED HOT SHUTDOWN, 1 RHR LOOP	4	200	173	193
2B	SORV AT ISOLATED HOT SHUTDOWN, 2 RHR LOOPS	0	1110 ⁽¹⁾	166	175
2C	NORMAL DEPRESSURIZATION AT ISOLATED HOT SHUTDOWN, 2 RHR LOOPS	4	100	177	187
3A	SBA-ACCIDENT MODE, 1 RHR LOOP	4 (ADS)	1745	160	186
3B	SBA-FAILURE OF SHUTDOWN COOLING MODE, 2 RHR LOOPS	4	100	177	186

(1) DUE TO SORV

NOTES TO TABLE 1-5.1-1

1. REACTOR OPERATION AT 105% OF RATED TURBINE THROTTLE STEAM FLOW (1658 MWt).
2. MINIMUM TECHNICAL SPECIFICATION SUPPRESSION POOL WATER VOLUME (58,900 ft³).
3. THE SUPPRESSION POOL HAS NO INITIAL VELOCITY.
4. WETWELL AND DRYWELL AIRSPACES ARE AT NORMAL OPERATING CONDITIONS.
5. OFF-SITE POWER IS AVAILABLE.
6. THE CONTROL VOLUME OF THE REACTOR INCLUDES THE REACTOR VESSEL, THE RECIRCULATION LINES, AND THE STEAM LINES FROM THE VESSEL TO THE INBOARD MSIV.
7. NORMAL AUTOMATIC OPERATION OF THE PLANT AUXILIARY SYSTEM (HIGH PRESSURE COOLANT INJECTION (HPCI), ADS).
8. THE CORE SPRAY PUMPS HAVE A MANUAL SHUTOFF AT VESSEL HIGH WATER LEVEL (LEVEL 8 ELEVATION). THEY ARE REACTIVATED WHEN THE LEVEL DROPS AS NEEDED TO MAINTAIN WATER LEVEL AND MAY BE SHUT OFF AGAIN.
9. CONTROL ROD DRIVE (CRD) FLOW IS MAINTAINED CONSTANT AT 8.33 LBM/SEC.
10. SRV (MANUAL, AUTOMATIC, ADS) CAPACITIES ARE AT 122.5% OF ASME-RATED FLOW TO CONSERVATIVELY CALCULATE MAXIMUM POOL TEMPERATURES.
11. THE LICENSED DECAY-HEAT CURVE (MAY-WITT) FOR CONTAINMENT ANALYSIS IS USED.
12. NO HEAT TRANSFER IS CONSIDERED IN THE DRYWELL OR WETWELL AIRSPACE.
13. THE MSIV'S CLOSE THREE SECONDS AFTER A ONE-HALF SECOND DELAY FOR THE ISOLATION SIGNAL.
14. OPERATOR ACTIONS ARE BASED ON NORMAL OPERATOR ACTION TIMES AND LICENSING BASIS DELAYS DURING THE GIVEN EVENT.
15. A SWITCHOVER TIME OF 16 MINUTES IS TAKEN TO SWITCH FROM THE POOL COOLING MODE TO THE SHUTDOWN COOLING MODE.

NOTES TO TABLE 1-5.1-1
(Concluded)

16. WHEN BOTH RHR LOOPS ARE OPERATING AND SHUTDOWN COOLING IS AVAILABLE, ONE RHR LOOP IS LEFT ALIGNED IN THE POOL COOLING MODE WHILE THE OTHER IS DIVERTED TO SHUTDOWN COOLING. THIS ASSUMPTION IS REASONABLE BECAUSE THE POOL IS AT A HIGH TEMPERATURE, AND BECAUSE A SINGLE RHR LOOP WILL EFFECTIVELY DEPRESSURIZE THE VESSEL VIA SHUTDOWN COOLING.
17. DRYWELL FAN COOLERS ARE AVAILABLE IN SORV EVENTS AND ISOLATION EVENTS TO KEEP THE DRYWELL PRESSURE BELOW THE HIGH DRYWELL PRESSURE TRIP SET POINT (2 PSIG).
18. THE ADS SYSTEM IS MODELED BY FULLY OPENING FOUR SRV'S IN THE ADS MODE. THE ADS SYSTEM MAY BE ACTUATED MANUALLY AT A HIGH SUPPRESSION POOL TEMPERATURE OF 120°F.
19. ALL RHR AND ECCS PUMPS HAVE 100% OF THEIR HORSEPOWER RATING CONVERTED TO A PUMP HEAT INPUT (BTU/SEC) AND ADDED DIRECTLY TO THE POOL AS AN ENTHALPY RISE OVER TIME OF PUMP OPERATION. THIS ASSUMPTION ADDS CONSERVATISM TO THE POOL TEMPERATURE RESULTS.
20. THE FEEDWATER SYSTEM HAS MOTOR-DRIVEN PUMPS WHICH SUPPLY FEEDWATER TO THE REACTOR VESSEL THROUGHOUT EACH EVENT. THE FEEDWATER TEMPERATURE IS TAKEN AS THE ACTUAL TEMPERATURE IN THE FEEDWATER SYSTEM. HOWEVER, FOR THAT PORTION OF THE FEEDWATER SYSTEM WHICH IS LOWER THAN 172°F, THE TEMPERATURE IS CONSERVATIVELY ASSUMED TO BE 172°F. FEEDWATER INJECTION IS DETERMINED BY THE FEEDWATER LEVEL CONTROLS.
21. THE SERVICE WATER TEMPERATURE FOR THE RHR HEAT EXCHANGERS IS KEPT CONSTANT AT 95°F, GIVING A HEAT TRANSFER CAPACITY OF 148.6 BTU/SEC-°F PER LOOP FOR THE 9600 GPM HEAT EXCHANGER FLOWRATE.
22. THE 12" RHR DISCHARGE LINE IS EQUIPPED WITH AN 8" NOZZLE AND IS DIRECTED PARALLEL TO FLOW IN THE DISCHARGE BAY.
23. THE BREAK FLOW MASS AND ENERGY ARE ADDED TO FLOW THROUGH THE QUENCHERS FOR SBA CASES. THIS APPROACH MAKES THE RESULTS OF SBA CASES MORE CONSERVATIVE BECAUSE IT MAINTAINS A "HOT SPOT" AROUND THE QUENCHERS AT ALL TIMES.
24. THE ANALYSES ARE TERMINATED WHEN THE POOL TEMPERATURE REACHES A MAXIMUM AND TURNS AROUND, OR WHEN THE STEAM DISCHARGING ACTIVITIES OF THE SRV'S ARE OVER.
25. THE OPERATOR WILL ATTEMPT TO RECLOSE AN SORV. BASED ON AVAILABLE OPERATING PLANT DATA PRIOR TO THE IMPLEMENTATION OF THE REQUIREMENTS OF IE BULLETIN 80-25 (REFERENCE 19), SORV'S HAVE BEEN SHOWN TO RECLOSE AT AN AVERAGE PRESSURE OF 260 PSIG. THE LOWEST RECLOSURE PRESSURE RECORDED WAS 50 PSIG, AND THIS VALUE IS CONSERVATIVELY ASSUMED FOR THIS ANALYSIS.
26. SRV'S IN THE AUTOMATIC MODE HAVE NORMAL SET POINTS.

Table 1-5.1-2

SUMMARY OF DAEC POOL TEMPERATURE RESPONSE
TO ADDITIONAL SRV TRANSIENTS

CASE NUMBER	EVENT	NUMBER OF SRV's MANUALLY OPENED	MAXIMUM COOLDOWN RATE (°F/hr)	MAXIMUM BULK POOL TEMPERATURE (°F)	MAXIMUM LOCAL POOL TEMPERATURE (°F)
(2) 1BX	SORV AT POWER, SPURIOUS ISOLATION, 2 RHR LOOPS	0	1110 ⁽¹⁾	182	194
(2) 2AX	RAPID DEPRESSURIZATION AT ISOLATED HOT SHUTDOWN, 1 RHR LOOP	4	200	174	194
(3) 1BY	SORV AT POWER, SPURIOUS ISOLATION, 2 RHR LOOPS	0	1110 ⁽¹⁾	181	194
(3) 2AY	RAPID DEPRESSURIZATION AT ISOLATED HOT SHUTDOWN, 1 RHR LOOP	4	200	173	193

- (1) DUE TO SORV.
- (2) THE SAME NOTES IN TABLE 1-5.1-1 APPLY TO THESE CASES EXCEPT NOTE 1. FOR THESE CASES, THE ANALYSES WERE PERFORMED AT 102% OF 105% OF RATED TURBINE THROTTLE STEAM FLOW (1,691 MWT).
- (3) THE SAME NOTES IN TABLE 1-5.1-1 APPLY TO THESE CASES EXCEPT NOTE 21. FOR THESE CASES, THE ANALYSES WERE PERFORMED WITH AN RHR HEAT EXCHANGER SERVICE WATER FLOW RATE OF 4,080 GPM GIVEN A HEAT TRANSFER COEFFICIENT OF 142.7 Btu/sec °F PER LOOP.

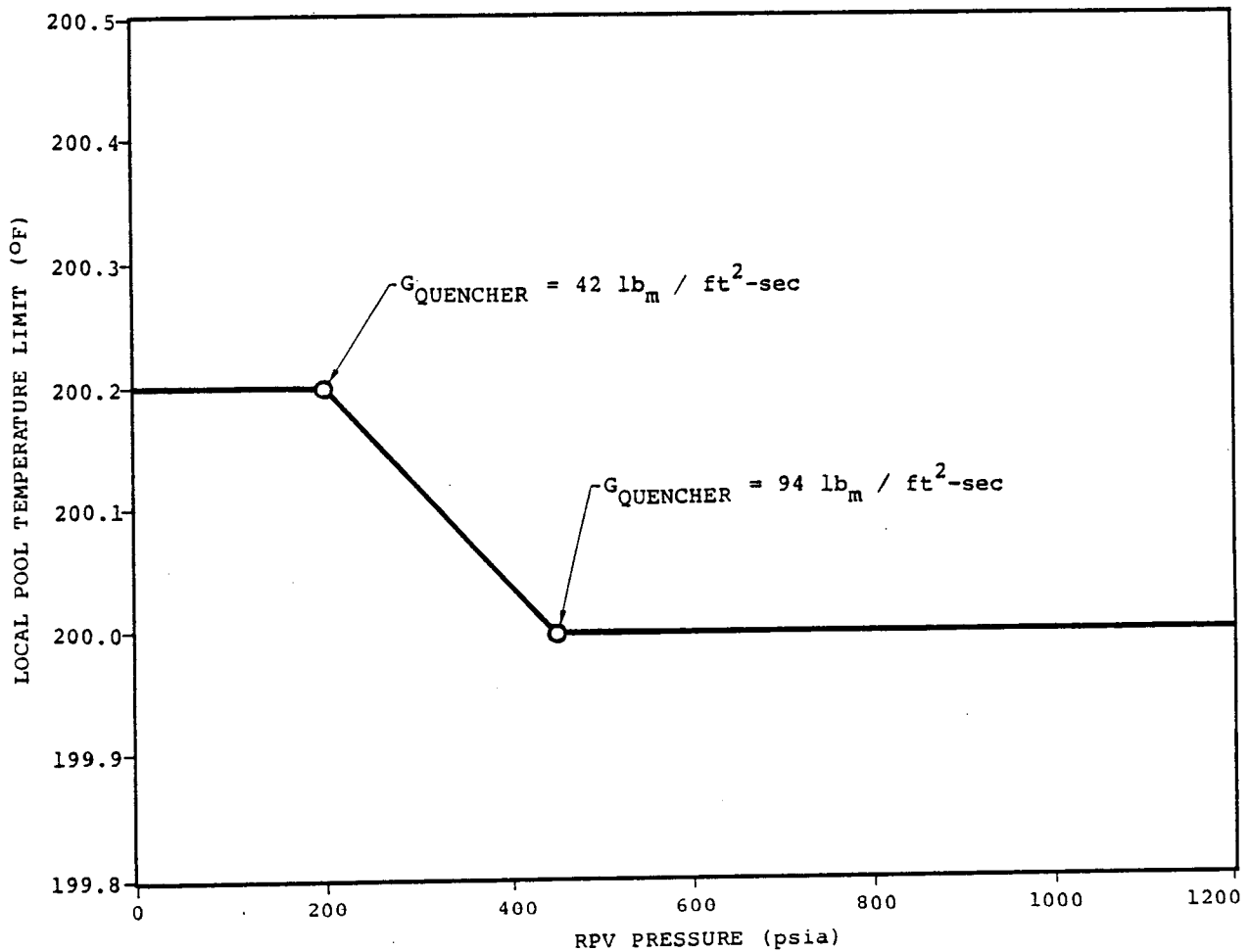


Figure 1-5.1-1

LOCAL POOL TEMPERATURE LIMIT FOR DUANE ARNOLD ENERGY CENTER

IOW-40-199-1
Revision 0

1-5.10

DAEC utilizes a Suppression Pool Temperature Monitoring System (SPTMS) to ensure that the suppression pool temperature is within the allowable Technical Specification limits. The following discussion describes the DAEC SPTMS design and demonstrates conformance to the criteria specified in Appendix A of NUREG-0661.

The DAEC SPTMS utilizes two separate channels of eight sensors per channel to measure temperature. The average temperature of the eight sensors of either channel represents the actual pool bulk temperature. These temperature sensors are seismically qualified and are located in Quality Group B thermowells, fed from an on-site emergency power supply. The thermowells are located around the suppression pool both inboard and outboard at an elevation just below the minimum water level.

An analysis was performed to ascertain the relationship between local temperature and bulk temperature of the suppression pool during transient events. The definitions of local, bulk temperature, and transient

events are those in NUREG-0661. A correlation between the local and bulk temperatures was predicted from this analysis. Then, utilizing the actual pool bulk temperature measured as described above, a conservative local temperature is determined by the correlation analysis to verify compliance with the Technical Specification temperature limits.

At present, only one channel of sensors determines the actual pool bulk temperature, using the DAEC plant computer. The second channel of sensors is installed and wired to the Control Room for future connection. The use of only one of the two monitoring channels is a temporary method to monitor suppression pool temperature, but it meets all the requirements of NUREG-0661. It is anticipated that both monitoring channels will be incorporated into the Safety Parameters Display System (SPDS), which will be implemented in the future.

LIST OF REFERENCES

1. "Mark I Containment Program Load Definition Report," General Electric Company, NEDO-21888, Revision 2, November 1981, including Errata and Addenda No. 1, April 1982.
2. "Mark I Containment Program Structural Acceptance Criteria Plant Unique Analysis Application Guide," Task Number 3.1.3, General Electric Company, NEDO-24583-1, October 1979.
3. "Mark I Containment Long-Term Program," Safety Evaluation Report, USNRC, NUREG-0661, July 1980.
4. "Final In-Plant Safety Relief Valve Discharge Test Report, Duane Arnold Energy Center," IOW-30-027, Volume I, Revision 1, March 18, 1982; Volumes II through IX, Revision 0, January 26, 1982.
5. ASME Boiler and Pressure Vessel Code, Section III, Division 1, 1977 Edition with Addenda up to and including Winter 1978.
6. "Damping Values for Seismic Design of Nuclear Power Plants," USNRC, Regulatory Guide 1.61, October 1973.
7. "The General Electric Pressure Suppression Containment Analytical Model," General Electric Company, NEDO-10320, April 1971; Supplement 1, July, 1971; Supplement 2, January 1973.
8. "Mark I Containment Program Plant Unique Load Definition," Duane Arnold Energy Center, General Electric Company, NEDO-24571, Revision 1, March 1982, including Errata and Addenda No. 1, October 1982.
9. "Mark I Containment Program Quarter-Scale Plant Unique Tests, Task Number 5.5.3, Series 2," General Electric Company, NEDE-21944-P, Volumes 1-4, April 1979.
10. "Mark I Containment Program Quarter-Scale Pressure Suppression Pool Swell Test Program: Supplemental Plant Unique Tests, Task Numbers 5.5.4/10.1," General Electric Company, NEDE-24615-P, Volumes 1-3, January 1980.

11. Patton, K.T., "Tables of Hydrodynamic Mass Factors for Translational Motion," ASME Manuscript, Chicago, November 7-11, 1965.
12. Miller, R.R., "The Effects of Frequency and Amplitude of Oscillation on the Hydrodynamic Masses of Irregularly-Shaped Bodies," MS Thesis, University of Rhode Island, Kingston, R.I., 1965.
13. Fitzsimmons, G. W. et al., "Mark I Containment Program Full-Scale Test Program Final Report," Task Number 5.11, General Electric Company, NEDE-24539-P, April 1979.
14. "Mark I Containment Program Letter Reports MI-LR-81-01 and MI-LR-81-01-P, Supplemental Full-Scale Condensation Test Results and Load Confirmation-Proprietary and Nonproprietary Information," General Electric Company, May 6, 1981.
15. "Mark I Containment Program - Full-Scale Test Program - Evaluation of Supplemental Tests," General Electric Company, NEDE-24539-P, Supplement 1, July 1981.
16. Hsiao, W. T. and Valandani, P., "Mark I Containment Program Analytical Model for Computing Air Bubble and Boundary Pressures Resulting from an SRV Discharge Through a T-Quencher Device," General Electric Company, NEDE-21878-P, August 1979.
17. Letter from T. A. Ippolito (NRC) to J. F. Quirk (GE) dated October 16, 1981.
18. "Suppression Pool Temperature Limits for BWR Containment," USNRC, NUREG-0783, Draft, July 1981.
19. "Operating Problems with Target Rock Safety-Relief Valves at BWR's," USNRC, Office of Inspection and Enforcement, IE Bulletin No. 80-25, December 19, 1980.
20. "Analytical Model for T-Quencher Water Jet Loads on Submerged Structures," General Electric Company, NEDE-25090-1-P, Revision 1, May 1981.